5-2012

Interactions of Nitric Oxide and Superoxide Pathways in Hyperglycemic Endothelial Cells

Steven Clay Rogers
University of Arkansas, Fayetteville

Interactions of Nitric Oxide and Superoxide Pathways in Hyperglycemic Endothelial Cells

Interactions of Nitric Oxide and Superoxide Pathways in Hyperglycemic Endothelial Cells

A dissertation submitted in partial fulfillment
of the requirements for the degree of
Doctor of Philosophy in Cell and Molecular Biology

By

Steven Clay Rogers
University of Central Arkansas
Bachelor of Science in Biology and Physics, 2005

May 2012
University of Arkansas

ABSTRACT

Cardiovascular complications arising from diabetic hyperglycemia represents one of the leading causes of death and greatest public health challenges of modern societies. Despite state-of-the-art glucose control, diabetic patients remain at a markedly increased risk of cardiovascular disease. The loss of endothelial function (the development of diabetic endothelial dysfunction) has been implicated in the development of numerous diabetic cardiovascular diseases. The endothelial cell produces many vasoactive substances, hormones and cytoprotective biological factors. Endothelial cells are also involved in and affected by the initiation of inflammatory responses through the release and interaction of cytokines and other immune system molecules. Therefore, regulation of these signaling molecules is extremely important to the health of the vascular endothelium and, consequently, damage to the cells ability to control vessel tone and inflammation is a known hallmark to numerous cardiovascular diseases. Much of recent research attention is directed towards the loss of the ability of the diabetic vasculature to produce nitric oxide (vasodilator and anti-inflammatory hormone, a key component of vascular homeostasis). The observation that endothelial cells in diabetes fail to produce sufficient amount of nitric oxide and fail to relax in response to the endothelium-dependent vasorelaxants (e.g. acetylcholine, bradykinin, shear stress, etc.) has been documented by multiple studies, both in animal models of the disease and in human studies. In this dissertation, we investigated the molecular and enzymatic mechanisms associated with the loss of nitric oxide bioavailability and increase in oxidant formation using a hyperglycemic human umbilical vein endothelial cell model. Our results indicate that while hyperglycemia decreases overall nitric oxide levels, generation of nitric oxide is paradoxically increased, validating previous modeling data published by our lab. Furthermore, we were able to indirectly confirm this concomitant increase in superoxide and

nitric oxide by showing a significant increase in the formation of nitrotyrosine in high glucose exposed endothelial cells. This illustrates that the parallel increase in superoxide and nitric oxide lead to increased reaction with one another, resulting in higher levels of the cytotoxic peroxynitrite molecule. To better understand the effects of angiotensin II and high glucose on gene regulation of oxidant generating enzymes involved in oxidative and nitrosative stress pathways, we performed real-time quantitative PCR for NADPH oxidase subunits and nitric oxide synthase isoforms in HUVEC's. Results from our studies show that stimulating effects of angiotensin II on the activity of endothelial cell NADPH oxidases is enhanced in high-glucose exposed HUVEC's. We also show that hyperglycemic endothelial cells are more sensitive to Ang II interaction, resulting in lower levels of nitric oxide bioavailability and increased nitrotyrosine formation. Our results also provide insight into the gene regulation of NADPH oxidase, eNOS and iNOS. Data shows that angiotensin II increases NADPH oxidase and iNOS mRNA levels in high-glucose exposed HUVECs, while eNOS expression is relatively unchanged. This further validates the hypothesis that high glucose initiates a protective response in endothelial cells by upregulating nitric oxide producing enzymes, iNOS, in an attempt to counteract/scavenge the increased production of superoxide by NADPH oxidase. This protective measure only exacerbates the oxidative and nitrosative stress environment of the cell, leading to increased cell damage and/or apoptosis. Studies in this dissertation will help [1][1][1]clarify the molecular mechanisms and interactions involved in hyperglycemia induced oxidative and nitrosative stress, providing improved focus for treatment design towards improving/reversing high glucose induced endothelial cell dysfunction.

This dissertation is approved for recommendation to the Graduate Council.

Dissertation Director

_____

Dr. Mahendra Kavdia

Thesis Committee:

_____

Dr. Robert Beitle

_____

Dr. Heidi Kluess

_____

Dr. Gisela Erf

DISSERTATION DUPLICATION RELEASE

I hereby authorize the University of Arkansas Libraries to duplicate this dissertation when needed for research and scholarship.

Agreed _____

Steven Clay Rogers

Refused _____

Steven Clay Rogers

ACKNOWLEDGEMENT

Although only my name appears on the cover of this dissertation, a great many people have contributed to its production. I owe my deepest gratitude to all those people who have made this dissertation possible and because of whom my graduate experience has been one that I will cherish forever. My deepest gratitude is to my advisor, Dr. Mahendra Kavdia. First and foremost, I would like to thank Dr. Kavdia for believing in me and giving me the opportunity to work with him. I have been amazingly fortunate to have an advisor who gave me the freedom to explore on my own, and at the same time the guidance to recognize my missteps and refocus my attention. Dr. Kavdia taught me how to question thoughts and express ideas. His patience and support helped me overcome many crisis situations and finish this dissertation. I hope that one day I will become as good an advisor to my students as Dr. Kavdia has been to me.

I would like to thank Dr. Heidi Kluess and her team (Audrey Stone and Kirk Evanson) for introducing me new ways to apply techniques learned in the lab towards investigating other realms of science. Those experiences help broaden my understanding of the complicated mechanisms occurring within my own research.

My thanks also go to Prabhakar Deonikar for teaching me the chemiluminescence assay and many other lab techniques and data analysis calculations.

A big thank you to my friends and colleagues at the lab: Duy Nguyen, Vladimir Ternovoi, Saptarshi Kar, Nisha Laksmanan, Madhuri K. and Jithesh V. for all your support and scientific dialogue.

I thank my parents, my sisters Amy and Amanda, my father in law Larry, mother in law Rhonda and all my other extended family members for their support in my endeavors.

Finally, and most importantly, I would like to thank my wife Amanda and son Baylor for being the source of my strength, for being an integral part of my life and for all the sacrifices they made for me to reach this stage of my life. The sacrifices they made are countless and can never be fully repaid.

DEDICATION

Dedicated to my Family

TABLE OF CONTENTS

CHAPTER 1

Introduction

1.1 Overview

The prevalence of type 2 diabetes is increasing at an alarming rate and is near epidemic proportions. According to the World Health Organization, the number of people worldwide with diabetes is expected to rise to nearly 400 million by 2025 [2]. Perhaps most alarming of all, an increasing number of children with type 2 diabetes have been reported in many of the developed countries; the United States, Japan, the United Kingdom, Australia and others. Clearly, type 2 diabetes is currently one of the largest threats to global health. With the increased risk of diabetic complications occurring over such a broad spectrum of the human race, knowledge of the body's response to hyperglycemia is needed to assist public health efforts in the reduction and treatment of Diabetes and its complications. Numerous epidemiological and basic science studies have highlighted the relationship between hyperglycemia and increased risk of cardiovascular disease. Impaired glucose tolerance and the metabolic syndrome often lead to development of type 2 diabetes. Hyperglycemia and the metabolic syndrome have been shown as causal factors of micro- and macrovascular disease. The risk of cardiovascular disease is increased threefold in patients with established metabolic syndrome [3].

Much is now known about the deleterious effects of high ambient glucose concentrations on the vasculature. Although the mechanisms are complex, a number of overlapping concepts seem to be prevalent among the numerous studies. The pathology of cardiovascular diseases associated with diabetes may ultimately be linked to oxidative and nitrosative stress and the development of inflammation, endothelial cell dysfunction and apoptosis. Research has shown that cross-talk between an expanding network of intracellular proteins and signaling molecules, coupled with the variability of responses in different cells and tissues has added to the complexity of diabetes-induced endothelial dysfunction. To date, a direct causal role for nitrosative and oxidative stress

and activation and/or inhibition of intracellular signaling intermediates in the overall pathogenesis of diabetes is unproven. However, a number of working hypotheses exists that attempt to explain the oxidative/nitrosative stress mechanisms associated with diabetic endothelial dysfunction, which results in the loss of vasoconstriction/vasodilation function due to imbalance of signaling molecule homeostasis.

1.2 Mechanisms of high glucose-induced endothelial cell dysfunction and death

1.2.1 High glucose-induced nitrosative and oxidative stress

One of the earliest detectable cell responses to high glucose exposure is the generation of reactive oxygen (ROS) and nitrogen species. Endothelial cells produce ROS such as superoxide and H_2O_2 similar to other types of nonphagocytic cells. Although excess amounts of ROS contribute to endothelial cell death and apoptosis, ROS have an important role at physiological concentrations and act as signaling molecules to mediate various biological responses. ROS are generated from a number of sources, including the mitochondrial electron transport system, xanthine oxidase, cytochrome p450, NADPH oxidase, uncoupled NO synthase (NOS) and myeloperoxidase. Activation and expression of these enzymatic sources of ROS in mammalian cells depend on the tissue and environmental context. There may also be complex interactions among different sources of ROS and feedback and feed forward regulation of ROS accumulation [4, 5].

Molecular O_2 is converted to superoxide by NADPH oxidase, and superoxide can be converted to H_2O_2 by superoxide dismutase (SOD), or to the highly reactive hydroxide ion by the Fenton or Haber–Weiss reactions, or to peroxinitrite by reacting with nitric oxide. Oxidative and nitrosative

stress play an important role in the development of diabetes complications, in both microvascular and macrovascular settings [6]. The metabolic abnormalities of diabetes cause excess superoxide production in endothelial cells of both large and small vessels, as well as in the myocardium. This increased superoxide production is known to cause the activation of five major pathways involved in the pathogenesis of diabetic complications: polyol pathway flux, increased formation of advanced glycation end products (AGEs), increased expression of the receptor for AGEs and its activating ligands, activation of protein kinase C isoforms and overactivity of the hexosamine pathway [7]. Superoxide production induced by high glucose is a well-described phenomenon and arises via a number of important enzymes; mitochondrial electron transport chain, NADPH oxidase (NOX), nitric oxide synthase (NOS) and xanthine oxidase (XO) [8].

Endothelial cells are unable to regulate glucose intake due to the intrinsic properties of the GLUT4 receptor. Consequently, chronic high glucose exposure leads to a buildup of glucose inside the endothelial cell [9, 10]. High intracellular glucose levels causes interruption of the electron transport chain at complex III, resulting in increased oxidation of molecular oxygen by coenzyme Q, yielding superoxide anions [11]. Therefore the normally efficient metabolism of glucose can, in response to stress such as hyperglycemia, lead to excess free-radical generation and oxidative stress.

Activation of NADPH oxidase and uncoupling of nitric oxide synthase are also significant in the contribution of excess free radical generation and decreased nitric oxide bioavailability in response to hyperglycemia. Our lab has previously predicted and shown that superoxide generation is increased and nitric oxide levels are decreased in human umbilical vein endothelial cells (HUVEC's) in response to high glucose [12]. This intracellular environment of both superoxide and nitric oxide greatly favors the formation of peroxynitrite. Peroxynitrite is an

important and powerful oxidizer of various proteins inside the endothelial cell. Nitration by peroxynitrite is a well-established posttranslational modification and attracts considerable interest in biomedical research, because it can alter protein function, is associated with acute and chronic disease states, and can be a predictor of disease risk [13]. The reactions between nitric oxide and superoxide do not necessarily result in oxidative damage and in some cases can even be cytoprotective.

Low levels of peroxynitrite are able to be detoxified by enzymatic and non-enzymatic systems [14]. Additional reactions of the peroxynitrite molecule lead to a number of other oxidative and nitrosative species. Protonation of peroxynitrite yields peroxynitrous acid, which may decompose to yield the oxidizing hydroxyl radical. Oxidation of peroxynitrite by CO_2 generates nitrosoperoxycarbonate. Decomposition of this short-lived radical produces nitrogen dioxide and the carbonate anion leading to further oxidation and nitration reactions [15, 16].

Many studies have demonstrated oxidative and nitrosative stress in cells following exposure to high glucose concentrations [17-20] and several have shown some beneficial effect of antioxidants [21-25]. However, care should be taken when interpreting data from studies of this type. Many of the techniques used to detect free radical species such as superoxide are not specific. Furthermore, the cellular half-life of these radicals is, at most, a few seconds given the number of possible reactants present. This is particularly true of peroxynitrite where oxidation and nitration reactions occur at very fast rates [14]. Therefore, studies involving detectors with relatively high reaction rates with the intended target, superoxide and nitric oxide, are needed to limit the potential for error. The efficacy of current fluorescent detectors specific for peroxynitrite is still under debate. The reactive species experiments performed in our lab utilize fluorescent probes known to react at high rates with their given targets, allowing for increased

accuracy in reactive species measurements. Despite these reservations, it is clear that oxidant formation is increased following exposure to high glucose and the oxidation and nitration products can be relatively detected both in vivo and in vitro. The detection of 3-nitrotyrosine in tissue sections is often used as an indicator of peroxynitrite induced oxidative stress and cellular injury. Increased nitrotyrosine staining has been detected in the proximal tubules of patients with diabetic nephropathy and in the renal cortex of diabetic rats [26, 27]. Peroxynitrite also directly causes oxidative DNA damage such as point mutation and double-strand breaks as well as lipid peroxidation [28-30]. Peroxynitrite was shown to activate caspases in HL-60 cells, but only caspase-3 was shown to be involved in apoptosis [31].

An additional source of high glucose-induced oxidative stress is via the polyol pathway. Here, glucose is reduced to sorbitol by aldose reductase in a process that consumes NADPH. Sorbitol is then converted to fructose by sorbitol dehydrogenase with the generation of NADH [32-34]. Glucose can undergo auto-oxidation or decomposition via numerous intermediates to yield reactive dicarbonyls glyoxal, methylglyoxal and 3-deoxyglucosone. These can then react with proteins to generate advanced glycation end products (AGEs) resulting in altered function that may lead, via ROS generation or NF-κB activation, to cell death. Many studies now implicate AGEs as mediators of diabetic pathophysiology [35].

The main underlying theme to these apoptotic cellular pathways is the condition of oxidative and nitrosative stress. From a molecular level, oxidative stress arises from increased production of ROS or reduced antioxidant capacity in cells or tissue. ROS are molecules with unpaired electrons, which can either accept another electron or transfer an electron to another molecule. The major intracellular form of ROS is superoxide, which may be converted to weaker or more stable ROS, like hydrogen peroxide or hydroxyl radicals, or to more aggressive compounds, like

peroxynitrite. As previously mentioned, ROS are normal by-products of cell metabolism through mitochondrial respiration or several oxidases, including NADPH oxidase, xanthine oxidase, cyclooxygenase, and lipoxygenase. ROS are required for maintaining normal cellular function, including scavenger and signal transduction roles. However, when cells are exposed to stress conditions such as hyperglycemia, a number of superoxide-producing enzymes are activated. The antioxidant mechanisms of the cell are overwhelmed, leading to the intracellular accumulation of excess superoxide. Endothelial nitric oxide synthase (eNOS) and SOD lose their ability to regulate superoxide levels and ultimately compound the problem of excess ROS/RNS production. The product of eNOS, nitric oxide, may react with superoxide to form peroxynitrite. Clarification of the complete major enzymatic biochemical pathways associated with hyperglycemia and their relative contribution towards inducing oxidative stress will greatly assist understanding of endothelial dysfunction. Furthermore, clarification of the early stages of enzymatic pathway activation due to high glucose stimulation in endothelial cells would be of large importance in understanding diabetic vascular pathology.

1.2.2 Involvement of NADPH oxidase

One of the major sources of ROS in endothelial cells is the NADPH oxidase system [36]. The activation of endothelial cell NADPH oxidase is a major hypothesis in the progression of high glucose induced oxidative and nitrosative stress. NADPH oxidase is activated in endothelial cells by growth factors, cytokines, shear stress, hypoxia, and G-protein coupled agonists [37]. In mammalian neutrophils, NADPH oxidase consists of the membrane-bound cytochrome b558 comprising the catalytic subunit gp91 phox (Nox2) and regulatory subunit p22 phox , as well as cytosolic subunits, p40 phox , p47 phox , and p67 phox, and the GTPase, Rac. The neutrophil

NADPH oxidase releases large amounts of O_2 in bursts, whereas the nonphagocytic, such as endothelial cell, NADPH oxidase(s) continuously produce low levels of O_2 intracellularly in basal state. However, these oxidant-producing enzymes can be further stimulated acutely by various agonists and growth factors [38]. In nonphagocytic cells, several human homologs of gp91 phox (also termed as Nox2) have been identified including Nox1, Nox3, Nox4, Nox5, and the dual oxidases (Duox1 and Duox2). In endothelial cells Nox1, Nox2, Nox4, and Nox5 are mainly expressed and Nox family members share the common binding sites for FAD, heme, and NADPH, and six transmembrane domains [39, 40]. Nox2 is the primary source of superoxide among all endothelial NADPH oxidase. The regulation of Nox1 activity requires p22 phox , as does Nox2 [41], and NoxO1 (Nox organizer 1) and NoxA1 (Nox activator 1)-respective homologs of p47 phox and p67 phox [42].

NADPH oxidase is activated by diverse stimuli including G-protein-coupled receptor agonists (angiotensin II and thrombin); cytokines (tumor necrosis factor and transforming growth factor); growth factors [VEGF (vascular endothelial growth factor), angiopoietin-1, PDGF, EGF, fibroblast growth factor and insulin]; hypoxia-reoxygenation or ischemia-reperfusion; and mechanical stimuli (shear stress) [4, 43]. The molecular mechanism of NADPH oxidase activation in endothelial cells has been better characterized for the Nox2-based oxidase and Nox1. In general, Nox2 oxidase activation of endothelial cells involves a translocation of cytosolic oxidase components (p47 phox, p67 phox, and Rac1) to the plasma membrane and association with cytochrome b558, which initiates the electron transfer process. The key post-translational modifications involved in oxidase activation are the phosphorylation of p47 phox and Rac activation [43, 44]. PKC isoforms are believed to be the major kinases responsible for p47 phox phosphorylation, although other kinases such as Src kinases, PI3 kinase (PI3K), Akt,

mitogen-activated protein kinases (MAP kinases) including p38 MAPK, JNK/SAPK, and ERK, and PAK (p21-activated kinase) may also play a role depending on the stimulus [5, 45].
Nox activation can also result in cell death. ROS can trigger apoptosis either indirectly through damage to DNA, lipids, and proteins or directly by ROS-mediated activation of signaling molecules [46]. Such pro-apoptotic signaling by ROS may occur through activation of MAP kinases, such as SAPK/JNK, ERK1/2, and p38 [43]. MAP kinase activation is known to occur in many instances through ROS-dependent inhibition of tyrosine phosphatase [47]. At higher ROS concentrations, hydrogen peroxide can inhibit caspases and thereby lead to a switch from apoptosis to necrosis [48]. High concentrations of ROS directly cause damage of DNA, lipids, and proteins that result in apoptosis [49].

1.2.3 Mitochondria-dependent mechanisms

Much more has been studied of the hypothesis regarding mitochondrial activation of oxidative stress and apoptotic pathways in diabetes. The current hypothesis linking mitochondria reactive oxygen species production to sustained hyperglycemia involves increased TCA activity, leading to increased electron delivery to the electron transport chain from NADH and $FADH_2$. Increased metabolic respiration occurs due to elevated intracellular glucose levels resulting from hyperglycemia. This condition hyperpolarizes the mitochondria membrane resulting in inhibition of complex I and III, which increases the electron transfer to O_2, producing superoxide [50]. Mitochondrial apoptosis is regulated by a large number of proteins that directly or indirectly activate or inhibit the activity of cysteine proteases. Several of these proteins share homology and comprise the Bcl-2 family of apoptosis regulators, of which there are three main groups defined according to the number and type of Bcl-2 homology (BH) domains they contain [51].

The pro-apoptotic proteins Bax and Bak contain multiple BH domains. BH3-only proteins inhibit the anti-apoptotic actions of Bcl-2 directly by binding and preventing its inhibition of Bax. Bax promotes mitochondrial membrane permeability, allowing the release of cytochrome *c* and formation of the apoptosome. This leads to activation of caspase-9 and, subsequently, caspase-3 [52].

High glucose causes mitochondrial membrane depolarization and loss of uncoupling proteins (UCP), especially UCP3, resulting in increased oxidative stress as well as release of cytochrome *c* and activation of caspases [53]. Uncoupling proteins are inner mitochondrial membrane proteins that can prevent ROS formation and maintain mitochondrial membrane potential [54]. The role of UCPs in apoptosis is not clear, however, and may depend on the nature of the stimuli and cell type. However, studies have shown that loss of UCP3 expression appears with high glucose-induced apoptosis [55]. Recent work has also shown that high glucose-induced superoxide generation causes DNA strand breaks and activation of poly(ADP)-ribose polymerase (PARP). In turn, PARP inhibits glyceraldehyde phosphate dehydrogenase (GAPDH) and leads to cell death. This study illustrates another potential role of mitochondrial ROS generation in high glucose-induced cell death [56].

The effects of high glucose on apoptotic cell death appear to be independent of hyperosmolarity of glucose, which induces necrosis in endothelial cells [3]. However, mitochondrial dependent apoptosis in high glucose endothelial cells has been linked to Bax and Bad translocation. Risso et al. showed that intermittent high glucose (5 mM followed by 25 mM daily over 14 days) was more effective at inducing mitochondrial Bax-mediated apoptosis than stable high glucose (25 mM continuously) [57]. Nakagami et al. showed that high glucose caused translocation of Bax to the mitochondrial membrane and subsequent caspase-3 and caspase-9 activation [58].

1.2.4 Nitric oxide synthase function/dysfunction and apoptosis

Lack of function or dysfunction of nitric oxide synthase represents another major hypothesis in the development of oxidative and nitrosative stress pathways in high glucose induced endothelial dysfunction. Three isozymes of nitric oxide synthase (NOS) have been identified in the current literature. Their cDNA- and protein structures as well as their genomic DNA structures have also been described. NOS I (nNOS, originally discovered in neurons) and NOS III (eNOS, originally discovered in endothelial cells) are relatively low output, Ca(2+)-activated enzymes whose main physiological function is signal transduction. NOS II (iNOS, originally discovered in cytokine-induced macrophages) is a high output enzyme which produces relatively higher amounts of nitric oxide [14]. Depending on the species, NOS II activity is largely or completely Ca(2+)-independent. All NOS produce nitric oxide by oxidizing guanidino nitrogen of L-arginine, utilizing molecular oxygen and NADPH as co-substrates. All isoforms contain FAD, FMN and heme iron and require the cofactor BH_4. NOS I and III are constitutively expressed in various cells, however, expression of these isoforms is subject to regulation [59]. TNF-alpha has been shown to reduce the expression of NOS III by a post-transcriptional mechanism that destabilizes the mRNA. Expression of NOS II is mainly regulated at the transcriptional level and can be induced in many cell types with LPS, cytokines, and other compounds [60].

Nitric oxide, produced by endothelial nitric oxide synthase (eNOS), is a key signaling molecule in vascular homeostasis [61]. Originally identified as endothelium-derived relaxing factor, nitric oxide is an important regulator of vascular tone and blood pressure. In addition, nitric oxide has multiple antiatherogenic roles, including anti-inflammatory, antithrombotic, antiproliferative, and antioxidant effects [62]. Loss of nitric oxide bioavailability is a cardinal feature of endothelial dysfunction that precedes the development of atherosclerosis and is an independent

predictor of cardiovascular disease risk [63, 64]. Several factors contribute to loss of nitric oxide bioavailability in endothelial dysfunction states, including eventual reduction in nitric oxide synthesis and nitric oxide scavenging by reactive oxygen species [65]. The regulation of nitric oxide production by eNOS is complex, but the cofactor tetrahydrobiopterin (BH_4) has emerged as a critical determinant of nitric oxide synthesis. Endothelial BH_4availability appears to be a key requirement for maintaining normal endothelial function [66].

In a number of studies where oxidative stress induces endothelial dysfunction, expression of eNOS has been shown to be paradoxically unchanged or increased. The mechanisms underlying expression changes of eNOS are not fully described, but may be associated with increases in secondary oxidative radicals such as hydrogen peroxide, which increases the expression of eNOS at the transcription and protein levels. The development of endothelial dysfunction in the presence of unchanged or increased eNOS levels suggests that the enzyme's function to produce nitric oxide may be limited. This decrease in nitric oxide production by eNOS may explain the reduced bioavailability of nitric oxide in the stressed endothelial cell. However, our data shows that although overall nitric oxide levels are decreased, nitric oxide production is increased in response to high glucose stimulation of endothelial cells [67]. This suggests that another significant source of nitric oxide appears during hyperglycemia-induced oxidative stress, presumably iNOS. Recent qPCR data from our lab shows that iNOS gene expression is significantly increased in HUVECs in as little as 1 hour exposure to high glucose. HUVEC gene expression of iNOS is further increased for 24 and 48 hour high glucose exposure. These data corroborate the theory that eNOS function is reduced and also converted to production of superoxide due to high glucose induced oxidative stress. Additionally, iNOS expression is increased, resulting in significantly higher nitric oxide production in the presence of elevated

superoxide production. All of these points taken together illustrate potent pathways for the development of nitrosative and oxidative stress within the high glucose exposed endothelial cell.

1.2.5 Role of nitration in endothelial cell dysfunction/apoptosis

The peroxynitrite anion is a short-lived oxidant species that is produced by the reaction of nitric oxide and superoxide radicals at diffusion-controlled rates (~1×10^{10} M–1 s–1) [68]. The sites of peroxynitrite formation are assumed to be spatially associated with the sources of superoxide (such as the plasma membrane NADPH oxidases or the mitochondrial respiratory complexes) because although nitric oxide is a relatively stable and highly diffusible free radical, superoxide is much shorter lived and has restricted diffusion across biomembranes [69]. The rates of peroxynitrite production in vivo in specific compartments have been estimated to be as high as 50–100 μM per min. The steady-state concentrations are estimated to be in the nanomolar concentration range, which, however, can be sustained for a long period of time [68]. So, under certain conditions such as hyperglycemic stress, exposure to peroxynitrite can be significant, considering the length of time of formation. Despite the short half-life of peroxynitrite at physiological pH (~10 ms), its ability to cross cell membranes suggests that peroxynitrite generated from a cellular source could influence surrounding cells within one to two cell diameters (~5–20 μm) [70]. When biological systems are exposed to peroxynitrite, a number of biological effects can occur, with adverse effects on the viability and function of cells. A fundamental reaction of peroxynitrite in biological systems is its fast reaction with carbon dioxide, which leads to the formation of carbonate and nitrogen dioxide radicals. Nitrogen dioxide can undergo reactions with biomolecules, resulting in nitrated compounds [71]. The

decomposition of peroxynitrite to form hydroxide ions may also be important in the initiation of lipid peroxidation processes [72].

Many biomolecules are oxidized and/or nitrated by peroxynitrite-derived radicals, including tyrosine residues, thiols, DNA and unsaturated fatty-acid-containing phospholipids. Tyrosine nitration, dimerization and hydroxylation by peroxynitrite to form 3-nitrotyrosine, 3,3′-dityrosine and 3,4′-dihydrophenylalanine, respectively, are completely dependent on free-radical pathways [73]. Thiols can also be oxidized by one-electron reactions by peroxynitrite-derived radicals. In DNA, purine nucleotides are vulnerable to oxidation. Also, peroxynitrite can cause deoxyribose oxidation and strand breaks [29]. The reaction of peroxynitrite-derived radicals with lipids leads to peroxidation and the formation of nitrated lipid oxidation. Lipid peroxidation processes may also assist in protein tyrosine oxidation and nitration in biomembranes and lipoproteins [72].

Peroxynitrite can promote the oxidation of co factors either by direct or free-radical-dependent mechanisms. Peroxynitrite-mediated oxidation of tetrahydrobiopterin (BH_4) to 5,6-dihydrobiopterin (and subsequently to 7,8-dihydrobiopterin) leads to the dysfunction of nitric oxide synthase, as BH_4 is an essential NOS cofactor. Another theory proposes that low levels of BH_4 can lead to its own further depletion, mediated by the NOS-dependent formation of peroxynitrite [74]. This hypothesized mechanism might also contribute to vascular endothelial dysfunction that is induced by oxidative stress in diseases such as diabetes.

An imbalance in the ratio of nitric oxide to superoxide anion due to increased superoxide levels has been shown to lead to an alteration in vascular reactivity. Under these conditions an increase in peroxynitrite formation, resulting from the reaction between nitric oxide and superoxide, is likely to occur. Peroxynitrite is responsible for nitration of tyrosine residues in proteins; therefore the presence of nitrotyrosine in plasma or intracellular proteins is considered indirect evidence of

peroxyntrite production and oxidative and nitrosative stress. Nitrotyrosine has been found in the plasma of patients with diabetes, but it is not detectable in the plasma of healthy controls. Nitrotyrosine plasma values are correlated with plasma glucose concentrations, and further studies exploring the effects of acute hyperglycemia on nitrotyrosine formation confirmed that nitrotyrosine is produced both in normal subjects during hyperglycemic clamp and in working hearts from rats during hyperglycemic perfusion. In a clinical study, glucose produced a decrease in endothelial function and an increase in nitrotyrosine in normal subjects and patients with diabetes [75].

1.2.6 Justification

Evidence for oxidative and nitrosative stress involvement in hyperglycemia-induced endothelial dysfunction is very strong. Taken together, these reports support the view that nitrosative stress and peroxyntrite-induced damage play a crucial role in multiple interrelated aspects of the pathogenesis of diabetes and its complications. Numerous studies have shown that diabetic patients have higher incidence of endothelial dysfunction and oxidant stress. The imbalance between superoxide and nitric oxide levels has the potential to damage the endothelial cell and lead to loss of vasomotor control. However, understanding of both nitric oxide and reactive oxygen species pathways and their interactions in hyperglycemia is unclear. Clarification of the molecular mechanisms involved in endothelial cell dysfunction is important for delineating effective treatment strategies. Neutralization of reactive nitrogen species or inhibition of upstream ROS pathways may emerge as novel approaches for the experimental therapy of diabetes, as well as for the prevention or reversal of its complications. However, without

complete knowledge of the numerous interactions involved in reactive oxygen and nitrogen species pathways, interventional treatments may create unintended damage or ineffective results.

1.3 Specific Aims

The overall goal of this study is to understand the interactions between high-glucose induced superoxide and nitric oxide in endothelial cells and their role in the development of oxidative and nitrosative stress, endothelial cell damage and apoptosis. To that end, we focused on the application of fluorescence detection techniques of nitric oxide and superoxide, contribution and gene regulation of enzymatic pathways involved in hyperglycemic stress and apoptosis and the role of the renin-angiotensin pathway in high-glucose endothelial cell dysfunction. The specific aims of this study are as follows:

Specific Aim 1: To study the reaction rates of fluorescent probes and their given reactive species, nitric oxide and superoxide, in a cell-free system

Specific Aim 2: To investigate the contribution levels and significance of endothelial and inducible nitric oxide synthase and NADPH oxidase in the development of oxidative and nitrosative stress and apoptosis in hyperglycemic endothelial cells

Specific Aim 3: To understand the effects of the renin-angiotensin pathway on cell damage and gene expression of endothelial and inducible nitric oxide synthase and NADPH in hyperglycemic endothelial cells

1.4 Significance

The results from our studies will enhance our current understanding of the complicated mechanisms associated with reduced nitric oxide availability and increased superoxide levels caused by hyperglycemia in endothelial cells. Increased understanding of the intracellular targets involved in high-glucose induced endothelial dysfunction will assist in the development of better drug design and treatment strategies for diabetic cardiovascular diseases.

1.5 References

[1] Brownlee, M. Biochemistry and molecular cell biology of diabetic complications. *Nature* **414:**813-820; 2001.

[2] Ceriello, A. Hyperglycaemia and the vessel wall: the pathophysiological aspects on the atherosclerotic burden in patients with diabetes. *Eur J Cardiovasc Prev Rehabil* **17 Suppl 1:**S15-19; 2010.

[3] Giacco, F.; Brownlee, M. Oxidative stress and diabetic complications. *Circ Res* **107:**1058-1070; 2010.

[4] Henriksen, E. J.; Diamond-Stanic, M. K.; Marchionne, E. M. Oxidative stress and the etiology of insulin resistance and type 2 diabetes. *Free Radic Biol Med*; 2010.

[5] Orasanu, G.; Plutzky, J. The pathologic continuum of diabetic vascular disease. *J Am Coll Cardiol* **53:**S35-42; 2009.

[6] Aronson, D. Hyperglycemia and the pathobiology of diabetic complications. *Adv Cardiol* **45:**1-16; 2008.

[7] Potdar, S.; Kavdia, M. NO/peroxynitrite dynamics of high glucose-exposed HUVECs: chemiluminescent measurement and computational model. *Microvasc Res* **78:**191-198; 2009.

[8] Rubbo, H.; Radi, R. Protein and lipid nitration: role in redox signaling and injury. *Biochim Biophys Acta* **1780:**1318-1324; 2008.

[9] Pacher, P.; Beckman, J. S.; Liaudet, L. Nitric oxide and peroxynitrite in health and disease. *Physiol Rev* **87:**315-424; 2007.

[10] Beckman, J. S.; Koppenol, W. H. Nitric oxide, superoxide, and peroxynitrite: the good, the bad, and ugly. *Am J Physiol* **271:**C1424-1437; 1996.

[11] Radi, R. Peroxynitrite reactions and diffusion in biology. *Chem Res Toxicol* **11:**720-721; 1998.

[12] Crabtree, M. J.; Smith, C. L.; Lam, G.; Goligorsky, M. S.; Gross, S. S. Ratio of 5,6,7,8-tetrahydrobiopterin to 7,8-dihydrobiopterin in endothelial cells determines glucose-elicited changes in NO vs. superoxide production by eNOS. *Am J Physiol Heart Circ Physiol* **294:**H1530-1540; 2008.

[13] Ge, Q. M.; Dong, Y.; Zhang, H. M.; Su, Q. Effects of intermittent high glucose on oxidative stress in endothelial cells. *Acta Diabetol* **47:**97-103; 2010.

[14] Piconi, L.; Quagliaro, L.; Assaloni, R.; Da Ros, R.; Maier, A.; Zuodar, G.; Ceriello, A. Constant and intermittent high glucose enhances endothelial cell apoptosis through mitochondrial superoxide overproduction. *Diabetes Metab Res Rev* **22:**198-203; 2006.

[15] Quagliaro, L.; Piconi, L.; Assaloni, R.; Da Ros, R.; Szabo, C.; Ceriello, A. Primary role of superoxide anion generation in the cascade of events leading to endothelial dysfunction and damage in high glucose treated HUVEC. *Nutr Metab Cardiovasc Dis* **17:**257-267; 2007.

[16] Ceriello, A.; dello Russo, P.; Amstad, P.; Cerutti, P. High glucose induces antioxidant enzymes in human endothelial cells in culture. Evidence linking hyperglycemia and oxidative stress. *Diabetes* **45:**471-477; 1996.

[17] Curcio, F.; Pegoraro, I.; Dello Russo, P.; Falleti, E.; Perrella, G.; Ceriello, A. Sod and GSH inhibit the high glucose-induced oxidative damage and the PDGF increased secretion in cultured human endothelial cells. *Thromb Haemost* **74:**969-973; 1995.

[18] Tsuneki, H.; Sekizaki, N.; Suzuki, T.; Kobayashi, S.; Wada, T.; Okamoto, T.; Kimura, I.; Sasaoka, T. Coenzyme Q10 prevents high glucose-induced oxidative stress in human umbilical vein endothelial cells. *Eur J Pharmacol* **566:**1-10; 2007.

[19] Ulker, S.; McMaster, D.; McKeown, P. P.; Bayraktutan, U. Antioxidant vitamins C and E ameliorate hyperglycaemia-induced oxidative stress in coronary endothelial cells. *Diabetes Obes Metab* **6:**442-451; 2004.

[20] Ungvari, Z.; Bagi, Z.; Feher, A.; Recchia, F. A.; Sonntag, W. E.; Pearson, K.; de Cabo, R.; Csiszar, A. Resveratrol confers endothelial protection via activation of the antioxidant transcription factor Nrf2. *Am J Physiol Heart Circ Physiol* **299:**H18-24; 2010.

[21] Ishii, N.; Patel, K. P.; Lane, P. H.; Taylor, T.; Bian, K.; Murad, F.; Pollock, J. S.; Carmines, P. K. Nitric oxide synthesis and oxidative stress in the renal cortex of rats with diabetes mellitus. *J Am Soc Nephrol* **12:**1630-1639; 2001.

[22] Thuraisingham, R. C.; Nott, C. A.; Dodd, S. M.; Yaqoob, M. M. Increased nitrotyrosine staining in kidneys from patients with diabetic nephropathy. *Kidney Int* **57:**1968-1972; 2000.

[23] Arteel, G. E.; Briviba, K.; Sies, H. Protection against peroxynitrite. *FEBS Lett* **445:**226-230; 1999.

[24] Niles, J. C.; Wishnok, J. S.; Tannenbaum, S. R. Peroxynitrite-induced oxidation and nitration products of guanine and 8-oxoguanine: structures and mechanisms of product formation. *Nitric Oxide* **14:**109-121; 2006.

[25] Shibuki, H.; Katai, N.; Yodoi, J.; Uchida, K.; Yoshimura, N. Lipid peroxidation and peroxynitrite in retinal ischemia-reperfusion injury. *Invest Ophthalmol Vis Sci* **41:**3607-3614; 2000.

[26] Zhuang, S.; Simon, G. Peroxynitrite-induced apoptosis involves activation of multiple caspases in HL-60 cells. *Am J Physiol Cell Physiol* **279:**C341-351; 2000.

[27] Samhan-Arias, A. K.; Tyurina, Y. Y.; Kagan, V. E. Lipid antioxidants: free radical scavenging versus regulation of enzymatic lipid peroxidation. *J Clin Biochem Nutr* **48:**91-95.

[28] Chung, S. S.; Ho, E. C.; Lam, K. S.; Chung, S. K. Contribution of polyol pathway to diabetes-induced oxidative stress. *J Am Soc Nephrol* **14:**S233-236; 2003.

[29] Takamura, Y.; Tomomatsu, T.; Kubo, E.; Tsuzuki, S.; Akagi, Y. Role of the polyol pathway in high glucose-induced apoptosis of retinal pericytes and proliferation of endothelial cells. *Invest Ophthalmol Vis Sci* **49:**3216-3223; 2008.

[30] Berrone, E.; Beltramo, E.; Solimine, C.; Ape, A. U.; Porta, M. Regulation of intracellular glucose and polyol pathway by thiamine and benfotiamine in vascular cells cultured in high glucose. *J Biol Chem* **281:**9307-9313; 2006.

[31] Circu, M. L.; Aw, T. Y. Glutathione and apoptosis. *Free Radic Res* **42:**689-706; 2008.

[32] Powell, L. A.; Nally, S. M.; McMaster, D.; Catherwood, M. A.; Trimble, E. R. Restoration of glutathione levels in vascular smooth muscle cells exposed to high glucose conditions. *Free Radic Biol Med* **31:**1149-1155; 2001.

[33] Beltramo, E.; Nizheradze, K.; Berrone, E.; Tarallo, S.; Porta, M. Thiamine and benfotiamine prevent apoptosis induced by high glucose-conditioned extracellular matrix in human retinal pericytes. *Diabetes Metab Res Rev* **25:**647-656; 2009.

[34] Allen, D. A.; Yaqoob, M. M.; Harwood, S. M. Mechanisms of high glucose-induced apoptosis and its relationship to diabetic complications. *J Nutr Biochem* **16:**705-713; 2005.

[35] Fujita, H.; Omori, S.; Ishikura, K.; Hida, M.; Awazu, M. ERK and p38 mediate high-glucose-induced hypertrophy and TGF-beta expression in renal tubular cells. *Am J Physiol Renal Physiol* **286:**F120-126; 2004.

[36] Yamagishi, S.; Matsui, T. Advanced glycation end products, oxidative stress and diabetic nephropathy. *Oxid Med Cell Longev* **3:**101-108.

[37] Ray, R.; Shah, A. M. NADPH oxidase and endothelial cell function. *Clin Sci (Lond)* **109:**217-226; 2005.

[38] Li, J. M.; Shah, A. M. Endothelial cell superoxide generation: regulation and relevance for cardiovascular pathophysiology. *Am J Physiol Regul Integr Comp Physiol* **287:**R1014-1030; 2004.

[39] Brown, D. I.; Griendling, K. K. Nox proteins in signal transduction. *Free Radic Biol Med* **47:**1239-1253; 2009.

[40] Datla, S. R.; Griendling, K. K. Reactive oxygen species, NADPH oxidases, and hypertension. *Hypertension* **56:**325-330; 2010.

[41] Paravicini, T. M.; Touyz, R. M. NADPH oxidases, reactive oxygen species, and hypertension: clinical implications and therapeutic possibilities. *Diabetes Care* **31 Suppl 2:**S170-180; 2008.

[42] BelAiba, R. S.; Djordjevic, T.; Petry, A.; Diemer, K.; Bonello, S.; Banfi, B.; Hess, J.; Pogrebniak, A.; Bickel, C.; Gorlach, A. NOX5 variants are functionally active in endothelial cells. *Free Radic Biol Med* **42:**446-459; 2007.

[43] Lassegue, B.; Griendling, K. K. NADPH oxidases: functions and pathologies in the vasculature. *Arterioscler Thromb Vasc Biol* **30:**653-661; 2010.

[44] Ambasta, R. K.; Kumar, P.; Griendling, K. K.; Schmidt, H. H.; Busse, R.; Brandes, R. P. Direct interaction of the novel Nox proteins with p22phox is required for the formation of a functionally active NADPH oxidase. *J Biol Chem* **279:**45935-45941; 2004.

[45] Gao, L.; Mann, G. E. Vascular NAD(P)H oxidase activation in diabetes: a double-edged sword in redox signalling. *Cardiovasc Res* **82:**9-20; 2009.

[46] Lee, M. Y.; Griendling, K. K. Redox signaling, vascular function, and hypertension. *Antioxid Redox Signal* **10:**1045-1059; 2008.

[47] Brandes, R. P.; Weissmann, N.; Schroder, K. NADPH oxidases in cardiovascular disease. *Free Radic Biol Med* **49:**687-706.

[48] Frey, R. S.; Gao, X.; Javaid, K.; Siddiqui, S. S.; Rahman, A.; Malik, A. B. Phosphatidylinositol 3-kinase gamma signaling through protein kinase Czeta induces NADPH oxidase-mediated oxidant generation and NF-kappaB activation in endothelial cells. *J Biol Chem* **281:**16128-16138; 2006.

[49] Paravicini, T. M.; Touyz, R. M. Redox signaling in hypertension. *Cardiovasc Res* **71:**247-258; 2006.

[50] Kamata, H.; Honda, S.; Maeda, S.; Chang, L.; Hirata, H.; Karin, M. Reactive oxygen species promote TNFalpha-induced death and sustained JNK activation by inhibiting MAP kinase phosphatases. *Cell* **120:**649-661; 2005.

[51] Fujita, R.; Ueda, H. Protein kinase C-mediated cell death mode switch induced by high glucose. *Cell Death Differ* **10:**1336-1347; 2003.

[52] Misiaszek, R.; Crean, C.; Joffe, A.; Geacintov, N. E.; Shafirovich, V. Oxidative DNA damage associated with combination of guanine and superoxide radicals and repair mechanisms via radical trapping. *J Biol Chem* **279:**32106-32115; 2004.

[53] Bashan, N.; Kovsan, J.; Kachko, I.; Ovadia, H.; Rudich, A. Positive and negative regulation of insulin signaling by reactive oxygen and nitrogen species. *Physiol Rev* **89:**27-71; 2009.

[54] Yang, Z.; Mo, X.; Gong, Q.; Pan, Q.; Yang, X.; Cai, W.; Li, C.; Ma, J. X.; He, Y.; Gao, G. Critical effect of VEGF in the process of endothelial cell apoptosis induced by high glucose. *Apoptosis* **13:**1331-1343; 2008.

[55] McKenzie, M. D.; Jamieson, E.; Jansen, E. S.; Scott, C. L.; Huang, D. C.; Bouillet, P.; Allison, J.; Kay, T. W.; Strasser, A.; Thomas, H. E. Glucose induces pancreatic islet cell apoptosis that requires the BH3-only proteins Bim and Puma and multi-BH domain protein Bax. *Diabetes* **59:**644-652.

[56] Vincent, A. M.; Olzmann, J. A.; Brownlee, M.; Sivitz, W. I.; Russell, J. W. Uncoupling proteins prevent glucose-induced neuronal oxidative stress and programmed cell death. *Diabetes* **53:**726-734; 2004.

[57] Rousset, S.; Alves-Guerra, M. C.; Mozo, J.; Miroux, B.; Cassard-Doulcier, A. M.; Bouillaud, F.; Ricquier, D. The biology of mitochondrial uncoupling proteins. *Diabetes* **53 Suppl 1:**S130-135; 2004.

[58] Li, Y.; Maedler, K.; Shu, L.; Haataja, L. UCP-2 and UCP-3 proteins are differentially regulated in pancreatic beta-cells. *PLoS One* **3:**e1397; 2008.

[59] Pacher, P.; Szabo, C. Role of poly(ADP-ribose) polymerase-1 activation in the pathogenesis of diabetic complications: endothelial dysfunction, as a common underlying theme. *Antioxid Redox Signal* **7:**1568-1580; 2005.

[60] Villanueva, C.; Giulivi, C. Subcellular and cellular locations of nitric oxide synthase isoforms as determinants of health and disease. *Free Radic Biol Med* **49:**307-316.

[61] Oess, S.; Icking, A.; Fulton, D.; Govers, R.; Muller-Esterl, W. Subcellular targeting and trafficking of nitric oxide synthases. *Biochem J* **396:**401-409; 2006.

[62] Ignarro, L. J. Nitric oxide as a unique signaling molecule in the vascular system: a historical overview. *J Physiol Pharmacol* **53:**503-514; 2002.

[63] Alp, N. J.; Channon, K. M. Regulation of endothelial nitric oxide synthase by tetrahydrobiopterin in vascular disease. *Arterioscler Thromb Vasc Biol* **24:**413-420; 2004.

[64] Bonetti, P. O.; Lerman, L. O.; Lerman, A. Endothelial dysfunction: a marker of atherosclerotic risk. *Arterioscler Thromb Vasc Biol* **23:**168-175; 2003.

[65] Reriani, M. K.; Lerman, L. O.; Lerman, A. Endothelial function as a functional expression of cardiovascular risk factors. *Biomark Med* **4:**351-360.

[66] Touyz, R. M.; Briones, A. M. Reactive oxygen species and vascular biology: implications in human hypertension. *Hypertens Res* **34:**5-14.

[67] Luiking, Y. C.; Engelen, M. P.; Deutz, N. E. Regulation of nitric oxide production in health and disease. *Curr Opin Clin Nutr Metab Care* **13:**97-104.

[68] Quijano, C.; Romero, N.; Radi, R. Tyrosine nitration by superoxide and nitric oxide fluxes in biological systems: modeling the impact of superoxide dismutase and nitric oxide diffusion. *Free Radic Biol Med* **39:**728-741; 2005.

[69] Szabo, C.; Ischiropoulos, H.; Radi, R. Peroxynitrite: biochemistry, pathophysiology and development of therapeutics. *Nat Rev Drug Discov* **6:**662-680; 2007.

[70] Ferrer-Sueta, G.; Radi, R. Chemical biology of peroxynitrite: kinetics, diffusion, and radicals. *ACS Chem Biol* **4:**161-177; 2009.

[71] Radi, R.; Peluffo, G.; Alvarez, M. N.; Naviliat, M.; Cayota, A. Unraveling peroxynitrite formation in biological systems. *Free Radic Biol Med* **30:**463-488; 2001.

[72] Bartesaghi, S.; Valez, V.; Trujillo, M.; Peluffo, G.; Romero, N.; Zhang, H.; Kalyanaraman, B.; Radi, R. Mechanistic studies of peroxynitrite-mediated tyrosine nitration in membranes using the hydrophobic probe N-t-BOC-L-tyrosine tert-butyl ester. *Biochemistry* **45:**6813-6825; 2006.

[73] Radi, R. Nitric oxide, oxidants, and protein tyrosine nitration. *Proc Natl Acad Sci U S A* **101:**4003-4008; 2004.

[74] Batthyany, C.; Schopfer, F. J.; Baker, P. R.; Duran, R.; Baker, L. M.; Huang, Y.; Cervenansky, C.; Branchaud, B. P.; Freeman, B. A. Reversible post-translational modification of proteins by nitrated fatty acids in vivo. *J Biol Chem* **281:**20450-20463; 2006.

CHAPTER 2

Critical Evaluation of DHE Fluorescence Measurement of Superoxide: Effect of Nitric Oxide and Superoxide Dismutase Presence

Abstract

An accurate detection of superoxide is desired to better understand numerous vascular pathologies. In this study, we performed mechanistic studies to understand the effectiveness of a currently used oxidative stress assay. We systematically evaluated the effect of nitric oxide ($^{\bullet}$NO) and superoxide dismutase (SOD) presence, two effective scavengers of superoxide, on the fluorescence measurement of superoxide. We also conducted a detailed reaction kinetic analysis of the dihydroethidium (DHE)-superoxide interaction. We used xanthine oxidase/hypoxanthine and spermine nonoate to produce superoxide and $^{\bullet}$NO, respectively. A microplate reader was used to measure DHE fluorescence detection of superoxide. SOD significantly decreased superoxide concentrations in the fluorescence assays. $^{\bullet}$NO showed an inhibitory effect on superoxide measurement at higher concentrations in DHE fluorescence measurements. The kinetic analysis resulted in a reaction rate constant of 1.1×10^3 $M^{-1}s^{-1}$ for DHE-superoxide reaction that is ~260× slower than the reported value of 2.6×10^5 $M^{-1}s^{-1}$. The lower reaction rate constant can explain a lack of DHE fluorescence in the presence of SOD. Results suggest that an accurate measurement of superoxide production may be difficult due to competitive interference from varying $^{\bullet}$NO and SOD levels; however net superoxide concentration may be quantified.

Key Words

DHE, Superoxide, Reaction rate constant, Nitric oxide, Kinetic analysis, Reaction, Oxidative stress

2.1 Introduction

Detection of superoxide has been an essential tool for exploring the various mechanisms occurring in physiological and experimental environments [76]. Xanthine oxidase (XO) catalysis of hypoxanthine oxidation to form superoxide is used widely in cell-free reactions in an experimental environment. Since 1990, fluorescence resulting from the oxidation of dihydroethidium (DHE) (also HE hydroethidine) has been used as a superoxide probe with much success [77]. DHE fluorescence is inhibited by superoxide scavengers such as SOD and NO [38]. For the detection of superoxide using DHE fluorescence, high performance liquid chromatography (HPLC), microplate reader analysis, and fluorometry have proven effective for both qualitatively and quantitatively determining superoxide concentrations [78]. For an accurate description of superoxide measurement an understanding of total reactive species interactions in an experiment is needed. Without this only qualitative measurements of superoxide are possible [79].

Products for the oxidation of DHE by superoxide are well established in the current literature. In the presence of superoxide, DHE is oxidized to 2-OH-ethidium and to a much lesser extent, ethidium. The main product, 2-hydroxyethidium, fluoresces at a wavelength measured with a maximum excitation and emission of 480 nm and 585 nm respectively [76, 80]. The product was also found to be stable within the cell, allowing for precise measurement of DHE fluorescence without risk of intraconversion variability. Fluorescence measurement of DHE yields superoxide concentrations specific for either intracellular or extracellular locations [81].

Oxidative stress within the vascular environment arises from excessive reactive oxygen species [82]. In normal vascular function, the endothelium maintains regulation of blood flow and vascular tone through a balance between vasodilators and vasoconstrictors. ROS also play an

important role in vascular homeostasis. Endothelial dysfunction resulting from oxidative stress is characterized by reduced vasodilation and increased concentrations of ROS including superoxide. The biological implications for accurate detection of superoxide levels within the vasculature are critical for understanding numerous pathologies involving endothelial dysfunction [83].

Nitric oxide is released from the endothelium in response to various agonist and shear stress. Endothelial nitric oxide is produced by catalysis of the amino acid L-arginine by endothelial nitric oxide synthase (eNOS) [84]. When released, nitric oxide is a potent vasodilator and antagonist against accumulation of superoxide within the vascular environment. In addition, nitric oxide and SOD inhibit oxidative stress by acting as an antioxidant in their regulatory interactions with superoxide. Contrarily, in conditions of oxidative stress, superoxide concentrations increase above effective nitric oxide and SOD levels. This leads to decreased bioavailability of nitric oxide and increased concentrations of superoxide and cytotoxic species, such as peroxynitrite and hydrogen peroxide [38].

In vivo, SOD and nitric oxide counteract superoxide. Previous studies have shown that disease pathologies such as hyperglycemia elevate both SOD and eNOS expression [21, 85]. However, the degree to which these species influence total superoxide production and affect DHE fluorescence detection is not fully understood. For this study, we determined the levels at which SOD and nitric oxide presence effect the fluorescence detection of superoxide. We also developed a reaction kinetic model to quantify DHE and superoxide interactions.

2.2 Materials and Methods

2.2.1 Materials:

Xanthine oxidase (XO), hypoxanthine, catalase, SOD, sodium hydroxide (NaOH), ferricytochrome-c and phosphate buffer solution (PBS) were obtained from Sigma Chemical Co. (St. Louis, MO, USA). Spermine nonoate was purchased from Calbiochem (Gibbstown, NJ, USA). Dihydroethidium (hydroethidine) was purchased from Invitrogen Corp. (Carlsbad, CA, USA).

2.2.2 Superoxide and nitric oxide sources:

Reactions were conducted in a BD Falcon 96-well plate with a transparent bottom holding a total reagent volume of 300 µL balanced with PBS (10 mM, pH 7.4). Superoxide was produced using a hypoxanthine and XO enzyme system. Excess catalase was used to remove hydrogen peroxide, which is generated by the dismutation of superoxide. Nitric oxide source was spermine nonoate, which was prepared in a 0.1 M NaOH (pH 12) stock solution for stable storage. Spermine nonoate releases NO at pH 7.4. Final concentrations of 1, 10, and 100 U/mL of SOD and 1, 10, 100 and 1000 µM of spermine nonoate were used to understand the effect of SOD and $^{\bullet}NO$ presence on DHE fluorescence.

2.2.3 Fluorescence measurement:

DHE reacts with superoxide to form mainly 2-OH-ethidium, however a secondary product ethidium can also form at low level [86]. The fluorescence from hydroxy-product (2-OH-ethidium) can be measured at excitation of either 396 or 510 nm with an emission at 585 nm.

Because of a higher contribution of ethidium fluorescence at 510 nm excitation wavelength, the excitation at 396 nm wavelength is advantageous for specific oxidation dependent of superoxide formation [87]. We measured the secondary product at 510/610 nm excitation/emission and observed a linear increase of ethidium over time and the amount of ethidium formation was less than 5% (data not shown).

Fluorescence was monitored with a Synergy 2 Multi-Detection Microplate Reader using Gen5 Microplate Data Collection & Analysis software (BioTek Instruments Inc., VT, USA). The excitation was set to 390/20 nm and emission to 585/40 nm for the detection of 2-OH-ethidium. The unreacted DHE levels were measured at excitation 360/40 and emission 460/40. The plate was read from the bottom, and sensitivity of the photomultiplier tube was set to 70. The fluorescence measurements were performed either for 30 or 120 minutes. For each of the experiments, the final concentrations were 1.5 mU/mL, 0.25 mM, 100 U/mL and 5μM for XO, HX, catalase and DHE, respectively in a 300 μL volume. All fluorescence values were corrected for the background fluorescence that was measured in PBS with DHE in the absence of XO.

2.2.4 Superoxide production:

Superoxide production was measured by the widely used assay of rapid reduction of ferricytochrome c [78, 88]. Absorbance readings at 550 nm were collected every minute for 30 minutes and a molar extinction coefficient 21,000 $M^{-1}cm^{-1}$ was used to calculate superoxide production. The absorbance assay volume was 300 μL in PBS with reagents including XO (1.5 mU/mL), hypoxanthine (0.25 mM), catalase (100 U/mL), and ferricytochrome c (81 μM).

2.2.5 DHE and superoxide reaction kinetic analysis:

To understand the kinetics of the DHE and superoxide reaction, we modified the kinetic analysis from an earlier study by Zhao et al. [80] that used the competition kinetic analysis to provide a rate constant of 2.6×10^5 $M^{-1}s^{-1}$ for superoxide and DHE reaction. However, based on our fluorescence measurements and model predictions, we propose a much lower reaction rate for superoxide and DHE reaction as described in the results section.

We consider the following reactions occurring in the system.

i). The reaction between DHE and superoxide yields a fluorescent product at a rate constant of k_{DHE} (=2.6×10^5 $M^{-1}s^{-1}$ [80] or 1.1×10^3 $M^{-1}s^{-1}$ proposed in this study) as follows:

$$\mathrm{DHE} + \mathrm{O_2^{\cdot -}} \xrightarrow{k_{DHE}} \text{Fluorescent Product (F)} \quad (1)$$

ii). When SOD is present, the reaction between superoxide and SOD occurs at a rate constant of 3×10^9 $M^{-1}s^{-1}$ as follows:

$$\mathrm{H_2O} + \mathrm{O_2^{\cdot -}} \xrightarrow{\mathrm{SOD},\ k_{SOD}} \frac{1}{2}\mathrm{O_2} + \frac{1}{2}\mathrm{H_2O_2} + \mathrm{OH^-} \quad (2)$$

iii). We included the dismutation of superoxide in our analysis. Earlier studies have indicated that this reaction is negligible [80, 89]; we also analyzed the effect of this reaction on the predictions. The rate constant for dismutation of superoxide is 8×10^7 $M^{-1}s^{-1}$ and the reaction occurs as follows:

$$\mathrm{HO_2^{\cdot}} + \mathrm{O_2^{\cdot -}} + \mathrm{H^+} \xrightarrow{k_D} \mathrm{O_2} + \mathrm{H_2O_2} \quad (3)$$

Thus, the mass balance equation for the species of interests, $O_2^{\cdot -}$, and DHE, can be written as

$$\frac{dC_{o_2^{\cdot -}}}{dt} = S_{o_2^{\cdot -}} - k_{DHE} C_{DHE} C_{o_2^{\cdot -}} - k_{SOD} C_{SOD} C_{o_2^{\cdot -}} - k_D C_{HO_2^{\cdot}} C_{o_2^{\cdot -}}, \quad (4)$$

$$\frac{dC_{DHE}}{dt} = -k_{DHE} C_{DHE} C_{o_2^{\cdot -}} \quad (5)$$

Note that, i) $S_{o_2^{\cdot -}}$ (0.76 μM/min) is the rate of superoxide production in the system, and ii) rate can be simplified assuming a rapid equilibrium of $HO_2^{\cdot}/O_2^{\cdot -}$ with $C_{HO_2^{\cdot}} / C_{o_2^{\cdot -}} = 0.0025$ based on pK_a=4.8.

Equations 4 and 5 were solved using MatLab® with an initial concentration of 5 μM for DHE and 0 nM for superoxide.

2.2.6 Statistical analysis:

Three runs were performed for each assay and all values represent the mean ± std deviation. A paired two sample t-test was performed to determine significance between SOD and $^{\cdot}$NO treatments against no treatment. $P < 0.05$ was deemed as significant.

2.3 Results

2.3.1 Fluorescence measurements of 2-OH- ethidium (main product of superoxide and DHE reaction) and unreacted DHE

DHE and superoxide reaction was observed using XO, HX, catalase and DHE at concentrations of 1.5 mU/mL, 0.25 mM, 100 U/mL and 5μM, respectively in a 300 μL volume. Fluorescence measurements of 2-OH-ethidium (396/585 nm, ex/em) and unreacted DHE (360/460 nm, ex/em) were conducted. Figure 1a and b shows the accumulation of 2-OH-ethidium and the remaining unreacted DHE, respectively in solution over 120 minutes. Both increase in 2-OH-ethidium and decrease in unreacted DHE occurred linearly with a fluorescence rate of 38.62 and –39.19 RFU/min, respectively for up to 90 min. After 90 min unreacted DHE levels became zero, consequently fluorescence of 2-OH-ethidium plateaued.

To validate that the unreacted DHE levels became zero, we added SOD (1 U/ml) and spermine nonoate (10 μM) to reduce available superoxide level for DHE reaction. As seen in Figure 1, in the presence of SOD and NO, increase in 2-OH-ethidium and decrease in unreacted DHE kept changing linearly over 120 min. This shows that DHE was still available for reaction after 120 min. However, the 2-OH-ethidium fluorescence rate decreased to 21.60 and 15.85 RFU/min and the unreacted DHE fluorescence rate changed to –25.41 and –15.58 RFU/min for NO and SOD, respectively.

2.3.2 Kinetic analysis of DHE and superoxide reaction

Using k_{DHE} of 2.6×10^5 $M^{-1}s^{-1}$, and $S_{o_2^{\cdot-}}$ (superoxide production rate) of 0.76 μM/min, we solved the kinetic model of DHE and superoxide reaction represented by Eqs 4 and 5. The unreacted

DHE and superoxide concentration profiles are shown in Figure 2a. Superoxide reached a steady-state concentration of 250 nM. To our surprise, the unreacted DHE concentration in the solution reduced to zero (less than 1 nM) within the first 10 min (Figure 2a). Using k_{DHE} of 2.6×10^5 $M^{-1}s^{-1}$, the fluorescence cannot increase linearly for 90 min in this system, as we observed in our experiments. In addition, this establishes that DHE, not superoxide, is the limiting factor for the continuation of the reaction.

2.3.3 A slower reaction rate constant for DHE and superoxide reaction

Next, we analyzed whether the long-term linear increase in DHE fluorescence can be explained from a slower reaction rate constant for the DHE and superoxide reaction using kinetic analysis. For this purpose, we obtained the time at which the RFU value was 63.2% of the maximum fluorescence value (1722 RFU) for the 5 μM DHE concentration experiments shown in Figure 1. This corresponds to the one time constant response for a first order system. The time was 68 min. We performed kinetic analysis by reducing the reaction rate of DHE with superoxide. The reaction rate was found to be 1.01×10^3 $M^{-1}s^{-1}$ for which 1.84 μM unreacted DHE (shows reaction is 63.2% complete with 63.2% of DHE consumed) remained after 68 min. Figure 2a shows the predicted unreacted DHE concentration profiles for 5 and 10 μM initial DHE concentrations. As seen, the unreacted DHE concentration is 0.85 and 1.8 μM for 5 and 10 μM initial DHE concentrations, respectively after 120 min.

We also show the unreacted DHE profiles for a reaction rate constant of 2×10^3 $M^{-1}s^{-1}$. Figure 2b shows the profiles for 5 and 10 μM initial DHE concentrations. As seen, the profiles plateau earlier. The unreacted DHE concentrations were 0.70 and 1.6 μM at 68 min and 0.35 and 0.45 μM at 120 min for 5 and 10 μM initial DHE concentrations, respectively. This clarifies that even

at a high reaction rate constant of 2×10^3 $M^{-1}s^{-1}$, the amount of unreacted DHE remaining is small and may not be sufficient for a linear increase in the DHE fluorescence.

Thus, the proposed reaction rate constant for the DHE and superoxide reaction (k_{DHE}) is 1.01×10^3 $M^{-1}s^{-1}$, which is ~260× lower than the previously reported value of 2.6×10^5 $M^{-1}s^{-1}$ [80].

2.3.4 DHE fluorescence is completely inhibited at 10 U/ml SOD concentration

DHE fluorescence from superoxide was measured for SOD concentrations of 0, 1, 10, and 100 U/mL. DHE background fluorescence was measured in PBS in the absence of SOD and XOD. The background fluorescence was 522 ± 12 relative fluorescence units (RFU) (n = 3) and did not change with time due to the absence of superoxide generation. Figure 4a shows the measurement of DHE fluorescence over 30 minutes. The presence of XO and hypoxanthine in PBS, containing DHE and catalase but no SOD, produced a significantly higher value of 1873 ± 69 RFU (n = 3, $p < 0.05$) after 30 min. The increase in fluorescence was linear, indicating a steady-state system with constant and uninhibited formation of superoxide and its interaction with DHE.

As the concentrations of SOD increased, DHE fluorescence values decreased (Figure 4a). This indicates that SOD was reducing the concentration of superoxide in the solution. SOD concentrations as low as 1 U/mL significantly decreased DHE fluorescence ($p < 0.05$). For the 10 and 100 U/mL SOD concentrations, DHE fluorescence was significantly abolished ($p < 0.05$) and were similar to background values produced by DHE and PBS alone. Absence of catalase was without effect (data not shown). Figure 4b shows the rate of DHE fluorescence in RFU per minute for a given SOD concentration. For 0 and 1 U/mL SOD concentration, the rate of DHE fluorescence are 33 ± 3 and 10 ± 2 RFU/min, respectively. Thus, even a small amount of SOD can reduce the rate of DHE fluorescence by 70 percent. At high SOD concentrations (10 and 100

U/mL), the rate of DHE fluorescence was negligible. This lack of change in DHE fluorescence suggests that there was very low superoxide concentration in the system to react with DHE at any time during the assay, though there was superoxide production from XO and hypoxanthine system. This indicates that SOD concentration of 10 U/mL or higher, will be able to scavenge all superoxide produced in this system.

2.3.5 DHE fluorescence is reduced in presence of nitric oxide

The effects of nitric oxide presence on the DHE fluorescence of superoxide were assessed using spermine nonoate concentrations of 0, 1, 10, 100 and 1000 μM. DHE and PBS fluorescence was measured to establish a background control for the nitric oxide assay; results averaged 521 ± 7 RFU (n = 3). Hypoxanthine, XO, DHE, catalase and PBS resulted in a RFU value of 2077 ± 24 RFU (n = 3) after 30 min, indicating the production of superoxide by the enzymatic system. Figure 5a shows the DHE fluorescence change with time in the presence of spermine nonoate. DHE fluorescence was directly related to the concentration of spermine nonoate present in the system; as spermine nonoate concentrations increased, RFU values decreased. For every spermine nonoate concentration, the increase in DHE fluorescence was linear indicating a steady-state system with constant and uninhibited formation of superoxide. Absence of catalase was without effect (data not shown). After 30 min, DHE fluorescence decreased to 1731 ± 93 ($p < 0.05$), 1449 ± 59 ($p < 0.05$), 839 ± 16 ($p < 0.05$) and 584 ± 7 ($p < 0.05$) RFU for spermine nonoate concentrations of 1, 10, 100 and 1000 μM, respectively.

Figure 5b shows the rate of DHE fluorescence in RFU per minute for each spermine nonoate concentration (0, 1, 10, 100, 1000 μM). DHE fluorescence in the absence of spermine nonoate resulted in the fluorescence rate of 24.3 ± 2.6 RFU per minute. Addition of 1, 10, 100, and 1000

μM spermine nonoate reduced the rate of DHE fluorescence to 20.5 ± 0.2, 15.4 ± 0.5, 5.1 ± 0.3 and 0.4 ± 0.4 RFU/min, respectively, which represents a 16, 37, 79 and 98 percent reduction in RFU/min values over that of 0 U/mL spermine nonoate value, respectively. The relationship of DHE fluorescence rate with spermine nonoate concentration is $y = -1.95 \ln(x) + 19.76$ with $r^2 = 0.996$, where y is the RFU/min and x is the spermine nonoate concentration. Spermine nonoate significantly reduced the rate of DHE fluorescence.

2.3.6 Kinetic analysis of DHE and superoxide reaction in the presence of SOD

Previous studies have raised concern regarding the detection of superoxide using DHE in the presence of in vivo SOD concentration range of μM [79]. The reasoning behind the concern is that the reaction rate constant of the reaction of superoxide with DHE (k_{DHE} =2.6-4 × 10^5 $M^{-1}s^{-1}$) is 1,000 times lower than that of the reaction rate constant of superoxide with SOD (k=3 × 10^9 $M^{-1}s^{-1}$). We estimate an even lower reaction rate of DHE with superoxide. To understand the effect of this lower reaction rate constant of 1.01 × 10^3 $M^{-1}s^{-1}$ in our experiments, we used Equations 4 and 5 to solve for profiles of DHE and superoxide for the 1, 10 and 100 U/ml (or 0.011, 0.11, and 1.1 μM) SOD concentrations used in this study. For the lower reaction rate constant of 1.01 × 10^3 $M^{-1}s^{-1}$, superoxide concentrations reached steady state values of 706, 70.6, 7.06 pM within a few seconds for SOD concentrations of 1, 10 and 100 U/ml, respectively. After 60 min, DHE remained unconsumed at 5 μM concentrations for 10 and 100 U/ml SOD but reduced by 0.1 μM for 1 U/ml SOD concentration. When we used the reaction rate constant of 2.6 × 10^5 $M^{-1}s^{-1}$, superoxide concentrations reached steady state values of 680, 70.2 and 7.06 pM within a few seconds for SOD concentrations of 1, 10 and 100 U/ml, respectively. After 60 min, DHE concentrations were 2.67, 4.68 and 4.97 μM for SOD concentrations of 1, 10 and 100

U/ml, respectively. Thus, only the lower reaction rate constant can explain no change in measured RFU for 10 and 100 U/ml of SOD concentrations and a small change in RFU for 1 U/ml SOD concentration as measured in this study and reported in Figure 3.

2.4 Discussion

Nitric oxide and SOD are two efficient scavengers of superoxide in cells and tissue, rendering measurement of superoxide complicated. In this study, we demonstrate the level at which nitric oxide and SOD effect superoxide measurements using DHE fluorescence. Using kinetic analysis of the experiments, a DHE-superoxide reaction rate constant of 1.1×10^3 $M^{-1}s^{-1}$ is proposed.

2.4.1 Superoxide measurements

A predictable cell-free superoxide generating system was utilized to achieve reliable measurements of superoxide concentrations for in vitro study of SOD and nitric oxide interactions using a common fluorescence detection method. A range of SOD and nitric oxide concentrations were examined by introducing nitric oxide, via spermine nonoate donation, and SOD directly into a superoxide environment. The system is free from reactive species interference found in the in-vivo detection of superoxide, allowing for a more accurate analysis of species interactions. We confirmed that DHE fluorescence occurred at significant rates from superoxide generated by the hypoxanthine/xanthine oxidase system. The presence of SOD or nitric oxide will reduce superoxide concentration, which directly affects DHE fluorescence detection.

Currently, there is question in the literature regarding the accuracy of fluorescence detection of the DHE-superoxide reaction [90]. The authors suggest that HPLC analysis is the only reliable

method for measurement of DHE detection of superoxide. Results from this study confirm through the simultaneous detection of 2-OH-ethidium accumulation and monitoring of unreacted DHE in solution that fluorescence measurements are specific for that of the DHE-superoxide reaction product reported in the literature. Using microplate reader fluorescence detection, we found that the rate of 2-OH-ethidium formation was equal to that of the decrease in unreacted DHE levels in solution. Therefore, we conclude that by using appropriate excitation and emission filters fluorescence measurement of DHE is an accurate method for the detection of in vitro superoxide levels.

Studies investigating reactive oxygen species have used several different methods to measure superoxide concentration, including DHE fluorescence, cytochrome c absorbance, lucigenin chemiluminescence, and HPLC [77, 91-93]. Data presented in this study regarding the limitations of DHE measurements are in agreement with other studies. Due to the extremely short half-life of superoxide and rapid reaction with SOD, DHE fluorescence detection is prone to underestimation of actual superoxide production [90, 94]. Additionally, Papapostolou et al. showed that DHE can react with various oxidants found within the cell, including cytochrome hemes of the mitochondria [95]. Shao et al. also demonstrated that certain potent diet antioxidants can greatly decrease superoxide concentration even in extreme acute oxidative stress [96]. DHE fluorescence measurements can describe quantitative measurements of localized superoxide concentration. However, total superoxide production measurements are not possible as reported [76] and, at best, will be an estimate due to the varying amount of superoxide consumption among various interactions with other species. Further experimental and computational studies are needed for the calibration of DHE fluorescence with superoxide.

2.4.2 Justification of DHE-superoxide reaction rate constant of 1.1×10^3 $M^{-1}s^{-1}$

Based on experimental measurements and computational modeling, we report a reaction rate of ~1.1×10^3 $M^{-1}s^{-1}$ that is ~260× lower than the previously reported value of 2.6×10^5 $M^{-1}s^{-1}$ [9]. The possible reasons for the discrepancy include: i) our kinetic analysis is more detailed with respect to the actual reaction occurring in the system, ii) we considered the dismutation of superoxide which will increase superoxide consumption that was not considered in previous study, and iii) we did not assume saturating concentrations of DHE (compared to superoxide flux), as the previous study, model analysis (Figure 5) and experimental measurements (Figure 6) show that DHE is the limiting factor in its reaction with superoxide.

In the presence of SOD, the experimental results of no DHE fluorescence in this study were similar to the absence of oxyethidium peak formation at SOD concentration of 100 U/ml [97]. Additionally, the lower reaction rate constant 1.1×10^3 $M^{-1}s^{-1}$ can justify no observed DHE fluorescence in our experiments for SOD levels above 0.11 μM (10 U/mL), whereas the higher reaction rate constant of 2.6×10^5 $M^{-1}s^{-1}$ will still lead to significant DHE fluorescence for SOD levels above 0.11 μM (10 U/mL).

2.4.3 Effect of SOD concentration on superoxide presence

This study analyzed the concentration levels at which SOD effects detection of superoxide using an in vitro system. SOD catalyzes dismutation of superoxide within the vascular environment to help maintain healthy endothelial function [98]. In the case of DHE detection of superoxide, fluorescence decreased with increasing SOD concentration (see Figure 4a). At low SOD concentration of 0.011 μM (1 U/mL), change in DHE fluorescence per minute was reduced by 70 percent. Furthermore, DHE fluorescence was nearly abolished at SOD concentrations above

0.11 μM (10 U/mL). Fink, et al. [97] reported similar findings using an endothelial cell model, with SOD completely eliminating induced superoxide formation due to angiotensin II administration. This data indicates that DHE measurements of superoxide production may be highly underestimated even in the presence of relatively low SOD competition. New evidence has also shown that apocynin may directly inhibit superoxide, much like SOD, rather than indirectly decrease its levels through the inhibition of NADPH-oxidase [99, 100]. Furthermore, other research has shown that apocynin is potentially a pro-oxidant, leading to the increased production of superoxide in endothelial cells [101]. In addition, the scavenging efficiency of vascular antioxidant systems in maintaining healthy blood flow and reactive oxygen species levels further complicates the accurate analysis of superoxide production [82]. Dependent on experimental conditions such as hypoxia, inflammation, atherosclerosis, SOD expression may up or down-regulate within the vascular environment and may vary widely on a spatial level [102, 103]. Consequently, DHE fluorescence can describe localized superoxide concentration rather than vascular superoxide production.

2.4.4 Effect of nitric oxide on superoxide concentrations

Nitric oxide is released from the endothelium in response to stimuli such as superoxide concentration increases in the vascular environment. However, in the case of oxidative stress, superoxide concentrations are elevated beyond effective nitric oxide levels [81]. Our objective was to evaluate the level at which nitric oxide influences the detection of superoxide production. Selemidis, et al. [77] reports that an increase in nitric oxide donor concentrations led to a dramatic decrease in superoxide production as measured by DHE fluorescence in endothelial cells. We show that in vitro DHE fluorescence measurement of superoxide significantly

decreased in the presence of nitric oxide. Spermine nonoate concentrations as low as 1 µM significantly decreased superoxide detection while 1 mM concentrations completely abolished DHE measurement (See Figure 5a). Cosentino reports that hyperglycemia upregulates the expression of nitric oxide synthase [85]. This may lead to local elevation of nitric oxide, however, spatial nitric oxide concentrations will vary widely. Consequently, dependent upon the nitric oxide environment of a given sample DHE superoxide production measurements may be over- or underestimated. A more accurate description of superoxide production may require DHE measurement in relation to nitric oxide, peroxynitrite and SOD concentrations in a given sample.

2.4.5 Pathological Implications of SOD and nitric oxide interactions

A complete understanding of species interactions is critical for reducing the risk of numerous disease pathologies. Concentrations of reactive oxygen species, such as superoxide, are tightly regulated in the normal functioning vascular system [98]. However, accumulation of superoxide within the vasculature, termed as oxidative stress, contributes to the development of a number of diseases, such as atherosclerosis, diabetes, and dyslipidemia [104, 105]. As superoxide concentrations increase, excess molecules react with nitric oxide to form the cytotoxic chemical peroxyntirite and effectively decrease the bioavailability of nitric oxide [106]. Consequently, a reliable method for quantifying superoxide levels is highly desirable. However, presently there is no method that will describe superoxide production without the problem of interference. Data presented in this study demonstrate that a full understanding of the competition between SOD, nitric oxide, and superoxide interactions are critical when using DHE fluorescence methods for in vivo measurements.

2.5 Conclusions

An accurate method for superoxide measurement would be highly beneficial to the potential diagnosis and treatment of a number of different health problems. The current study describes some of the necessary considerations for experimental measurement and analysis of superoxide concentrations in the presence of SOD and nitric oxide. DHE measurement of superoxide in conjunction with the relative amount of nitric oxide, SOD and peroxynitrite present may provide a more accurate description of oxidative stress. A detailed kinetic analysis resulted in a DHE and superoxide reaction rate constant of ~1.1×10^3 $M^{-1}s^{-1}$ that is ~260× lower than the previously reported value of 2.6×10^5 $M^{-1}s^{-1}$. The lower reaction rate constant can explain a lack of DHE fluorescence in the presence of SOD.

Acknowledgements

This study was supported by AHA grant # 0530050N and NIH grant # R01 HL084337.

Abbreviations

DHE Dihydroethidium

$^{\bullet}$NO Nitric oxide

PBS Phosphate buffer solution

SOD Superoxide dismutase

XO Xanthine oxidase

2.6 References

[1] C.D. Georgiou, I. Papapostolou, N. Patsoukis, T. Tsegenidis, T. Sideris, An ultrasensitive fluorescent assay for the in vivo quantification of superoxide radical in organisms, Anal Biochem 347 (2005) 144-151.

[2] S. Selemidis, G.J. Dusting, H. Peshavariya, B.K. Kemp-Harper, G.R. Drummond, Nitric oxide suppresses NADPH oxidase-dependent superoxide production by S-nitrosylation in human endothelial cells, Cardiovasc Res 75 (2007) 349-358.

[3] T.M. Paravicini, R.M. Touyz, NADPH oxidases, reactive oxygen species, and hypertension: clinical implications and therapeutic possibilities, Diabetes Care 31 Suppl 2 (2008) S170-180.

[4] K.R. Messner, J.A. Imlay, In vitro quantitation of biological superoxide and hydrogen peroxide generation, Methods Enzymol 349 (2002) 354-361.

[5] F.R. Laurindo, D.C. Fernandes, C.X. Santos, Assessment of superoxide production and NADPH oxidase activity by HPLC analysis of dihydroethidium oxidation products, Methods Enzymol 441 (2008) 237-260.

[6] H. Zhao, S. Kalivendi, H. Zhang, J. Joseph, K. Nithipatikom, J. Vasquez-Vivar, B. Kalyanaraman, Superoxide reacts with hydroethidine but forms a fluorescent product that is distinctly different from ethidium: potential implications in intracellular fluorescence detection of superoxide, Free Radic Biol Med 34 (2003) 1359-1368.

[7] H.M. Peshavariya, G.J. Dusting, S. Selemidis, Analysis of dihydroethidium fluorescence for the detection of intracellular and extracellular superoxide produced by NADPH oxidase, Free Radic Res 41 (2007) 699-712.

[8] M.M. Tarpey, D.A. Wink, M.B. Grisham, Methods for detection of reactive metabolites of oxygen and nitrogen: in vitro and in vivo considerations, Am J Physiol Regul Integr Comp Physiol 286 (2004) R431-444.

[9] M.M. Hartge, T. Unger, U. Kintscher, The endothelium and vascular inflammation in diabetes, Diab Vasc Dis Res 4 (2007) 84-88.

[10] H.A. Hadi, J.A. Suwaidi, Endothelial dysfunction in diabetes mellitus, Vasc Health Risk Manag 3 (2007) 853-876.

[11] A. Ceriello, P. dello Russo, P. Amstad, P. Cerutti, High glucose induces antioxidant enzymes in human endothelial cells in culture. Evidence linking hyperglycemia and oxidative stress, Diabetes 45 (1996) 471-477.

[12] F. Cosentino, K. Hishikawa, Z.S. Katusic, T.F. Luscher, High glucose increases nitric oxide synthase expression and superoxide anion generation in human aortic endothelial cells, Circulation 96 (1997) 25-28.

[13] H. Zhao, J. Joseph, H.M. Fales, E.A. Sokoloski, R.L. Levine, J. Vasquez-Vivar, B. Kalyanaraman, Detection and characterization of the product of hydroethidine and intracellular superoxide by HPLC and limitations of fluorescence, Proc Natl Acad Sci U S A 102 (2005) 5727-5732.

[14] K.M. Robinson, M.S. Janes, M. Pehar, J.S. Monette, M.F. Ross, T.M. Hagen, M.P. Murphy, J.S. Beckman, Selective fluorescent imaging of superoxide in vivo using ethidium-based probes, Proc Natl Acad Sci U S A 103 (2006) 15038-15043.

[15] V. Massey, The microestimation of succinate and the extinction coefficient of cytochrome c, Biochim Biophys Acta 34 (1959) 255-256.

[16] J. Vasquez-Vivar, J. Whitsett, P. Martasek, N. Hogg, B. Kalyanaraman, Reaction of tetrahydrobiopterin with superoxide: EPR-kinetic analysis and characterization of the pteridine radical, Free Radic Biol Med 31 (2001) 975-985.

[17] J. Zielonka, B. Kalyanaraman, Hydroethidine- and MitoSOX-derived red fluorescence is not a reliable indicator of intracellular superoxide formation: another inconvenient truth, Free Radic Biol Med 48 983-1001.

[18] C.A. Papaharalambus, K.K. Griendling, Basic mechanisms of oxidative stress and reactive oxygen species in cardiovascular injury, Trends Cardiovasc Med 17 (2007) 48-54.

[19] S. Dikalov, K.K. Griendling, D.G. Harrison, Measurement of reactive oxygen species in cardiovascular studies, Hypertension 49 (2007) 717-727.

[20] D.C. Fernandes, J. Wosniak, Jr., L.A. Pescatore, M.A. Bertoline, M. Liberman, F.R. Laurindo, C.X. Santos, Analysis of DHE-derived oxidation products by HPLC in the assessment of superoxide production and NADPH oxidase activity in vascular systems, Am J Physiol Cell Physiol 292 (2007) C413-422.

[21] J. Zielonka, J. Vasquez-Vivar, B. Kalyanaraman, Detection of 2-hydroxyethidium in cellular systems: a unique marker product of superoxide and hydroethidine, Nat Protoc 3 (2008) 8-21.

[22] J. Zielonka, M. Hardy, B. Kalyanaraman, HPLC study of oxidation products of hydroethidine in chemical and biological systems: ramifications in superoxide measurements, Free Radic Biol Med 46 (2009) 329-338.

[23] I. Papapostolou, N. Patsoukis, C.D. Georgiou, The fluorescence detection of superoxide radical using hydroethidine could be complicated by the presence of heme proteins, Anal Biochem 332 (2004) 290-298.

[24] Z.H. Shao, J.T. Xie, T.L. Vanden Hoek, S. Mehendale, H. Aung, C.Q. Li, Y. Qin, P.T. Schumacker, L.B. Becker, C.S. Yuan, Antioxidant effects of American ginseng berry extract in cardiomyocytes exposed to acute oxidant stress, Biochim Biophys Acta 1670 (2004) 165-171.

[25] B. Fink, K. Laude, L. McCann, A. Doughan, D.G. Harrison, S. Dikalov, Detection of intracellular superoxide formation in endothelial cells and intact tissues using dihydroethidium and an HPLC-based assay, Am J Physiol Cell Physiol 287 (2004) C895-902.

[26] R.J. Esper, R.A. Nordaby, J.O. Vilarino, A. Paragano, J.L. Cacharron, R.A. Machado, Endothelial dysfunction: a comprehensive appraisal, Cardiovasc Diabetol 5 (2006) 4.

[27] S. Heumuller, S. Wind, E. Barbosa-Sicard, H.H. Schmidt, R. Busse, K. Schroder, R.P. Brandes, Apocynin is not an inhibitor of vascular NADPH oxidases but an antioxidant, Hypertension 51 (2008) 211-217.

[28] R.M. Touyz, Apocynin, NADPH oxidase, and vascular cells: a complex matter, Hypertension 51 (2008) 172-174.

[29] M. Vejrazka, R. Micek, S. Stipek, Apocynin inhibits NADPH oxidase in phagocytes but stimulates ROS production in non-phagocytic cells, Biochim Biophys Acta 1722 (2005) 143-147.

[30] S. Dimmeler, C. Hermann, J. Galle, A.M. Zeiher, Upregulation of superoxide dismutase and nitric oxide synthase mediates the apoptosis-suppressive effects of shear stress on endothelial cells, Arterioscler Thromb Vasc Biol 19 (1999) 656-664.

[31] M. Horiuchi, M. Tsutsui, H. Tasaki, T. Morishita, O. Suda, S. Nakata, S. Nihei, M. Miyamoto, R. Kouzuma, M. Okazaki, N. Yanagihara, T. Adachi, Y. Nakashima, Upregulation of vascular extracellular superoxide dismutase in patients with acute coronary syndromes, Arterioscler Thromb Vasc Biol 24 (2004) 106-111.

[32] A. Ceriello, Possible role of oxidative stress in the pathogenesis of hypertension, Diabetes Care 31 Suppl 2 (2008) S181-184.

[33] J.D. Cohen, Overview of physiology, vascular biology, and mechanisms of hypertension, J Manag Care Pharm 13 (2007) S6-8.

[34] T. Munzel, C. Sinning, F. Post, A. Warnholtz, E. Schulz, Pathophysiology, diagnosis and prognostic implications of endothelial dysfunction, Ann Med 40 (2008) 180-196.

Figure Legends

Figure 1. Experimental reaction profile for DHE fluorescence detection of superoxide for 120 minutes. (a) Results shown are for fluorescence detection of the DHE (5μM) and superoxide reaction product 2-OH ethidium using a microplate reader set at excitation 390/20 nm and emission 585/20. A cell-free XO/hypoxanthine system was used to generate superoxide and readings were taken every 2 minutes for 120 minutes. Detection of superoxide using DHE increases linearly until saturation of the dye occurs at approximately the 100 minute reading. (b) Data shows the fluorescence monitoring of the unreacted portion of DHE, excitation 360/40 and emission 460/40, remaining in solution at each time point. The amount of unreacted DHE in the system decreases linearly until being quenched at approximately 100 minutes.

Figure 2. Unreacted DHE concentration profiles using kinetic analysis. a). The DHE concentration profiles are shown for 5 and 10 μM initial DHE concentrations for 120 min for a reaction rate of (k_{DHE}) 1.01×10^3 $M^{-1}s^{-1}$. We performed kinetic analysis by reducing the reaction rate of DHE with superoxide to better fit the experimental observation of DHE fluorescence in Figure 6. We obtained the time (=68 min) at which the RFU value was 63.2% of the maximum fluorescence value (1722 RFU) for 5 μM DHE concentration experiments in Figure 6 (which corresponds to one time constant response for a first order system). The reaction rate for which 1.84 μM unreacted DHE (63.2 % of DHE consumed) was at 68 min was 1.01×10^3 $M^{-1}s^{-1}$. The superoxide concentrations reached steady-state concentration of 250 nM not shown. b). The DHE concentration profiles for a higher reaction rate of (k_{DHE}) 2.0×10^3 $M^{-1}s^{-}$

[1] is shown for 5 and 10 μM initial DHE concentrations for 120 min. Note that, the DHE concentration fall more sharply and reach a plateau at an earlier time points.

Figure 3. Superoxide and DHE concentration profiles using kinetic Analysis. The reaction rate constant of DHE and superoxide reaction used was 2.6×10^5 $M^{-1}s^{-1}$. The superoxide concentration reached a steady-state concentration of 250 nM. The unreacted DHE concentration in the solution reduced to less than 1 nM within first 10 min. This indicates that DHE fluorescence cannot increase linearly over 30 min in experimental measurement as seen in Figure 1.

Figure 4. Fluorescence of DHE for the reaction of hypoxanthine with XO in the presence of SOD. (a). The results shown are for SOD concentrations of 1, 10, and 100 U/mL with a total run time of 30 minutes (n = 3). DHE fluorescence of superoxide was measured using a microplate reader and cell-free XO/hypoxanthine system. RFU values were inversely proportional to SOD concentrations. (b)**.** The data represents the average change in DHE fluorescence per minute for the reaction of hypoxanthine with XO in the presence of catalase and SOD. Values were calculated by taking the slope of the linear-fit curve for each fluorescence readings.

Figure 5. Fluorescence of DHE for the reaction of hypoxanthine with XO in the presence of nitric oxide. (a). The data shows DHE fluorescence for superoxide detection in the presence of SPERMINE NONOATE (n = 3). Fluorescence was measured using a microplate reader and best-fit lines were calculated based on linear-regression. (b). The results shown represent the change in RFU per minute for each measured nitric oxide concentration. Values were calculated by plotting the slopes for each of the nitric oxide concentrations.

Figure 6. Measurement of DHE fluorescence at 5 and 10 μM initial DHE concentrations for 120 min. The increase in RFU plateaus around 100 min for the 5 μM initial DHE concentration but remains increasing for 10 μM DHE.

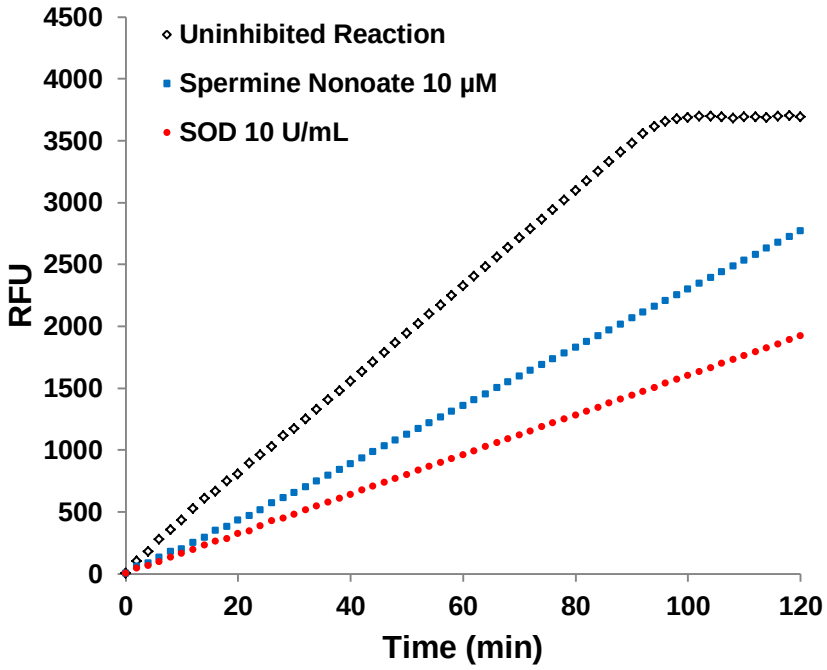
Uninhibited Reaction
Spermine Nonoate 10 µM
SOD 10 U/mL
RFU
4500
4000
3500
3000
2500
2000
1500
1000
500
0
0
20
40
60
80
100
120
Time (min)

Figure 1a

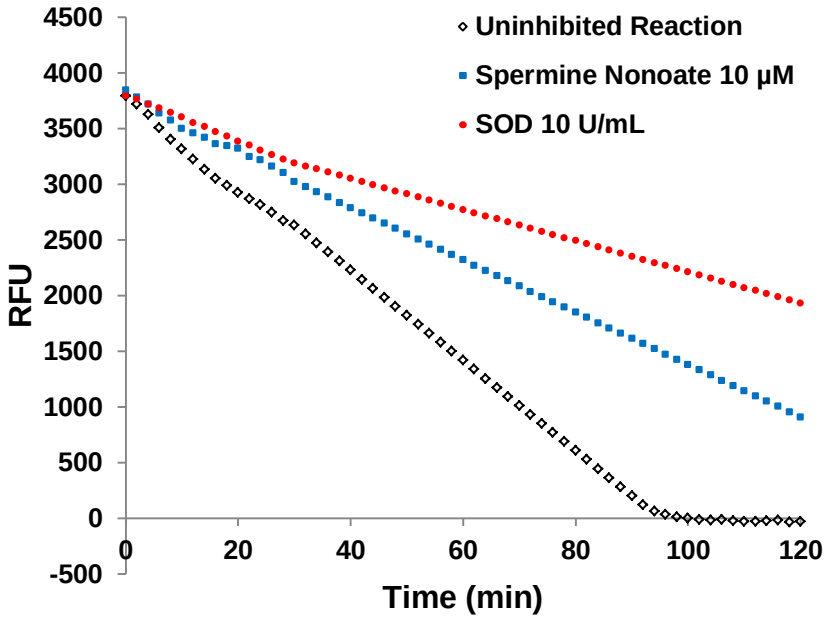
Uninhibited Reaction
Spermine Nonoate 10 µM
SOD 10 U/mL
RFU
4500
4000
3500
3000
2500
2000
1500
1000
500
0
-500
0
20
40
60
80
100
120
Time (min)

Figure 1b

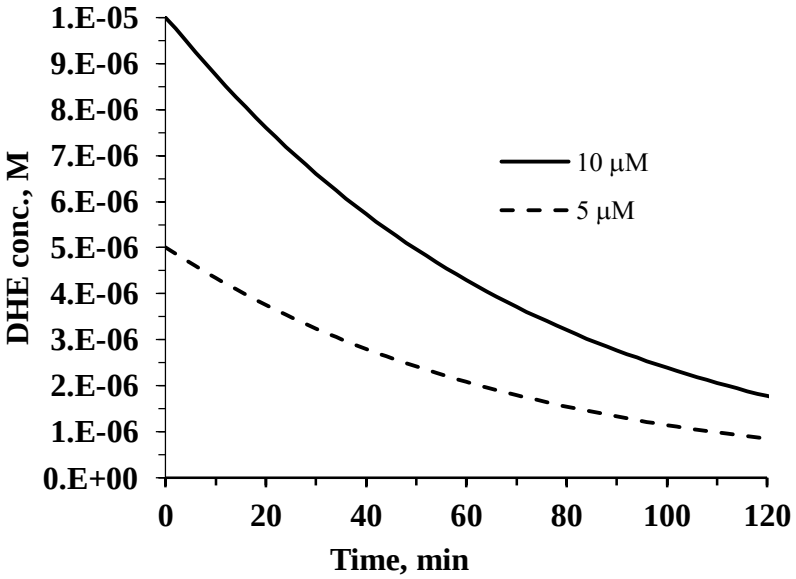
1.E-05
9.E-06
8.E-06
7.E-06
6.E-06
5.E-06
4.E-06
3.E-06
2.E-06
1.E-06
0.E+00
DHE conc., M
0
20
40
60
80
100
120
Time, min
10 μM
5 μM

Figure 2a

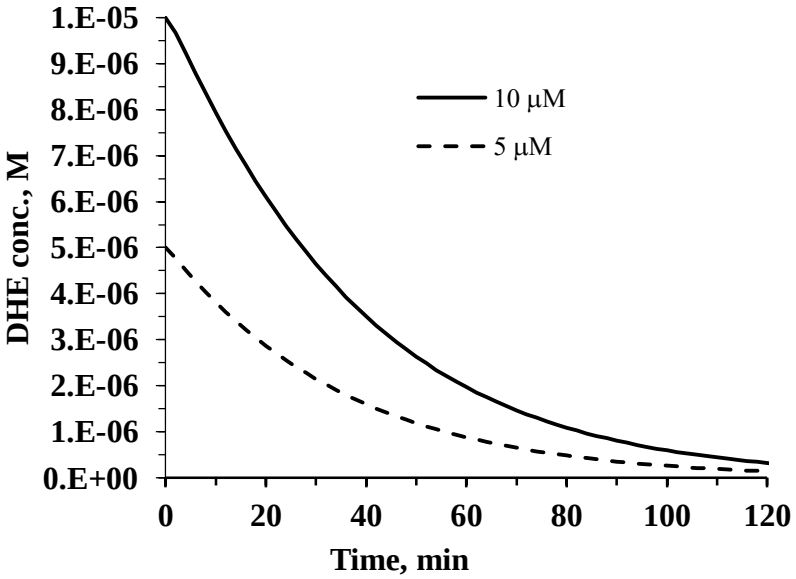
1.E-05
9.E-06
8.E-06
7.E-06
6.E-06
5.E-06
4.E-06
3.E-06
2.E-06
1.E-06
0.E+00
DHE conc., M
10 μM
5 μM
0
20
40
60
80
100
120
Time, min

Figure 2b

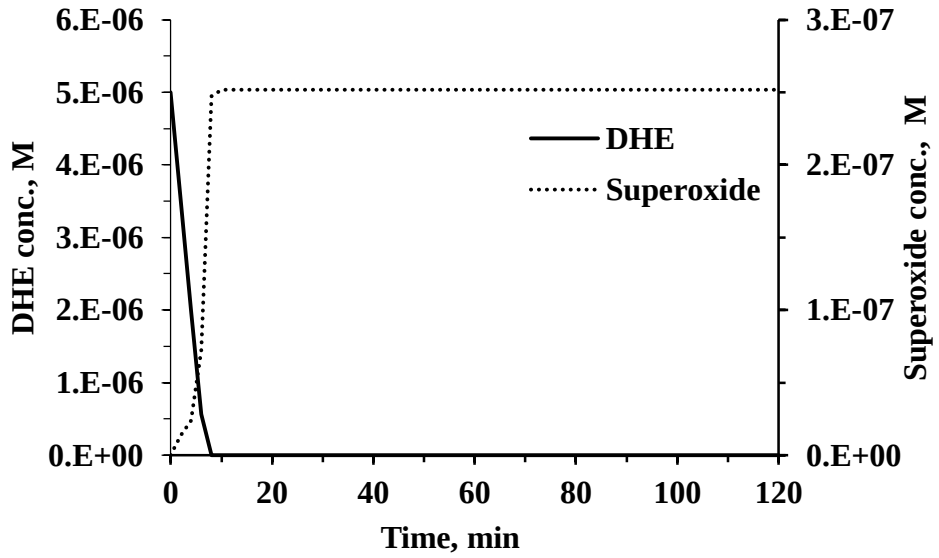
6.E-06
5.E-06
4.E-06
3.E-06
2.E-06
1.E-06
0.E+00
DHE conc., M
3.E-07
2.E-07
1.E-07
0.E+00
Superoxide conc., M
DHE
Superoxide
0
20
40
60
80
100
120
Time, min

Figure 3

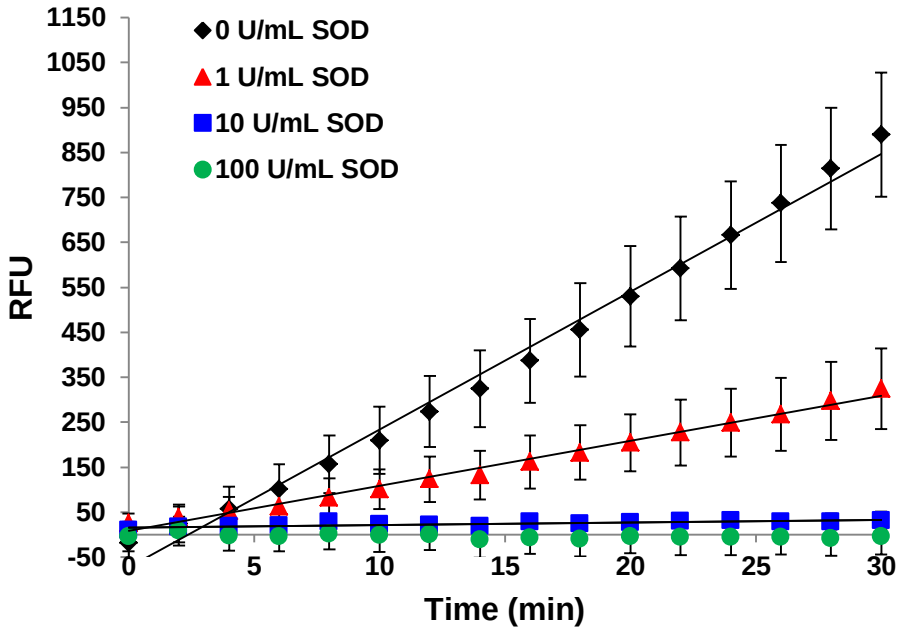
0 U/mL SOD
1 U/mL SOD
10 U/mL SOD
100 U/mL SOD
RFU
1150
1050
950
850
750
650
550
450
350
250
150
50
-50
0
5
10
15
20
25
30
Time (min)

Figure 4a

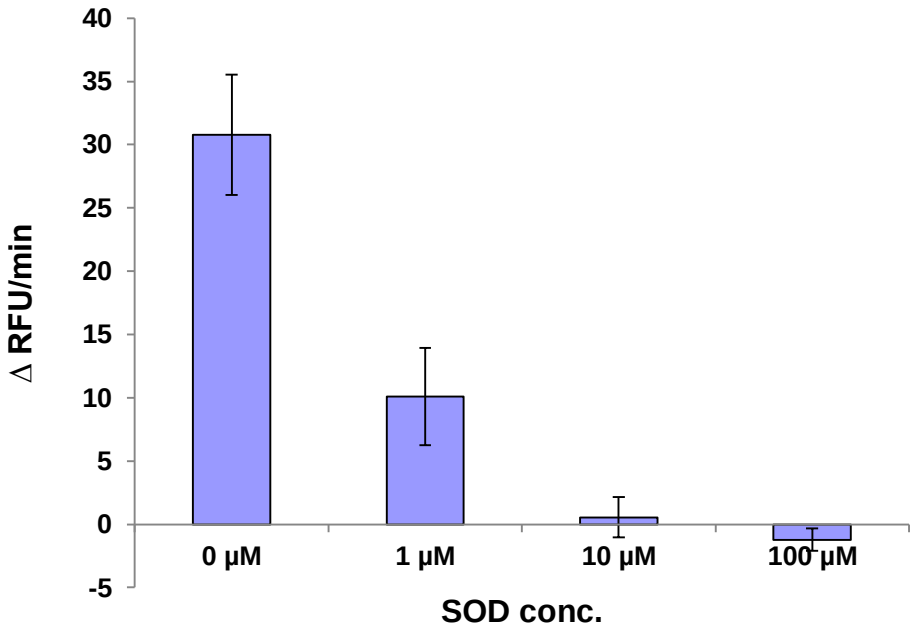

Figure 4b

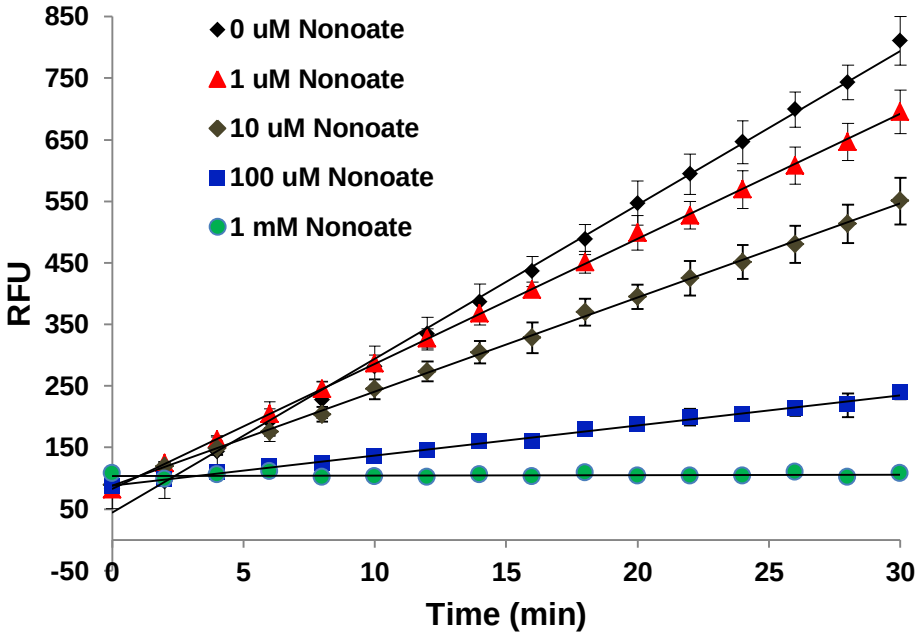
0 uM Nonoate
1 uM Nonoate
10 uM Nonoate
100 uM Nonoate
1 mM Nonoate
RFU
850
750
650
550
450
350
250
150
50
-50
0
5
10
15
20
25
30
Time (min)

Figure 5a

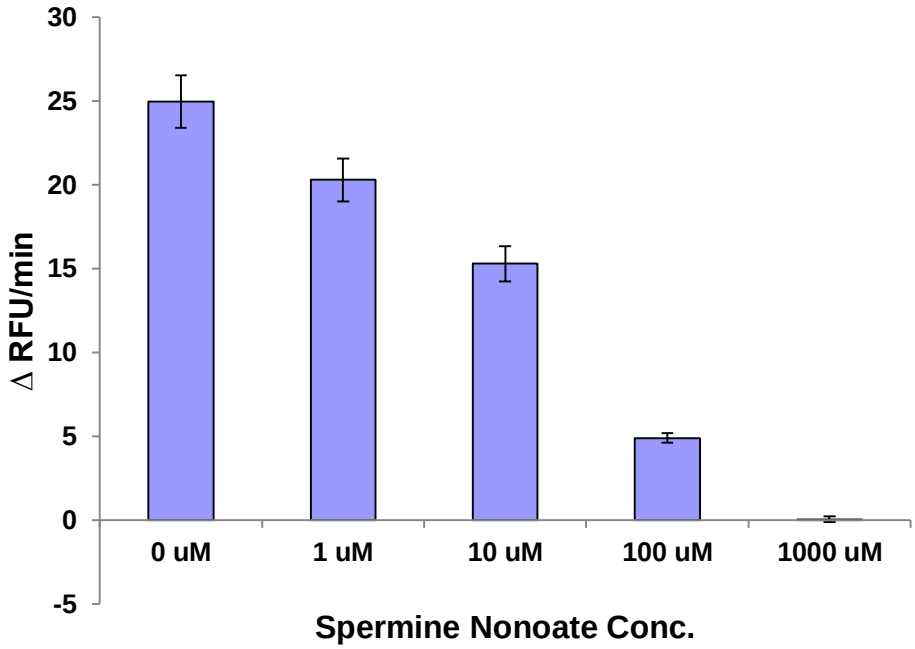
30
25
20
15
10
5
0
-5
Δ RFU/min
0 uM
1 uM
10 uM
100 uM
1000 uM
Spermine Nonoate Conc.

Figure 5b

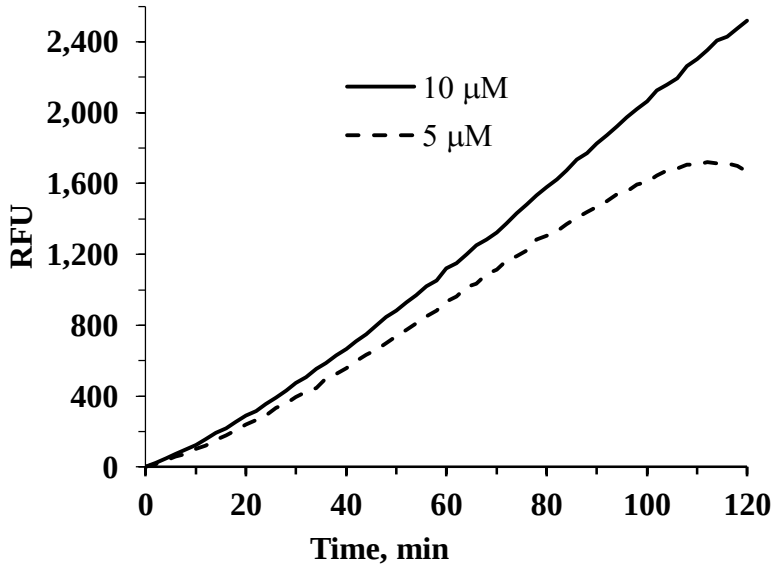
2,400
2,000
1,600
1,200
800
400
0
RFU
10 μM
5 μM
0
20
40
60
80
100
120
Time, min

Figure 6

CHAPTER 3

Mechanistic Study of Nitrosative and Oxidative Stress in High Glucose Exposed HUVEC's

Abstract (250 words)

Pathogenesis of diabetes-related vascular complications involves progression of oxidative and nitrosative stress, leading to endothelial dysfunction and cell death. A major characteristic of hyperglycemia is increased reactive oxygen species. Superoxide interacts readily with nitric oxide to form the cytotoxic oxidant peroxynitrite. This leads to formation of nitrated proteins, reduction of BH_4/BH_2 ratios and nitric oxide levels, and activation of apoptotic caspase pathways. In this study, we examine the effect of high glucose on endothelial superoxide, and nitric oxide levels, nitrotyrosine and apoptosis. HUVECs were exposed to 1, 24 and 48 hour control (5 mM) and high glucose (25 mM) conditions in the presence of L-NAME (100 μM), apocynin (300 μM), or SOD (100 units/ml). Fluorescence dyes dihydroethidium and DAF-FM DA were used to detect superoxide and nitric oxide, respectively. Nitrotyrosine formation was measured using competitive ELISA and immunocytofluorescence. Apoptosis was measured using Hoechst 33342 fluorescence. Results showed that 48 hour high glucose exposure upregulates NADPH oxidase activation, leading to 87% increase in intracellular superoxide levels and 32% decrease in nitric oxide bioavailability. Additionally, results show that nitric oxide production is increased 28% in high glucose exposed endothelial cells. HUVEC's exposed to high glucose for 24 hours show 62% increase in nitrotyrosine levels compared to that of normal glucose cells. Finally, our results suggest that increased production of peroxynitrite and decreased nitric oxide levels induces significant apoptosis via caspase denitroslyation. Inhibition of NADPH oxidase activity lead to restoration of nitric oxide bioavailability and reduction of hyperglycemia induced apoptosis. The results indicate that treatment strategies towards reducing NADPH oxidase activity and increasing nitric oxide levels will help reverse the damaging effects of high glucose on endothelial cells.

Key Words

Diabetes, Hyperglycemia, Endothelial cells, Nitrosative stress, Oxidative stress, Endothelial dysfunction

3.1 Introduction

Current literature supports that nitrosative and oxidative stress are strongly involved in endothelial dysfunction and the pathogenesis of diabetes [42, 107, 108]. This stress condition is characterized by the imbalance between free radical production and available antioxidants in vasculature tissue. It is widely accepted that the pathologic pathway is facilitated by a loss in nitric oxide bioavailability, mediated by increased superoxide production [109, 110]. A hallmark of diabetic vascular disease is reduction or loss of nitric oxide activity, leading to poor vessel tone and inflammation [111]. Furthermore, nitrosative stress leads to increased nitration/nitrosylation events, resulting in cell damage and activation of apoptosis signaling cascades [14]. A number of enzymatic sources of superoxide exist within endothelial cells such as NADPH oxidase, mitochondrial electron transport chain, xanthine oxidase, cyclooxygenase and uncoupled endothelial nitric oxide synthase (eNOS) [112]. However, the significance, involvement and contribution of these enzymes in nitrosative and oxidative stress are still not completely understood.

In the vasculature, eNOS production of nitric oxide is an important regulator of physiological vessel tone and inflammation [113]. During normal conditions, nitric oxide production occurs at low, basal levels as a pro-life molecule and to facilitate important signaling events. Stress induces an increase in reactive oxygen and nitrogen species, leading to decreased nitric oxide bioavailability and increased cell damage/death [114, 115]. Decreased eNOS-derived nitric oxide bioavailability and endothelial dysfunction are hallmarks for a number of vascular pathologies such as diabetes, atherosclerosis and hypertension [116, 117]. While the mechanistic basis for reduced nitric oxide bioavailability is uncertain, both slowed nitric oxide synthesis and accelerated nitric oxide scavenging by reactive oxygen species (ROS), such as superoxide, have

been implicated as pathogenic [118]. In contrast, levels of eNOS protein are typically unchanged or paradoxically increased. Additionally, our lab has previously predicted that nitric oxide production concomitantly increases along with superoxide in response to high glucose exposure [12].

Oxidative stress, due to excessive superoxide generation, is thought to underlie and trigger the development of endothelial dysfunction in chronic vascular conditions as seen in diabetes [62]. According to Paravinci, NADPH oxidase is a multi-subunit enzyme that catalyzes O_2^- production by the 1-electron reduction of O_2 using NADPH or NADH as the electron donor: $2O_2 + NADPH \rightarrow 2 \cdot O_2^- + NADP^+ + H^+$. NADPH oxidase was originally found in neutrophils and the basic enzyme structure has five subunits: p47phox, p67phox, p40phox, p22phox, and the catalytic subunit gp91phox (also termed "Nox2") [38, 119]. Inactive NOX enzymes exist as unincorporated protein structures with the subunits, p47phox, p67phox, and p40phox in the cytosol. Only p22phox and gp91phox are found in the membrane, as a heterodimeric protein referred to as cytochrome b558. When the cell is exposed to sufficient stimuli, phosphorylation of p47phox acts as the activator and the remaining cytosolic subunits form a complex that translocates to the membrane. Translocation to the membrane results in the association of the cytosolic subunits with the existing cytochrome b558 unit to assemble the active oxidase, which transfers electrons from the substrate to O_2, forming $\cdot O_2^-$ [120]. Additionally, activation of the NOX enzyme requires the presence and activity of co-factors such as Rac (1 or 2) and Rap 1A [121, 122]. Among the different enzymatic sources of ROS reported to be activated by hyperglycemia, NADPH oxidase appears to play a major role. Higher vascular NADPH oxidase activity has been detected in diabetic patients and, more importantly, endothelial NADPH oxidase activity is markedly increased by high glucose levels [123]. Therefore, focusing on

mechanisms leading to NADPH oxidase activation may reveal further molecular details involved in diabetes-induced vascular injury.

Uncoupled eNOS represents another potentially important enzymatic generator of superoxide in hyperglycemic conditions. A deficiency of 5,6,7,8-tetrahydrobiopterin (BH_4) results in eNOS uncoupling, which is associated with increased superoxide and decreased $NO^{\bullet}$ production. BH_4 is an essential cofactor of eNOS and its oxidation in the setting of diabetes and other chronic vasoinflammatory conditions can cause reduced cofactor availability and uncoupling of eNOS [17, 124]. Hyperglycemia-induced superoxide production may lead to increased interactions with NO and elevated peroxynitrite (ONOO-) levels. BH_4 has been suggested as a target for oxidation by $ONOO^{-}$, a product of the superoxide and nitric oxide reaction. The immediate product of the reaction between ONOO- and BH_4 is the trihydrobiopterin radical (BH_3) which is further oxidized to 7,8-dihydrobiopterin (BH_2). Studies have shown that the ratio of BH_4 and BH_2 is an important indicator of the level of eNOS uncoupling [17].

Identification of the complete major enzymatic biochemical pathways associated with hyperglycemia induced oxidative stress may potentially lead to novel diabetic drug treatment therapies. Furthermore, clarification of the early stages of enzymatic pathway activation due to high glucose stimulation in endothelial cells would be of importance in understanding diabetic vascular pathology. The aim of this study is to quantify the contribution levels of NADPH oxidase and eNOS towards excess intracellular superoxide presence and decreased nitric oxide bioavailability. Additionally, we quantify the downstream cellular effects of superoxide-nitric oxide interactions through the measurement of nitrotyrosine, an indirect marker of peroxynitrite. Lastly, we investigate the impact of high glucose exposure on endothelial cell death. Overall, our focus is on the level of enzymatic involvement in the initiation of these nitrosative and oxidative

stress pathways in hyperglycemia. We specifically show that short-term hyperglycemia causes increased intracellular superoxide and decreased nitric oxide presence in HUVEC's. NADPH oxidase appears to contribute the greatest portion of superoxide generation. Furthermore, nitric oxide bioavailability is greatly reduced in hyperglycemic cells, apparently from increased superoxide interaction and uncoupled eNOS.

3.2 Materials and Methods

3.2.1 Materials

Pooled HUVEC's, trypsin-EDTA, trypsin neutralizing solution (TNS), HEPES, phenol red-free EBM and EGM-2 bullet kits were obtained from Lonza (Walkersville, PA). Glucose, SOD, apocynin, and L-NAME were purchased from Sigma-Aldrich (St. Louis, MO). Hoechst 33342, DHE, DAF-FM diacetate, Alexa-594 goat anti-rabbit secondary antibody and DAPI nuclear staining probe were acquired from Invitrogen Molecular Probes (Carlsbad, California). Nitrotyrosine ELISA kit and nitrotyrosine monoclonal rabbit primary antibody were obtained from Millipore (Billerica, MA).

3.2.2 Human Umbilical Vein Endothelial Cell Culture and Treatment Incubation

Pooled primary cell line HUVEC's were cultured in BD falcon 75 cm^2 flasks containing EGM-2 supplemented with 2% heat irradiated fetal bovine serum. The culture flasks were incubated at 37°C in 5% CO_2. Primary cultures were fluid changed 24 hours after seeding and were subcultured upon reaching 80-90% confluence by the use of 0.25% trypsin-EDTA, inactivated by TNS. Only passages 2-4 were used in the study to avoid passage-dependent cellular

modifications. Upon confluency HUVEC's were passaged and seeded at equal density (1 x 10^4 per well) onto BD Falcon 96 well microplates and allowed to attach overnight in fresh growth media. Once confluent, fresh basal media was then added and treated HUVEC's were incubated with 25mM high glucose for 1, 24 or 48 hours. After glucose treatment cells were then incubated for 1 hour with each respective enzymatic inhibitor or superoxide scavenger; L-NAME (100 μM), apocynin (300 μM), or SOD (100 units/ml). Treated basal media was then removed from the well and replaced with phenol-red free basal media to avoid possible fluorescence measurement interference. Cells were then incubated with either 5 μM DHE or 5 μM DAF-FM diacetate for 20 minutes for the measurement of superoxide and NO respectively. Basal media containing either DHE or DAF-FM diacetate was then aspirated from the well and the cells were washed three times with phenol-red free EBM to remove any extracellular fluorescence presence. Fresh phenol-red free media and all respective chemical treatments were added back into each well before fluorescence detection. Osmotic control was assured by incubating HUVEC's with 25mM mannitol for 1, 24 or 48 hours.

3.2.3 Fluorescence Measurement of Superoxide and NO Presence

Fluorescence of DHE and DAF-FM diacetate was monitored with a Synergy 2 Multi-Detection Microplate Reader using Gen5 Microplate Data Collection & Analysis software (BioTek Instruments Inc., VT, USA). The fluorescence software was programmed to collect readings every two minutes for 30 minutes. For DHE detection of intracellular superoxide the excitation was set to 485/20 nm and emission to 590/35 nm according to Fernandes et al. [93]. DAF-FM diacetate detection of intracellular nitric oxide was measured at excitation 485/20 and emission 545/40 [125]. The plate was read from the bottom and sensitivity of the photomultiplier tube was

set to 70. For each assay, final concentrations for each of the treatments were as follows: 5.5 mM and 25 mM glucose, 100 µM L-name, 300 µM apocynin, 100 µM L-name + 300 µM apocynin, 100 U/mL SOD.

3.2.4 Fluorescence Microscopy of Superoxide and NO in HUVEC's

Fluorescence microscopy was performed using an Olympus IX81 motorized inverted microscope, Hamamatsu ORCA high resolution digital camera and IPLab 4.0 image analysis software. HUVEC's were seeded at equal density onto BD Falcon 12 well plates. Treatment times and concentrations were identical to the above fluorometric protocols for both DHE and DAF-FM diacetate. After chemical treatments, images were immediately acquired using the fluorescence microscope detection software and appropriate filters for DHE and DAF-FM diacetate.

3.2.5 Nitrotyrosine Immunocytofluorescence

Following respective normal glucose and 24 hour glucose treatment, cells were washed briefly with cold PBS and fixed for 15 min with 4% formalin. The fixative was removed by washing with PBS and cells were permeabilized with 0.1% Triton X-100/0.1% sodium citrate for 2 min on ice. Cells were washed with PBS and blocked with 3% BSA in PBS for 1 h, followed by overnight incubation at 4°C with primary rabbit nitrotyrosine antibody diluted (1:200) in antibody diluent (1.5% BSA and 0.5% skim milk in PBS). The following day cells were washed with PBS-T and incubated with the secondary antibody, Alexa-594 goat anti-rabbit IgG, for 30 minutes at room temperature in the dark. Cells were rinsed with PBS-T and nuclear counterstaining was initiated using DAPI for 10 minutes at room temperature and were washed

with PBS. Nitrotyrosine staining was evaluated with an Olympus IX81 motorized inverted microscope, Hamamatsu ORCA high resolution digital camera and IPLab 4.0 image analysis software.

3.2.6 Nitrotyrosine ELISA

We used a competitive ELISA to measure intracellular nitrotyrosine concentrations. HUVEC's were grown to confluence in 6 well plates and treated with either normal or high glucose 1, 24 or 48 hours. Additionally, cells were treated with either 300 μM L-NAME, 100 μM apopcynin or 100 U/mL SOD to evaluate contribution of each respective enzymatic pathway responsible for the increased peroxynitrite formation. HUVEC's were lysed using a standard RIPA buffer protocol and protein content was standardized via Bradford assay. Equal amounts of protein were then aliquoted for use in the ELISA. High binding plates were first coated with antigen, nitrated BSA, and blocked. Next, the competitive ELISA was performed using a nitrotyrosine antibody and a HUVEC lysate sample. HRP-conjugated goat anti-rabbit IgG and LumiGLO® were used for chemiluminescence detection of nitrotyrosine.

First, 100 μL of 5 μg/mL nitrated BSA in 50mM carbonate buffer was added to each well. Next, the plate was incubated for 2 hours at 37°C to ensure adequate binding. The wells were then emptied by inverting the plate over a sink. The plate was then washed two times with 1X TBS-T, then soaked for 2-3 minutes in 1X TBS. Next, we blotted the plate on absorbent paper to remove excess liquid. To eliminate unspecific binding of the antibody, 150 μL per well of 1X blocking buffer was added to each well and the plate was incubated at 37°C for 1 hour. Lastly, the microplate wells were emptied by inverting the plate over a sink and the plate was blotted on absorbent paper to remove excess liquid.

Next, 50 µL of HUVEC sample was added to the appropriate wells. Then 50 µL of 2X rabbit anti-nitrotyrosine primary antibody was added to each well. The plates were incubated at 37°C for 60 minutes. Next, the wells were emptied by inverting the plate over a sink. We then washed the plate once with TBS-T and three times with 1X TBS to remove all bound antibody-nitrotyrosine complexes. The wells were then emptied by inverting the plate over a sink and the plate was blotted on absorbent paper to remove excess liquid. Now, 100 µL of the secondary 1X goat anti-rabbit IgG, HRP-conjugated antibody was added to each well. The plate was incubated at 37°C for 60 minutes to bind the labeled secondary antibody to any remaining primary antibody on the well surface. The plate was then washed two times with 1X TBS-T and twice with TBS to remove any unbound secondary antibody. The wells were then emptied by inverting the plate over a sink and the plate was blotted on absorbent paper to remove excess liquid. Finally, 75 µL of freshly prepared LumiGLO® chemiluminescent substrate was added to each well and the plate was incubated at room temperature for 10 minutes to complete the reaction. Measurement of nitrotyrosine was performed through the detection of luminescence as relative light units (RLU) using a BioTek Synergy 2 Multi-Detection Microplate Reader. A standard curve using known concentrations of nitrated BSA was generated to provide concentration analysis of each respectively treated HUVEC sample. To generate a standard curve (0-1200 µg/mL nitrated BSA) we used the following procedure recommended by the manufacturer, Millipore (Figure 7c). Briefly, we prepared the 2400 µg/mL nitrated BSA standard in 1X blocking buffer as described previously. Next, we prepared 3-fold serial dilutions of the 2400 µg/mL nitrated BSA standard in microfuge tubes (transfer 55 µL of the 2400 µg/mL nitrated BSA standard to 110 µL of 1X blocking buffer, mixing thoroughly before the next transfer. Repeat this process to make successive 3-fold dilutions). Lastly, we used 110 µL of 1X blocking

buffer in the last tube for the background. Each assay point used 50 μL as described in the previous Elisa protocol and was performed in duplicate. The concentrations of nitrated proteins that inhibit anti-nitrotyrosine antibody binding were estimated from the standard curve and are expressed as nitro-BSA equivalents, i.e. an equivalent concentration of 3-nitrotyrosine in nitro-BSA that produces the equivalent inhibition as the nitrated proteins.

3.2.7 24 and 48 hour Hyperglycemia Induced Apoptosis in HUVEC's

Apoptosis was detected through nuclear fluorescence staining using Hoechst 33342 with an excitation/emission maxima of 350/460 nm. HUVEC's were seeded at equal density onto BD Falcon 12 well plates and once confluent incubated with normal or high (25 mM) glucose for 24 or 48 hours. Following glucose treatment, endothelial cells were incubated in EBM phenol red-free basal media with 10 μM Hoechst 33342 for 10 minutes. HUVEC's were then washed with fresh basal media and images were acquired immediately using the appropriate filters and methods described in the previous section. Hoechst 33342 binds more readily to condensed chromatin in the nucleus of apoptotic cells. Therefore, a stronger fluorescence signal indicates larger presence of condensed chromatin and apoptosis [126].

3.2.8 Statistical analysis

Statistical analysis was performed using JMP Statistical Discovery Software Version 8.0 (SAS Institute, USA). All data are expressed as the mean ± standard deviation. Statistical differences were assessed using the two-way analysis of variance (ANOVA) test. Differences were considered statistically significant at a value of $p < 0.05$.

3.3 Results

3.3.1 Superoxide and NO Presence in HUVEC's after 1 hour High Glucose Treatment

We first tested whether there was an immediate effect of a high glucose environment on intracellular superoxide and nitric oxide presence in HUVEC's. Figure 1a shows the RFU change in DHE fluorescence for HUVEC's treated with high glucose for 1 hour during the course of the fluorometric measurement for 30 minutes after washing. Cells treated with normal and high glucose showed no difference in DHE fluorescence. High glucose cells treated with L-name showed a 190% increase in fluorescence, while those treated with SOD or apocynin showed a decrease of 56% and 44%, respectively. Cells incubated with the combined L-name/apocynin treatment showed an increase of 160% in DHE fluorescence. Figure 1b illustrates the level of DHE fluorescence intensity for each hyperglycemic treatment through fluorescence microscopy. Figure 2a shows the RFU change over time for DAF-FM DA detection of nitric oxide in the same environment. Again, there was no difference in DAF-FM DA fluorescence among normal and high glucose treatments. High glucose cells treated with apocynin and SOD showed an increase in DAF-FM fluorescence of 142% and 127%, respectively. Treatment with L-NAME resulted in a decrease of 20% for DAF-DA detection of nitric oxide. Combined treatment of L-NAME and apocynin gave a fluorescence reduction of 12%. Figure 2b shows the qualitative levels of DAF-FM fluorescence intensity for each hyperglycemic treatment through fluorescence microscopy.

3.3.2 Superoxide and NO Presence in HUVEC's after 24 hour Hyperglycemic Treatment

Next we characterized the effect of short term high glucose exposure on the different enzymatic pathways that are thought to contribute to intracellular superoxide and nitric oxide presence in HUVEC's. Figure 3a illustrates the change in DHE fluorescence for HUVEC's incubated in hyperglycemic conditions for 24 hours. The graph shows that hyperglycemic cells showed an increase of 165% in DHE fluorescence compared to that of normal glucose cells. Additionally, hyperglycemic cells treated with L-name showed a 200% increase in fluorescence over that of normal glucose cells. HUVEC's incubated in high glucose and treated with apocynin or SOD showed a 31% and 47% decrease in DHE fluorescence, respectively. The combined treatment of L-name/apocynin on hyperglycemic cells showed a return in fluorescence values near that of normal glucose cells. Figure 3b illustrates the level of DHE fluorescence intensity for each hyperglycemic treatment through fluorescence microscopy. Figure 4a shows the change in DAF-DAF-FM fluorescence over time for HUVEC's incubated in high glucose for 24 hours. Hyperglycemic cells resulted in a decrease of 27% in DAF-FM fluorescence compared to that of normal glucose HUVEC's. High glucose cells treated with apocynin and SOD showed an increase in fluorescence of 116% and 112%, respectively. Cells treated with high glucose and L-NAME resulted in a 42% reduction in DAF-DA fluorescence. Hyperglycemic cells incubated with a combined treatment of L-NAME and apocynin showed a decrease of 12% in fluorescence. Figure 4b shows the qualitative levels of DAF-FM DA fluorescence intensity for each hyperglycemic treatment through fluorescence microscopy.

3.3.3 Superoxide and NO Presence in HUVEC's after 48 hour Hyperglycemic Treatment

The next sets of experiments were performed to determine whether a more chronic exposure to hyperglycemia enhanced or altered the effects of enzymatic contribution to intracellular

superoxide and nitric oxide presence. Figure 5a illustrates the change in DHE fluorescence over time for HUVEC's incubated in high glucose for 48 hours. Cells treated with high glucose showed an increase of 187% in DHE fluorescence as compared to that of normal glucose cells. Cells treated with high glucose and L-NAME resulted in 209% increase in DHE fluorescence. Hyperglycemic cells incubated in apocynin and SOD showed a fluorescence decrease of 8% and 23% compared to that of normal cells, respectively. Combined treatment of L-NAME and apocynin in hyperglycemic cells gave an increase of 123% in DHE fluorescence measurement. Figure 6a shows the change in DAF-FM fluorescence for HUVEC's incubated in hyperglycemic conditions for 48 hours. Cells incubated in high glucose showed a decrease DAF-FM fluorescence of 32% compared to that of normal glucose HUVEC's. Treatment with high glucose and L-NAME resulted in a fluorescence decrease of 48%. Hyperglycemic cells incubated with a combined treatment of L-NAME and apocynin gave a 19% reduction in fluorescence. Hyperglycemic cells treated with apocynin and SOD showed a return of DAF-FM fluorescence back to normal glucose levels.

3.3.4 Nitric Oxide and Superoxide Production in HUVEC's Exposes to High Glucose

As indicated in the fluorometric data, increases in RFU for both DHE and DAF-FM were linear. Therefore, we calculated the slopes (rate of change over time in RFU) for each of the superoxide and nitric oxide measurements as a quantitative measurement for rate of production. Table 1 shows the rate of superoxide production for 1, 24 and 48 normal and high glucose exposure. Normal glucose showed no significant change in rate of superoxide production over any time period. Additionally, for 1 hr exposure there was no difference between that of normal and high glucose. However, 24 and 48 hr high glucose treatments showed a progressively higher

significant increase over time compared to that of normal glucose for the same treatment time. Treatment of 24 and 48 hr high glucose exposed endothelial cells with L-NAME resulted in an even greater significant increase in superoxide production rate than that of normal glucose HUVEC's. When apocynin and SOD were added to HUVECs treated with high glucose for 24 and 48 hr the increase in superoxide production over time was abolished and restored to production levels lower than that of normal glucose treated cells. Rates of nitric oxide production for 1, 24 and 48 normal and high glucose exposure are shown in Table 2. Normal glucose showed no significant change in rate of nitric oxide production over any time period. Additionally, for 1 hr normal and high glucose exposure there was no difference between nitric oxide production rates. However, 24 and 48 hr high glucose treatments showed a significant decrease over time compared to that of normal glucose for the same treatment time. Nitric oxide production was further decreased by treatment of 24 and 48 hr high glucose exposed cells with L-NAME. Interestingly, when we removed the competition of superoxide by treating the 24 and 48 hr high glucose treated cells with apocynin and SOD, we observed a significant increase in nitric oxide production over time compared to that of normal glucose HUVEC's.

3.3.5 Nitrotyrosine Levels in Normal and Hyperglycemic HUVEC's

The downstream effect of increased superoxide-nitric oxide interactions, via peroxynitrite was quantified. Nitrotyrosine is well known to be an indirect marker for peroxynitrite inside cells and tissue [73]. First we visualized the increase in nitrotyrosine presence between normal and 24 hr high glucose exposed HUVEC's using immunocytofluorescence microscopy. Figure 7a illustrates that exposure to high glucose for 24 hr is sufficient to increase peroxynitrite formation in endothelial cells. Endothelial cells exposed to high glucose for 24 hours show substantially

more immunofluorescence when compared visually with that of normal glucose cells. We then quantified the concentration of intracellular nitrotryosine using an established competitive ELISA. Figure 7b shows the concentration of nitrotyrosine for HUVEC's treated with high glucose for 1, 24 and 48 hr. There was very little difference in nitrotyrosine concentrations among all the different treatment groups for 1 hr high glucose exposure. There was no statistical difference in nitrotyrosine concentrations between normal glucose and 1 hr high glucose treated HUVEC's. Endothelial cells exposed to 24 and 48 hr high glucose showed a significant increase in intracellular nitrotyrosine concentration compared to that of normal glucose cells. L-NAME treatment of 24 and 48 hr high glucose exposed HUVEC's also showed a significant increase in nitrotyrosine concentration compared to that of normal glucose cells. Treatment of 24 and 48 hr high glucose exposed HUVEC's with apocynin and SOD was shown to restore nitrotyrosine concentrations near to those of normal glucose cells.

3.3.6 Analysis of Apoptosis in HUVEC's after 24 and 48 hour hyperglycemic treatment

Lastly, we were interested in the prevalence of apoptosis as a result of hyperglycemia exposure in endothelial cells. For this purpose, we treated HUVEC's with 25 mM high glucose for 24 and 48 hours and compared Hoechst 33342 nuclear fluorescence staining to that of normal glucose treated cells. Figure 8 qualitatively shows the presence of condensed nuclear chromatin for normal, 24 and 48 hour high glucose HUVEC's. Endothelial cells in normal glucose media show little to no apoptosis as evidenced by the lack of significant Hoechst 33342 fluorescence. HUVEC's exposed to both 24 and 48 hour high glucose show progressively increased nuclear fluorescence, indicating a high concentration of condensed chromatin and apoptosis, with 48

hour exposure being the most significant. Interestingly, as seen in Figure 8, most of the apoptosis occurs in clusters within the endothelial cell monolayer.

3.4 Discussion

Type-2 diabetes is characterized by chronically elevated glucose levels in the vasculature as a result of insulin resistance and decreased insulin secretion [127]. Endothelial cells are unable to regulate glucose intake due to the intrinsic properties of the GLUT4 receptor. Consequently, chronic high glucose exposure leads to a buildup of glucose inside the endothelial cell [128]. This condition increases mitochondrial function and superoxide leakage, activates stress pathways (NF-κB, p38 MAPK, JNK/SAPK, PKC, AGE/RAGE, sorbitol) and increases reactive oxygen species production [1]. Oxidative and nitrosative stress pathways induce an imbalance of vascular reactive species homeostasis and can be a contributor or consequence of endothelial dysfunction. Numerous enzymatic pathways contribute to oxidative and nitrosative stress. Enzymes such as NADPH oxidase, uncoupled eNOS and the mitochondrial electron transport chain are all implicated in the production of superoxide [42].

Our study focuses on quantifying the contribution levels of NADPH oxidase and eNOS towards hyperglycemia induced superoxide generation, nitrosative stress and depletion of nitric oxide bioavailability in HUVEC's. We show that 24 and 48 hr hyperglycemia exposure is sufficient to increase nitric oxide production in HUVEC's. We also show that upregulation of nitric oxide generation is accompanied by a comparatively greater increase in superoxide production. This excess intracellular superoxide presence leads to decreased nitric oxide bioavailability, increased formation of peroxynitrite and endothelial cell damage/death.

3.4.1 NOS Function and Nitrosative Stress in Hyperglycemic HUVEC's

Structure of nitric oxide synthase is described as a homodimer consisting of an oxygenase and reductase domain, binding-dependent upon the cofactor tetrahydrobiopterin [129]. Proper function of eNOS is dependent upon the dimer to monomer ratio of the enzyme. Pathology such as diabetes induces "uncoupling" of the enzyme, leading to higher levels of the monomer form of eNOS due to a lower ratio of 5,6,7,8-tetrahydrobiopterin to 7,8-dihydrobiopterin [17]. Due to the dysfunction of eNOS and increased levels of superoxide, NO bioavailability decreases and peroxynitrite levels increase.

Studies have shown that augmentation of intracellular BH_4 levels restores endothelial nitric oxide synthase function and nitric oxide bioavailability in the presence of high glucose [130]. Interestingly, our data shows that NO production increases, presumably in the attempt to provide antioxidant support against increased production of superoxide (see Tables 1 and 2). From our data and the current literature; it is not clear what enzymatic source(s) is responsible for the increased production of nitric oxide. Increase in gene and/or protein expression levels of eNOS may account for the increase. Activation or increase in gene and/or protein expression of iNOS may also be responsible for this source of increased nitric oxide production and, consequently, nitrosative stress. Ultimately, this antioxidant defense mechanism leads to increased peroxynitrite formation, caspase activation and apoptosis. Our results support that hyperglycemia alters the role of nitric oxide from that of a vasoprotective, signaling molecule to cytotoxic and apoptotic.

3.4.2 Hyperglycemia Induced NADPH oxidase Activity and Oxidative Stress

NADPH oxidase may act as both a pro- and anti- oxidative stress enzyme, depending upon the local cellular environment [42, 112, 119, 131]. In normal function, the enzyme induces antioxidant defenses via ROS-mediated activation of intracellular redox signaling pathways [36]. However, overproduction of ROS leads to eNOS uncoupling, mitochondrial dysfunction, and an impaired redox balance due to depletion of NADPH and impaired Nrf2/ARE-mediated gene expression [131]. Recent studies in the identification of vascular NADPH oxidase subunits and their subcellular localization/regulation have shown that increased NADPH oxidase expression and cytosolic subunit translocation to the membrane results in increased superoxide presence [38, 127, 132].

Our results indicate that NADPH oxidase is the main source of superoxide in hyperglycemic HUVEC's. We show that hyperglycemic endothelial cells treated with apocynin, an NADPH oxidase inhibitor, showed intracellular superoxide return to levels lower than that of normal glucose cells (see Figures 1a, 3a, 5a). These data are in agreement with a previous study which shows inhibition of Rac-1, an important NADPH oxidase cofactor, protected against hyperglycemic injury in a murine model [133]. Rac-1 assembly with membrane bound NADPH oxidase subunits is needed for the activation and production of superoxide by this enzyme. Together, these data suggests that activation of NADPH oxidase is the most significant contributor of hyperglycemic induced superoxide in endothelial cells. We also found that, although NADPH oxidase accounted for most of the excess superoxide presence, treatment of hyperglycemic HUVEC's with SOD still showed intracellular superoxide presence which was significantly lower than that of apocynin treated cells. These results suggest that there is another source of hyperglycemic induced superoxide within the endothelial cell. Our findings support the

hypothesis of increased nitric oxide inactivation by O_2^- as an important mechanism for hyperglycemic endothelial dysfunction.

3.4.3 Level of Nitrotyrosine and Apoptosis in HUVEC's Exposed to High Glucose

Because peroxynitrite is a highly transient species with a biological half-life [10–20 ms [134]] much shorter than that of nitric oxide [1–30 s [135]], it cannot be directly measured. One of the molecular footprints left by the reactions of this reactive nitrogen species with intracellular biomolecules is the nitration of protein tyrosine residues to 3-nitrotyrosine [14, 136]. This well-established posttranslational modification attracts considerable interest in biomedical research, because it can alter protein function, is associated with acute and chronic disease states, and can be a predictor of disease risk. The reactions between nitric oxide and superoxide do not necessarily result in oxidative damage and in some cases can even be cytoprotective. Low levels of peroxynitrite are able to be detoxified by enzymatic and non-enzymatic systems [137].

Results from this study verify a small intracellular presence of peroxynitrite through the detection of a low concentration of nitrotyrosine in normal glucose HUVEC's. However, in response to high glucose exposure and subsequent increases in nitric oxide and superoxide production and interaction, we show that nitrotyrosine concentration is highly elevated in 24 and 48 hr hyperglycemic HUVEC's. These results corroborate ex vivo findings by previous work with perfused rat hearts exposed to short term high glucose [138]. Additionally, our findings show that this significant increase in nitrotyrosine formation is largely mediated by NADPH oxidase activity in response to high glucose exposure. We were able to virtually abolish the high glucose stimulated increase in nitrotyrosine concentration with treatment of apocynin (Figure 7b).

Increased peroxynitrite and nitration events are thought to be major participants in endothelial cell apoptosis [73]. Mitochondrial proteins have been shown to be nitrated *in vitro* and *in vivo*, including MnSOD, aconitase, cytochrome *c*, voltage-dependent anion channel, ATPase, and succinyl-CoA oxoacid-CoA transferase [73, 139]. According to Radi, the nitration inactivation of MnSOD can lead to enhanced intramitochondrial peroxynitrite formation, which in turn triggers apoptotic signaling of cell death, in part by the thiol oxidation-dependent assembly of the permeability transition pore [73]. Our results using Hoechst 33342 fluorescence detection of condensed nuclear chromatin show that apoptotic events increase relative to time of high glucose exposure. Normal glucose HUVEC's showed no evidence of condensed chromatin over any of the tested time periods, while 24 and 48 hour high glucose exposure produced increasingly higher Hoechst 33342 fluorescence (Figure 8).

In conclusion, low basal production of nitric oxide promotes a pro-life intracellular environment through the nitrosylation, and consequent inactivation, of caspases 1 and 3 [140]. Enhanced endothelial cell nitric oxide and superoxide production in response to stress results in greater incidence of protein nitrosylation [141]. This pathway represents an additional and, perhaps, more prominent mode of nitrosative stress involvement in hyperglycemic endothelial cell apoptosis [142].

3.5 References

1. Newsholme, P., et al., *Diabetes associated cell stress and dysfunction: role of mitochondrial and non-mitochondrial ROS production and activity.* J Physiol, 2007. **583**(Pt 1): p. 9-24.

2. Shaw, J.E., R.A. Sicree, and P.Z. Zimmet, *Global estimates of the prevalence of diabetes for 2010 and 2030.* Diabetes research and clinical practice, 2010. **87**(1): p. 4-14.

3. Allen, D.A., M.M. Yaqoob, and S.M. Harwood, *Mechanisms of high glucose-induced apoptosis and its relationship to diabetic complications.* The Journal of nutritional biochemistry, 2005. **16**(12): p. 705-13.

4. Li, J.M. and A.M. Shah, *Endothelial cell superoxide generation: regulation and relevance for cardiovascular pathophysiology.* Am J Physiol Regul Integr Comp Physiol, 2004. **287**(5): p. R1014-30.

5. Brown, D.I. and K.K. Griendling, *Nox proteins in signal transduction.* Free Radic Biol Med, 2009. **47**(9): p. 1239-53.

6. Brownlee, M., *Biochemistry and molecular cell biology of diabetic complications.* Nature, 2001. **414**(6865): p. 813-20.

7. Ceriello, A., *Hyperglycaemia and the vessel wall: the pathophysiological aspects on the atherosclerotic burden in patients with diabetes.* Eur J Cardiovasc Prev Rehabil, 2010. **17 Suppl 1**: p. S15-9.

8. Giacco, F. and M. Brownlee, *Oxidative stress and diabetic complications.* Circ Res, 2010. **107**(9): p. 1058-70.

9. Henriksen, E.J., M.K. Diamond-Stanic, and E.M. Marchionne, *Oxidative stress and the etiology of insulin resistance and type 2 diabetes.* Free Radic Biol Med, 2010.

10. Orasanu, G. and J. Plutzky, *The pathologic continuum of diabetic vascular disease.* J Am Coll Cardiol, 2009. **53**(5 Suppl): p. S35-42.

11. Aronson, D., *Hyperglycemia and the pathobiology of diabetic complications.* Adv Cardiol, 2008. **45**: p. 1-16.

12. Potdar, S. and M. Kavdia, *NO/peroxynitrite dynamics of high glucose-exposed HUVECs: chemiluminescent measurement and computational model.* Microvasc Res, 2009. **78**(2): p. 191-8.

13. Rubbo, H. and R. Radi, *Protein and lipid nitration: role in redox signaling and injury.* Biochim Biophys Acta, 2008. **1780**(11): p. 1318-24.

14. Pacher, P., J.S. Beckman, and L. Liaudet, *Nitric oxide and peroxynitrite in health and disease.* Physiol Rev, 2007. **87**(1): p. 315-424.

15. Beckman, J.S. and W.H. Koppenol, *Nitric oxide, superoxide, and peroxynitrite: the good, the bad, and ugly.* Am J Physiol, 1996. **271**(5 Pt 1): p. C1424-37.

16. Radi, R., *Peroxynitrite reactions and diffusion in biology.* Chem Res Toxicol, 1998. **11**(7): p. 720-1.

17. Crabtree, M.J., et al., *Ratio of 5,6,7,8-tetrahydrobiopterin to 7,8-dihydrobiopterin in endothelial cells determines glucose-elicited changes in NO vs. superoxide production by eNOS.* Am J Physiol Heart Circ Physiol, 2008. **294**(4): p. H1530-40.

18. Ge, Q.M., et al., *Effects of intermittent high glucose on oxidative stress in endothelial cells.* Acta Diabetol, 2010. **47**(Suppl 1): p. 97-103.

19. Piconi, L., et al., *Constant and intermittent high glucose enhances endothelial cell apoptosis through mitochondrial superoxide overproduction.* Diabetes Metab Res Rev, 2006. **22**(3): p. 198-203.

20. Quagliaro, L., et al., *Primary role of superoxide anion generation in the cascade of events leading to endothelial dysfunction and damage in high glucose treated HUVEC.* Nutr Metab Cardiovasc Dis, 2007. **17**(4): p. 257-67.

21. Ceriello, A., et al., *High glucose induces antioxidant enzymes in human endothelial cells in culture. Evidence linking hyperglycemia and oxidative stress.* Diabetes, 1996. **45**(4): p. 471-7.

22. Curcio, F., et al., *Sod and GSH inhibit the high glucose-induced oxidative damage and the PDGF increased secretion in cultured human endothelial cells.* Thromb Haemost, 1995. **74**(3): p. 969-73.

23. Tsuneki, H., et al., *Coenzyme Q10 prevents high glucose-induced oxidative stress in human umbilical vein endothelial cells.* Eur J Pharmacol, 2007. **566**(1-3): p. 1-10.

24. Ulker, S., et al., *Antioxidant vitamins C and E ameliorate hyperglycaemia-induced oxidative stress in coronary endothelial cells.* Diabetes Obes Metab, 2004. **6**(6): p. 442-51.

25. Ungvari, Z., et al., *Resveratrol confers endothelial protection via activation of the antioxidant transcription factor Nrf2.* Am J Physiol Heart Circ Physiol, 2010. **299**(1): p. H18-24.

26. Ishii, N., et al., *Nitric oxide synthesis and oxidative stress in the renal cortex of rats with diabetes mellitus.* J Am Soc Nephrol, 2001. **12**(8): p. 1630-9.

27. Thuraisingham, R.C., et al., *Increased nitrotyrosine staining in kidneys from patients with diabetic nephropathy.* Kidney Int, 2000. **57**(5): p. 1968-72.

28. Arteel, G.E., K. Briviba, and H. Sies, *Protection against peroxynitrite.* FEBS Lett, 1999. **445**(2-3): p. 226-30.

29. Niles, J.C., J.S. Wishnok, and S.R. Tannenbaum, *Peroxynitrite-induced oxidation and nitration products of guanine and 8-oxoguanine: structures and mechanisms of product formation.* Nitric Oxide, 2006. **14**(2): p. 109-21.

30. Shibuki, H., et al., *Lipid peroxidation and peroxynitrite in retinal ischemia-reperfusion injury.* Invest Ophthalmol Vis Sci, 2000. **41**(11): p. 3607-14.

31. Zhuang, S. and G. Simon, *Peroxynitrite-induced apoptosis involves activation of multiple caspases in HL-60 cells.* Am J Physiol Cell Physiol, 2000. **279**(2): p. C341-51.

32. Chung, S.S., et al., *Contribution of polyol pathway to diabetes-induced oxidative stress.* J Am Soc Nephrol, 2003. **14**(8 Suppl 3): p. S233-6.

33. Takamura, Y., et al., *Role of the polyol pathway in high glucose-induced apoptosis of retinal pericytes and proliferation of endothelial cells.* Invest Ophthalmol Vis Sci, 2008. **49**(7): p. 3216-23.

34. Berrone, E., et al., *Regulation of intracellular glucose and polyol pathway by thiamine and benfotiamine in vascular cells cultured in high glucose.* J Biol Chem, 2006. **281**(14): p. 9307-13.

35. Yamagishi, S. and T. Matsui, *Advanced glycation end products, oxidative stress and diabetic nephropathy.* Oxid Med Cell Longev. **3**(2): p. 101-8.

36. Ray, R. and A.M. Shah, *NADPH oxidase and endothelial cell function.* Clin Sci (Lond), 2005. **109**(3): p. 217-26.

37. Datla, S.R. and K.K. Griendling, *Reactive oxygen species, NADPH oxidases, and hypertension.* Hypertension, 2010. **56**(3): p. 325-30.

38. Paravicini, T.M. and R.M. Touyz, *NADPH oxidases, reactive oxygen species, and hypertension: clinical implications and therapeutic possibilities.* Diabetes Care, 2008. **31 Suppl 2**: p. S170-80.

39. BelAiba, R.S., et al., *NOX5 variants are functionally active in endothelial cells.* Free Radic Biol Med, 2007. **42**(4): p. 446-59.

40. Lassegue, B. and K.K. Griendling, *NADPH oxidases: functions and pathologies in the vasculature.* Arterioscler Thromb Vasc Biol, 2010. **30**(4): p. 653-61.

41. Ambasta, R.K., et al., *Direct interaction of the novel Nox proteins with p22phox is required for the formation of a functionally active NADPH oxidase.* J Biol Chem, 2004. **279**(44): p. 45935-41.

42. Gao, L. and G.E. Mann, *Vascular NAD(P)H oxidase activation in diabetes: a double-edged sword in redox signalling.* Cardiovasc Res, 2009. **82**(1): p. 9-20.

43. Lee, M.Y. and K.K. Griendling, *Redox signaling, vascular function, and hypertension.* Antioxid Redox Signal, 2008. **10**(6): p. 1045-59.

44. Brandes, R.P., N. Weissmann, and K. Schroder, *NADPH oxidases in cardiovascular disease.* Free Radic Biol Med. **49**(5): p. 687-706.

45. Frey, R.S., et al., *Phosphatidylinositol 3-kinase gamma signaling through protein kinase Czeta induces NADPH oxidase-mediated oxidant generation and NF-kappaB activation in endothelial cells.* J Biol Chem, 2006. **281**(23): p. 16128-38.

46. Paravicini, T.M. and R.M. Touyz, *Redox signaling in hypertension.* Cardiovasc Res, 2006. **71**(2): p. 247-58.

47. Kamata, H., et al., *Reactive oxygen species promote TNFalpha-induced death and sustained JNK activation by inhibiting MAP kinase phosphatases.* Cell, 2005. **120**(5): p. 649-61.

48. Fujita, R. and H. Ueda, *Protein kinase C-mediated cell death mode switch induced by high glucose.* Cell Death Differ, 2003. **10**(12): p. 1336-47.

49. Misiaszek, R., et al., *Oxidative DNA damage associated with combination of guanine and superoxide radicals and repair mechanisms via radical trapping.* J Biol Chem, 2004. **279**(31): p. 32106-15.

50. Bashan, N., et al., *Positive and negative regulation of insulin signaling by reactive oxygen and nitrogen species.* Physiol Rev, 2009. **89**(1): p. 27-71.

51. Yang, Z., et al., *Critical effect of VEGF in the process of endothelial cell apoptosis induced by high glucose.* Apoptosis, 2008. **13**(11): p. 1331-43.

52. McKenzie, M.D., et al., *Glucose induces pancreatic islet cell apoptosis that requires the BH3-only proteins Bim and Puma and multi-BH domain protein Bax.* Diabetes. **59**(3): p. 644-52.

53. Vincent, A.M., et al., *Uncoupling proteins prevent glucose-induced neuronal oxidative stress and programmed cell death.* Diabetes, 2004. **53**(3): p. 726-34.

54. Rousset, S., et al., *The biology of mitochondrial uncoupling proteins.* Diabetes, 2004. **53 Suppl 1**: p. S130-5.

55. Li, Y., et al., *UCP-2 and UCP-3 proteins are differentially regulated in pancreatic beta-cells.* PLoS One, 2008. **3**(1): p. e1397.

56. Pacher, P. and C. Szabo, *Role of poly(ADP-ribose) polymerase-1 activation in the pathogenesis of diabetic complications: endothelial dysfunction, as a common underlying theme.* Antioxid Redox Signal, 2005. **7**(11-12): p. 1568-80.

57. Quagliaro, L., et al., *Intermittent high glucose enhances apoptosis related to oxidative stress in human umbilical vein endothelial cells: the role of protein kinase C and NAD(P)H-oxidase activation.* Diabetes, 2003. **52**(11): p. 2795-804.

58. Nakagami, H., et al., *Hepatocyte growth factor prevents endothelial cell death through inhibition of bax translocation from cytosol to mitochondrial membrane.* Diabetes, 2002. **51**(8): p. 2604-11.

59. Villanueva, C. and C. Giulivi, *Subcellular and cellular locations of nitric oxide synthase isoforms as determinants of health and disease.* Free Radic Biol Med. **49**(3): p. 307-16.

60. Oess, S., et al., *Subcellular targeting and trafficking of nitric oxide synthases.* Biochem J, 2006. **396**(3): p. 401-9.

61. Ignarro, L.J., *Nitric oxide as a unique signaling molecule in the vascular system: a historical overview.* J Physiol Pharmacol, 2002. **53**(4 Pt 1): p. 503-14.

62. Alp, N.J. and K.M. Channon, *Regulation of endothelial nitric oxide synthase by tetrahydrobiopterin in vascular disease.* Arterioscler Thromb Vasc Biol, 2004. **24**(3): p. 413-20.

63. Bonetti, P.O., L.O. Lerman, and A. Lerman, *Endothelial dysfunction: a marker of atherosclerotic risk.* Arterioscler Thromb Vasc Biol, 2003. **23**(2): p. 168-75.

64. Reriani, M.K., L.O. Lerman, and A. Lerman, *Endothelial function as a functional expression of cardiovascular risk factors.* Biomark Med. **4**(3): p. 351-60.

65. Touyz, R.M. and A.M. Briones, *Reactive oxygen species and vascular biology: implications in human hypertension.* Hypertens Res. **34**(1): p. 5-14.

66. Luiking, Y.C., M.P. Engelen, and N.E. Deutz, *Regulation of nitric oxide production in health and disease.* Curr Opin Clin Nutr Metab Care. **13**(1): p. 97-104.

67. Potdar, S. and M. Kavdia, *NO/Peroxynitrite Dynamics of High Glucose Exposed HUVECs: Chemiluminescent Measurement and Computational Model.* Microvasc Res, 2009.

68. Quijano, C., N. Romero, and R. Radi, *Tyrosine nitration by superoxide and nitric oxide fluxes in biological systems: modeling the impact of superoxide dismutase and nitric oxide diffusion.* Free Radic Biol Med, 2005. **39**(6): p. 728-41.

69. Szabo, C., H. Ischiropoulos, and R. Radi, *Peroxynitrite: biochemistry, pathophysiology and development of therapeutics.* Nat Rev Drug Discov, 2007. **6**(8): p. 662-80.

70. Ferrer-Sueta, G. and R. Radi, *Chemical biology of peroxynitrite: kinetics, diffusion, and radicals.* ACS Chem Biol, 2009. **4**(3): p. 161-77.

71. Radi, R., et al., *Unraveling peroxynitrite formation in biological systems.* Free Radic Biol Med, 2001. **30**(5): p. 463-88.

72. Bartesaghi, S., et al., *Mechanistic studies of peroxynitrite-mediated tyrosine nitration in membranes using the hydrophobic probe N-t-BOC-L-tyrosine tert-butyl ester.* Biochemistry, 2006. **45**(22): p. 6813-25.

73. Radi, R., *Nitric oxide, oxidants, and protein tyrosine nitration.* Proc Natl Acad Sci U S A, 2004. **101**(12): p. 4003-8.

74. Kuzkaya, N., et al., *Interactions of peroxynitrite, tetrahydrobiopterin, ascorbic acid, and thiols: implications for uncoupling endothelial nitric-oxide synthase.* The Journal of biological chemistry, 2003. **278**(25): p. 22546-54.

75. Ceriello, A., et al., *Effect of atorvastatin and irbesartan, alone and in combination, on postprandial endothelial dysfunction, oxidative stress, and inflammation in type 2 diabetic patients.* Circulation, 2005. **111**(19): p. 2518-24.

76. Georgiou, C.D., et al., *An ultrasensitive fluorescent assay for the in vivo quantification of superoxide radical in organisms.* Anal Biochem, 2005. **347**(1): p. 144-51.

77. Selemidis, S., et al., *Nitric oxide suppresses NADPH oxidase-dependent superoxide production by S-nitrosylation in human endothelial cells.* Cardiovasc Res, 2007. **75**(2): p. 349-58.

78. Messner, K.R. and J.A. Imlay, *In vitro quantitation of biological superoxide and hydrogen peroxide generation.* Methods Enzymol, 2002. **349**: p. 354-61.

79. Laurindo, F.R., D.C. Fernandes, and C.X. Santos, *Assessment of superoxide production and NADPH oxidase activity by HPLC analysis of dihydroethidium oxidation products.* Methods Enzymol, 2008. **441**: p. 237-60.

80. Zhao, H., et al., *Superoxide reacts with hydroethidine but forms a fluorescent product that is distinctly different from ethidium: potential implications in intracellular fluorescence detection of superoxide.* Free Radic Biol Med, 2003. **34**(11): p. 1359-68.

81. Peshavariya, H.M., G.J. Dusting, and S. Selemidis, *Analysis of dihydroethidium fluorescence for the detection of intracellular and extracellular superoxide produced by NADPH oxidase.* Free Radic Res, 2007. **41**(6): p. 699-712.

82. Tarpey, M.M., D.A. Wink, and M.B. Grisham, *Methods for detection of reactive metabolites of oxygen and nitrogen: in vitro and in vivo considerations.* Am J Physiol Regul Integr Comp Physiol, 2004. **286**(3): p. R431-44.

83. Hartge, M.M., T. Unger, and U. Kintscher, *The endothelium and vascular inflammation in diabetes.* Diab Vasc Dis Res, 2007. **4**(2): p. 84-8.

84. Hadi, H.A. and J.A. Suwaidi, *Endothelial dysfunction in diabetes mellitus.* Vasc Health Risk Manag, 2007. **3**(6): p. 853-76.

85. Cosentino, F., et al., *High glucose increases nitric oxide synthase expression and superoxide anion generation in human aortic endothelial cells.* Circulation, 1997. **96**(1): p. 25-8.

86. Zhao, H., et al., *Detection and characterization of the product of hydroethidine and intracellular superoxide by HPLC and limitations of fluorescence.* Proc Natl Acad Sci U S A, 2005. **102**(16): p. 5727-32.

87. Robinson, K.M., et al., *Selective fluorescent imaging of superoxide in vivo using ethidium-based probes.* Proc Natl Acad Sci U S A, 2006. **103**(41): p. 15038-43.

88. Massey, V., *The microestimation of succinate and the extinction coefficient of cytochrome c.* Biochim Biophys Acta, 1959. **34**: p. 255-6.

89. Vasquez-Vivar, J., et al., *Reaction of tetrahydrobiopterin with superoxide: EPR-kinetic analysis and characterization of the pteridine radical.* Free Radic Biol Med, 2001. **31**(8): p. 975-85.

90. Zielonka, J., J. Vasquez-Vivar, and B. Kalyanaraman, *Detection of 2-hydroxyethidium in cellular systems: a unique marker product of superoxide and hydroethidine.* Nat Protoc, 2008. **3**(1): p. 8-21.

91. Papaharalambus, C.A. and K.K. Griendling, *Basic mechanisms of oxidative stress and reactive oxygen species in cardiovascular injury.* Trends Cardiovasc Med, 2007. **17**(2): p. 48-54.

92. Dikalov, S., K.K. Griendling, and D.G. Harrison, *Measurement of reactive oxygen species in cardiovascular studies.* Hypertension, 2007. **49**(4): p. 717-27.

93. Fernandes, D.C., et al., *Analysis of DHE-derived oxidation products by HPLC in the assessment of superoxide production and NADPH oxidase activity in vascular systems.* Am J Physiol Cell Physiol, 2007. **292**(1): p. C413-22.

94. Zielonka, J., M. Hardy, and B. Kalyanaraman, *HPLC study of oxidation products of hydroethidine in chemical and biological systems: ramifications in superoxide measurements.* Free Radic Biol Med, 2009. **46**(3): p. 329-38.

95. Papapostolou, I., N. Patsoukis, and C.D. Georgiou, *The fluorescence detection of superoxide radical using hydroethidine could be complicated by the presence of heme proteins.* Anal Biochem, 2004. **332**(2): p. 290-8.

96. Shao, Z.H., et al., *Antioxidant effects of American ginseng berry extract in cardiomyocytes exposed to acute oxidant stress.* Biochim Biophys Acta, 2004. **1670**(3): p. 165-71.

97. Fink, B., et al., *Detection of intracellular superoxide formation in endothelial cells and intact tissues using dihydroethidium and an HPLC-based assay.* Am J Physiol Cell Physiol, 2004. **287**(4): p. C895-902.

98. Esper, R.J., et al., *Endothelial dysfunction: a comprehensive appraisal.* Cardiovasc Diabetol, 2006. **5**: p. 4.

99. Heumuller, S., et al., *Apocynin is not an inhibitor of vascular NADPH oxidases but an antioxidant.* Hypertension, 2008. **51**(2): p. 211-7.

100. Touyz, R.M., *Apocynin, NADPH oxidase, and vascular cells: a complex matter.* Hypertension, 2008. **51**(2): p. 172-4.

101. Vejrazka, M., R. Micek, and S. Stipek, *Apocynin inhibits NADPH oxidase in phagocytes but stimulates ROS production in non-phagocytic cells.* Biochim Biophys Acta, 2005. **1722**(2): p. 143-7.

102. Dimmeler, S., et al., *Upregulation of superoxide dismutase and nitric oxide synthase mediates the apoptosis-suppressive effects of shear stress on endothelial cells.* Arterioscler Thromb Vasc Biol, 1999. **19**(3): p. 656-64.

103. Horiuchi, M., et al., *Upregulation of vascular extracellular superoxide dismutase in patients with acute coronary syndromes.* Arterioscler Thromb Vasc Biol, 2004. **24**(1): p. 106-11.

104. Ceriello, A., *Possible role of oxidative stress in the pathogenesis of hypertension.* Diabetes Care, 2008. **31 Suppl 2**: p. S181-4.

105. Cohen, J.D., *Overview of physiology, vascular biology, and mechanisms of hypertension.* J Manag Care Pharm, 2007. **13**(5 Suppl): p. S6-8.

106. Munzel, T., et al., *Pathophysiology, diagnosis and prognostic implications of endothelial dysfunction.* Ann Med, 2008. **40**(3): p. 180-96.

107. Evans, J.L., et al., *Oxidative stress and stress-activated signaling pathways: a unifying hypothesis of type 2 diabetes.* Endocr Rev, 2002. **23**(5): p. 599-622.

108. Szabo, C., *Role of nitrosative stress in the pathogenesis of diabetic vascular dysfunction.* Br J Pharmacol, 2009. **156**(5): p. 713-27.

109. Huang, P.L., *eNOS, metabolic syndrome and cardiovascular disease.* Trends Endocrinol Metab, 2009. **20**(6): p. 295-302.

110. Ceriello, A. and R. Testa, *Antioxidant anti-inflammatory treatment in type 2 diabetes.* Diabetes Care, 2009. **32 Suppl 2**: p. S232-6.

111. Heitzer, T., et al., *Endothelial dysfunction, oxidative stress, and risk of cardiovascular events in patients with coronary artery disease.* Circulation, 2001. **104**(22): p. 2673-8.

112. Wolin, M.S., M. Ahmad, and S.A. Gupte, *The sources of oxidative stress in the vessel wall.* Kidney Int, 2005. **67**(5): p. 1659-61.

113. Sessa, W.C., *Regulation of endothelial derived nitric oxide in health and disease.* Mem Inst Oswaldo Cruz, 2005. **100 Suppl 1**: p. 15-8.

114. Chatterjee, A., S.M. Black, and J.D. Catravas, *Endothelial nitric oxide (NO) and its pathophysiologic regulation.* Vascul Pharmacol, 2008. **49**(4-6): p. 134-40.

115. Deonikar, P. and M. Kavdia, *A computational model for nitric oxide, nitrite and nitrate biotransport in the microcirculation: Effect of reduced nitric oxide consumption by red blood cells and blood velocity.* Microvasc Res.

116. Bian, K., M.F. Doursout, and F. Murad, *Vascular system: role of nitric oxide in cardiovascular diseases.* J Clin Hypertens (Greenwich), 2008. **10**(4): p. 304-10.

117. Naseem, K.M., *The role of nitric oxide in cardiovascular diseases.* Mol Aspects Med, 2005. **26**(1-2): p. 33-65.

118. Koh, K.K., P.C. Oh, and M.J. Quon, *Does reversal of oxidative stress and inflammation provide vascular protection?* Cardiovasc Res, 2009. **81**(4): p. 649-59.

119. Datla, S.R. and K.K. Griendling, *Reactive oxygen species, NADPH oxidases, and hypertension.* Hypertension. **56**(3): p. 325-30.

120. Touyz, R.M., G. Yao, and E.L. Schiffrin, *c-Src induces phosphorylation and translocation of p47phox: role in superoxide generation by angiotensin II in human vascular smooth muscle cells.* Arterioscler Thromb Vasc Biol, 2003. **23**(6): p. 981-7.

121. Bokoch, G.M. and T. Zhao, *Regulation of the phagocyte NADPH oxidase by Rac GTPase.* Antioxid Redox Signal, 2006. **8**(9-10): p. 1533-48.

122. Lassegue, B. and K.K. Griendling, *NADPH oxidases: functions and pathologies in the vasculature.* Arterioscler Thromb Vasc Biol. **30**(4): p. 653-61.

123. Guzik, T.J., et al., *Mechanisms of increased vascular superoxide production in human diabetes mellitus: role of NAD(P)H oxidase and endothelial nitric oxide synthase.* Circulation, 2002. **105**(14): p. 1656-62.

124. Crabtree, M.J., et al., *Quantitative regulation of intracellular endothelial nitric-oxide synthase (eNOS) coupling by both tetrahydrobiopterin-eNOS stoichiometry and biopterin redox status: insights from cells with tet-regulated GTP cyclohydrolase I expression.* J Biol Chem, 2009. **284**(2): p. 1136-44.

125. Mikirova, N.A., T.E. Ichim, and N.H. Riordan, *Anti-angiogenic effect of high doses of ascorbic acid.* J Transl Med, 2008. **6**: p. 50.

126. Dive, C., et al., *Analysis and discrimination of necrosis and apoptosis (programmed cell death) by multiparameter flow cytometry.* Biochim Biophys Acta, 1992. **1133**(3): p. 275-85.

127. Tabit, C.E., et al., *Endothelial dysfunction in diabetes mellitus: molecular mechanisms and clinical implications.* Rev Endocr Metab Disord. **11**(1): p. 61-74.

128. Brownlee, M., *The pathobiology of diabetic complications: a unifying mechanism.* Diabetes, 2005. **54**(6): p. 1615-25.

129. Li, H. and T.L. Poulos, *Structure-function studies on nitric oxide synthases.* J Inorg Biochem, 2005. **99**(1): p. 293-305.

130. Cai, S., J. Khoo, and K.M. Channon, *Augmented BH4 by gene transfer restores nitric oxide synthase function in hyperglycemic human endothelial cells.* Cardiovasc Res, 2005. **65**(4): p. 823-31.

131. Trachootham, D., et al., *Redox regulation of cell survival.* Antioxid Redox Signal, 2008. **10**(8): p. 1343-74.

132. Choi, H., et al., *Mechanism of angiotensin II-induced superoxide production in cells reconstituted with angiotensin type 1 receptor and the components of NADPH oxidase.* J Biol Chem, 2008. **283**(1): p. 255-67.

133. Vecchione, C., et al., *Selective Rac-1 inhibition protects from diabetes-induced vascular injury.* Circ Res, 2006. **98**(2): p. 218-25.

134. Denicola, A., J.M. Souza, and R. Radi, *Diffusion of peroxynitrite across erythrocyte membranes.* Proc Natl Acad Sci U S A, 1998. **95**(7): p. 3566-71.

135. Ignarro, L.J., *Biosynthesis and metabolism of endothelium-derived nitric oxide.* Annu Rev Pharmacol Toxicol, 1990. **30**: p. 535-60.

136. Beckmann, J.S., et al., *Extensive nitration of protein tyrosines in human atherosclerosis detected by immunohistochemistry.* Biol Chem Hoppe Seyler, 1994. **375**(2): p. 81-8.

137. Trujillo, M., G. Ferrer-Sueta, and R. Radi, *Peroxynitrite detoxification and its biologic implications.* Antioxid Redox Signal, 2008. **10**(9): p. 1607-20.

138. Ceriello, A., et al., *Acute hyperglycemia induces nitrotyrosine formation and apoptosis in perfused heart from rat.* Diabetes, 2002. **51**(4): p. 1076-82.

139. Turko, I.V., et al., *Protein tyrosine nitration in the mitochondria from diabetic mouse heart. Implications to dysfunctional mitochondria in diabetes.* J Biol Chem, 2003. **278**(36): p. 33972-7.

140. Sun, J., C. Steenbergen, and E. Murphy, *S-nitrosylation: NO-related redox signaling to protect against oxidative stress.* Antioxid Redox Signal, 2006. **8**(9-10): p. 1693-705.

141. Gow, A.J., et al., *Biological significance of nitric oxide-mediated protein modifications.* Am J Physiol Lung Cell Mol Physiol, 2004. **287**(2): p. L262-8.

142. Benhar, M. and J.S. Stamler, *A central role for S-nitrosylation in apoptosis.* Nat Cell Biol, 2005. **7**(7): p. 645-6.

143. Matchar, D.B., et al., *Systematic review: comparative effectiveness of angiotensin-converting enzyme inhibitors and angiotensin II receptor blockers for treating essential hypertension.* Annals of internal medicine, 2008. **148**(1): p. 16-29.

144. Koh, K.K., I. Sakuma, and M.J. Quon, *Role of renin-angiotensin system blockades in reciprocal relationship between insulin resistance and endothelial dysfunction.* Hypertension, 2010. **56**(6): p. e169; author reply e170.

145. Liu, Z., *The renin-angiotensin system and insulin resistance.* Current diabetes reports, 2007. **7**(1): p. 34-42.

146. Fonseca, V.A., *Insulin resistance, diabetes, hypertension, and renin-angiotensin system inhibition: reducing risk for cardiovascular disease.* Journal of clinical hypertension, 2006. **8**(10): p. 713-20; quiz 721-2.

147. Feener, E.P. and G.L. King, *Endothelial dysfunction in diabetes mellitus: role in cardiovascular disease.* Heart failure monitor, 2001. **1**(3): p. 74-82.

148. Ye, G., et al., *Catalase protects cardiomyocyte function in models of type 1 and type 2 diabetes.* Diabetes, 2004. **53**(5): p. 1336-43.

149. Luscher, T.F., et al., *Diabetes and vascular disease: pathophysiology, clinical consequences, and medical therapy: Part II.* Circulation, 2003. **108**(13): p. 1655-61.

150. Creager, M.A., et al., *Diabetes and vascular disease: pathophysiology, clinical consequences, and medical therapy: Part I.* Circulation, 2003. **108**(12): p. 1527-32.

151. Singh, M., G.A. Mensah, and G. Bakris, *Pathogenesis and clinical physiology of hypertension.* Cardiology clinics, 2010. **28**(4): p. 545-59.

152. Rodrigo, R., J. Gonzalez, and F. Paoletto, *The role of oxidative stress in the pathophysiology of hypertension.* Hypertension research : official journal of the Japanese Society of Hypertension, 2011. **34**(4): p. 431-40.

153. Endemann, D.H. and E.L. Schiffrin, *Nitric oxide, oxidative excess, and vascular complications of diabetes mellitus.* Current hypertension reports, 2004. **6**(2): p. 85-9.

154. Cai, H., *Hydrogen peroxide regulation of endothelial function: origins, mechanisms, and consequences.* Cardiovascular research, 2005. **68**(1): p. 26-36.

155. Lassegue, B. and K.K. Griendling, *NADPH oxidases: functions and pathologies in the vasculature.* Arteriosclerosis, thrombosis, and vascular biology, 2010. **30**(4): p. 653-61.

156. Daiber, A., *Redox signaling (cross-talk) from and to mitochondria involves mitochondrial pores and reactive oxygen species.* Biochimica et biophysica acta, 2010. **1797**(6-7): p. 897-906.

157. Forstermann, U. and W.C. Sessa, *Nitric oxide synthases: regulation and function.* European heart journal, 2011.

158. Nickenig, G., *Should angiotensin II receptor blockers and statins be combined?* Circulation, 2004. **110**(8): p. 1013-20.

159. Bluher, M., J. Kratzsch, and R. Paschke, *Plasma levels of tumor necrosis factor-alpha, angiotensin II, growth hormone, and IGF-I are not elevated in insulin-resistant obese individuals with impaired glucose tolerance.* Diabetes care, 2001. **24**(2): p. 328-34.

160. Burnier, M. and A. Zanchi, *Blockade of the renin-angiotensin-aldosterone system: a key therapeutic strategy to reduce renal and cardiovascular events in patients with diabetes.* Journal of hypertension, 2006. **24**(1): p. 11-25.

161. Garrido, A.M. and K.K. Griendling, *NADPH oxidases and angiotensin II receptor signaling.* Molecular and cellular endocrinology, 2009. **302**(2): p. 148-58.

162. Desideri, G., et al., *Angiotensin II inhibits endothelial cell motility through an AT1-dependent oxidant-sensitive decrement of nitric oxide availability.* Arteriosclerosis, thrombosis, and vascular biology, 2003. **23**(7): p. 1218-23.

163. Drummond, G.R., et al., *Combating oxidative stress in vascular disease: NADPH oxidases as therapeutic targets.* Nature reviews. Drug discovery, 2011. **10**(6): p. 453-71.

164. Nishikawa, T., et al., *Impact of mitochondrial ROS production on diabetic vascular complications.* Diabetes research and clinical practice, 2007. **77 Suppl 1**: p. S41-5.

165. Karagiannis, A., et al., *The role of renin-angiotensin system inhibition in the treatment of hypertension in metabolic syndrome: are all the angiotensin receptor blockers equal?* Expert opinion on therapeutic targets, 2007. **11**(2): p. 191-205.

166. Prasad, A. and A.A. Quyyumi, *Renin-angiotensin system and angiotensin receptor blockers in the metabolic syndrome.* Circulation, 2004. **110**(11): p. 1507-12.

167. Gabriely, I., et al., *Hyperglycemia modulates angiotensinogen gene expression.* American journal of physiology. Regulatory, integrative and comparative physiology, 2001. **281**(3): p. R795-802.

168. Dikalov, S.I., et al., *Distinct roles of Nox1 and Nox4 in basal and angiotensin II-stimulated superoxide and hydrogen peroxide production.* Free radical biology & medicine, 2008. **45**(9): p. 1340-51.

169. Groop, P.H., C. Forsblom, and M.C. Thomas, *Mechanisms of disease: Pathway-selective insulin resistance and microvascular complications of diabetes.* Nature clinical practice. Endocrinology & metabolism, 2005. **1**(2): p. 100-10.

170. Lavrentyev, E.N., A.M. Estes, and K.U. Malik, *Mechanism of high glucose induced angiotensin II production in rat vascular smooth muscle cells.* Circulation research, 2007. **101**(5): p. 455-64.

171. Touyz, R.M., *Reactive oxygen species, vascular oxidative stress, and redox signaling in hypertension: what is the clinical significance?* Hypertension, 2004. **44**(3): p. 248-52.

172. Touyz, R.M., et al., *Angiotensin II and endothelin-1 regulate MAP kinases through different redox-dependent mechanisms in human vascular smooth muscle cells.* Journal of hypertension, 2004. **22**(6): p. 1141-9.

173. Virdis, A., et al., *Role of NAD(P)H oxidase on vascular alterations in angiotensin II-infused mice.* Journal of hypertension, 2004. **22**(3): p. 535-42.

174. Li, Y., G. Lappas, and M.B. Anand-Srivastava, *Role of oxidative stress in angiotensin II-induced enhanced expression of Gi(alpha) proteins and adenylyl cyclase signaling in A10 vascular smooth muscle cells.* American journal of physiology. Heart and circulatory physiology, 2007. **292**(4): p. H1922-30.

175. Ichiki, T., et al., *Downregulation of angiotensin II type 1 receptor gene transcription by nitric oxide.* Hypertension, 1998. **31**(1 Pt 2): p. 342-8.

176. Zhang, H., et al., *Angiotensin II-induced superoxide anion generation in human vascular endothelial cells: role of membrane-bound NADH-/NADPH-oxidases.* Cardiovascular research, 1999. **44**(1): p. 215-22.

177. Gragasin, F.S., et al., *Estrogen reduces angiotensin II-induced nitric oxide synthase and NAD(P)H oxidase expression in endothelial cells.* Arteriosclerosis, thrombosis, and vascular biology, 2003. **23**(1): p. 38-44.

178. Takaya, T., et al., *Angiotensin II type 1 receptor blocker telmisartan suppresses superoxide production and reduces atherosclerotic lesion formation in apolipoprotein E-deficient mice.* Atherosclerosis, 2006. **186**(2): p. 402-10.

179. Koh, K.K., P.C. Oh, and M.J. Quon, *Does reversal of oxidative stress and inflammation provide vascular protection?* Cardiovascular research, 2009. **81**(4): p. 649-59.

180. Endres, M. and U. Laufs, *Effects of statins on endothelium and signaling mechanisms.* Stroke; a journal of cerebral circulation, 2004. **35**(11 Suppl 1): p. 2708-11.

181. Radi, R., *Nitric oxide, oxidants, and protein tyrosine nitration.* Proceedings of the National Academy of Sciences of the United States of America, 2004. **101**(12): p. 4003-8.

182. Dweik, R.A., *Nitric oxide, hypoxia, and superoxide: the good, the bad, and the ugly!* Thorax, 2005. **60**(4): p. 265-7.

Figure Legends

Figure 1. DHE intracellular superoxide detection in HUVEC's exposed to high glucose for 1 hour. (a) Data shown are for fluorometer measurement of DHE (5μM) in HUVEC's exposed to normal glucose (5.5 mM) or high glucose (25 mM) for 1 hour. Microplate reader was set at excitation 485/20 nm and emission 590/35 nm. (b) Results show the DHE fluorescence imaging of intracellular superoxide in HUVEC's exposed to normal or high glucose for 1 hour.

Figure 2. DAF-FM diacetate intracellular nitric oxide detection in HUVEC's exposed to high glucose for 1 hour. (a) Results shown are for fluorometer measurement of DAF-FM diacetate (5μM) in HUVEC's exposed to normal glucose (5.5 mM) or high glucose (25 mM) for 1 hour. Microplate reader was set at excitation 485/20 and emission 545/40. (b) Data shows the DAF-FM diacetate fluorescence imaging of intracellular intracellular nitric oxide in HUVEC's exposed to normal or high glucose for 1 hour.

Figure 3. DHE intracellular superoxide detection in HUVEC's exposed to high glucose for 24 hours. (a) Data shown are for fluorometer measurement of DHE (5μM) in HUVEC's exposed to normal glucose (5.5 mM) or high glucose (25 mM) for 24 hours. Microplate reader was set at excitation 485/20 nm and emission 590/35 nm. (b) Data shows the DHE fluorescence imaging of intracellular superoxide in HUVEC's exposed to normal or high glucose for 24 hours.

Figure 4. DAF-FM diacetate intracellular nitric oxide detection in HUVEC's exposed to high glucose for 24 hours. (a) Results shown are for fluorometer measurement of DAF-FM diacetate (5μM) in HUVEC's exposed to normal glucose (5.5 mM) or high

glucose (25 mM) for 24 hours. Microplate reader was set at excitation 485/20 and emission 545/40. (b) Data shows the DAF-FM diacetate fluorescence imaging of intracellular intracellular nitric oxide in HUVEC's exposed to normal or high glucose for 24 hours.

Figure 5. DHE intracellular superoxide detection in HUVEC's exposed to high glucose for 48 hours. (a) Results shown are for fluorometer measurement of DHE (5µM) in HUVEC's exposed to normal glucose (5.5 mM) or high glucose (25 mM) for 48 hours. Microplate reader was set at excitation 485/20 nm and emission 590/35 nm. (b) Data shows the DHE fluorescence imaging of intracellular superoxide in HUVEC's exposed to normal or high glucose for 48 hours.

Figure 6. DAF-FM diacetate intracellular nitric oxide detection in HUVEC's exposed to high glucose for 48 hours. (a) Results shown are for fluorometer measurement of DAF-FM diacetate (5µM) in HUVEC's exposed to normal glucose (5.5 mM) or high glucose (25 mM) for 48 hours. Microplate reader was set at excitation 485/20 and emission 545/40. (b) Data shows the DAF-FM diacetate fluorescence imaging of intracellular intracellular nitric oxide in HUVEC's exposed to normal or high glucose for 48 hours.

Figure 7. Immunocytochemistry detection of nitrotyrosine in HUVEC's exposed to normal and high glucose for 1, 24 and 48 hours. Nitrotyrosine Standard Curve (a) Data shown represent nitrotryosine presence in HUVEC's exposed to normal glucose (5.5 mM) or high glucose (25 mM) for 24 hours. Endothelial cells were formalin fixed and treated with primary nitrotyrosine antibodies. HUVEC's were then treated with Alexa 594-labeled secondary antibodies for immunocytofluorescence imaging. (b) Results

shown are for luminescence measurement of horseradish peroxidase-labeled secondary antibodies and LumiGLO® chemiluminescent substrate using a microplate reader in HUVEC's exposed to normal glucose and 1, 24 and 48 hour high glucose. (c) A standard curve using known concentrations of nitrated BSA was generated to provide concentration analysis of each respectively treated HUVEC sample. To generate a standard curve (0-1200 μg/mL nitrated BSA) we used the procedure recommended by the manufacturer, Millipore. We prepared the 2400 μg/mL nitrated BSA standard in 1X blocking buffer. Next, we prepared 3-fold serial dilutions of the 2400 μg/mL nitrated BSA standard in microfuge tubes (transfer 55 μL of the 2400 μg/mL nitrated BSA standard to 110 μL of 1X blocking buffer, mixing thoroughly before the next transfer. Repeat this process to make successive 3-fold dilutions). Lastly, we used 110 μL of 1X blocking buffer in the last tube for the background. Each assay point used 50 μL as used in the sample protocol and was performed in duplicate. The concentrations of nitrated proteins that inhibit anti-nitrotyrosine antibody binding were estimated from the standard curve and are expressed as nitro-BSA equivalents, i.e. an equivalent concentration of 3-nitrotyrosine in nitro-BSA that produces the equivalent inhibition as the nitrated proteins.

Figure 8. Hoechst 33342 nuclear fluorescence staining to detect hyperglycemia induced apoptosis. The figure shown is for apoptosis analysis of HUVEC's exposed to normal glucose (5.5 mM), 24 or 48 hour high glucose (25 mM) using Hoechst 33342 fluorescence dye detection. Cells were formalin fixed and stained with Hoechst 33342. Hoechst binds more readily to condensed chromatin found in apoptotic cells. Therefore, greater observed fluorescence shows increased presence of condensed

chromatin and apoptosis. Normal glucose HUVEC's show weak widespread fluorescence, indicating generic Hoechst dye staining of healthy nuclei. HUVEC's exposed to 24 and 48 hour high glucose show increasing levels of Hoechst fluorescence, indicating greater levels of apoptosis as high glucose exposure increases.

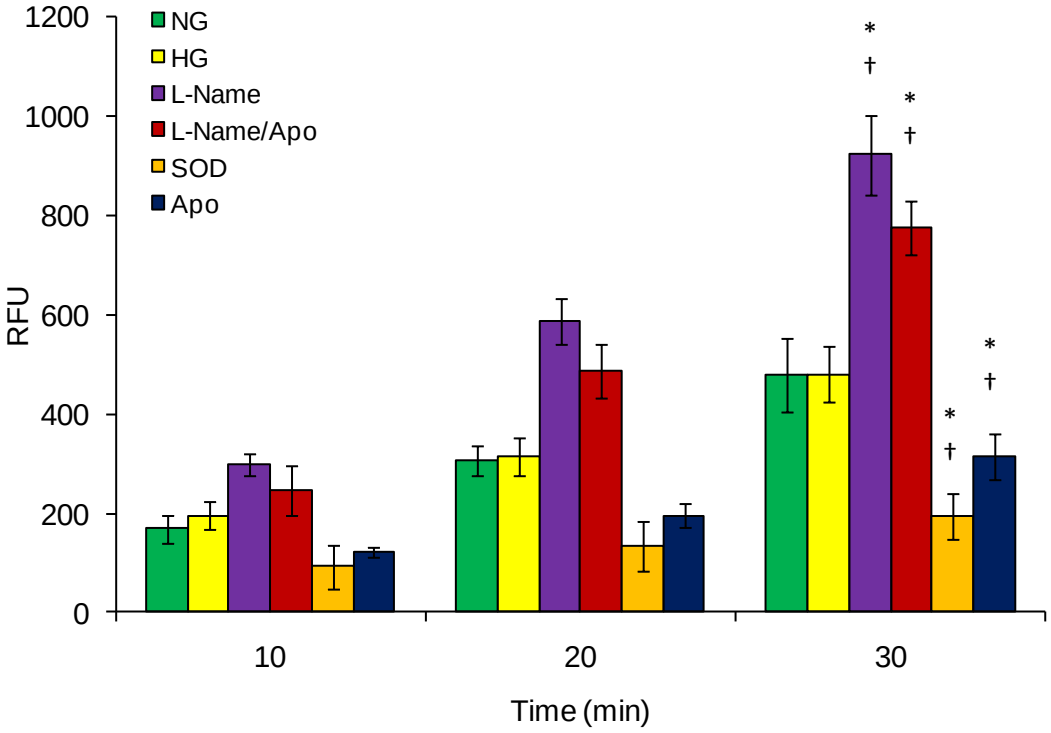
1200
1000
800
600
400
200
0
RFU
NG
HG
L-Name
L-Name/Apo
SOD
Apo
*
†
10
20
30
Time (min)

Figure 1a

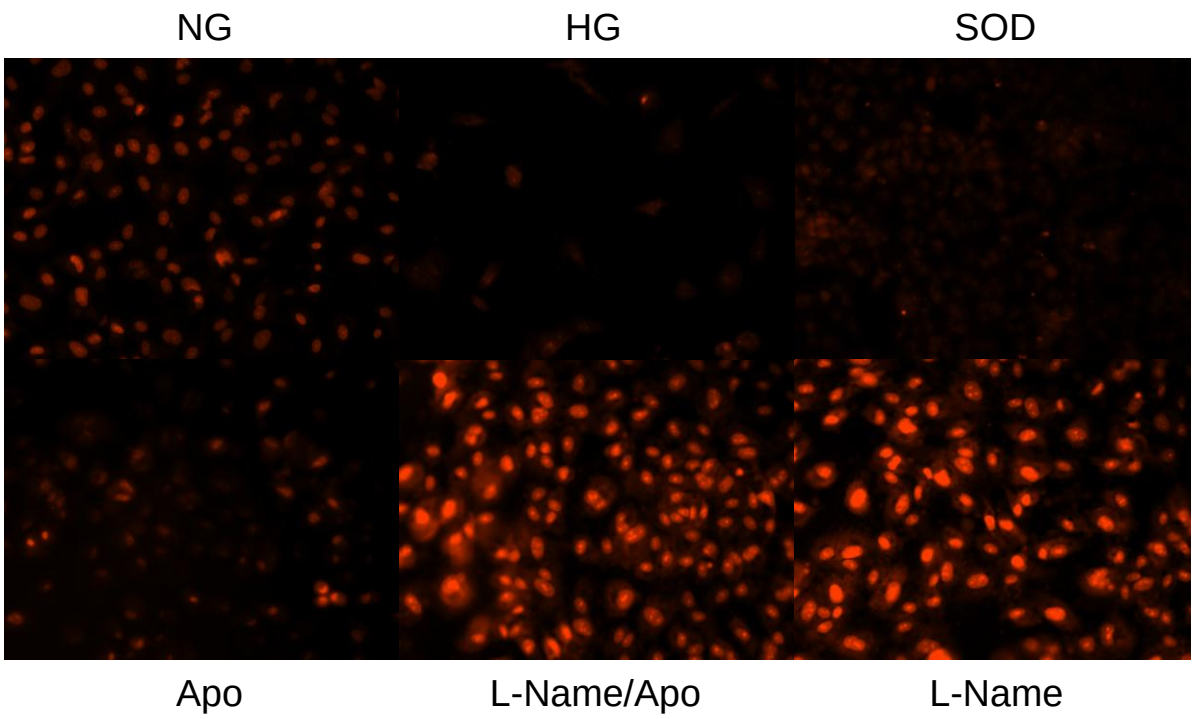

Figure 1b

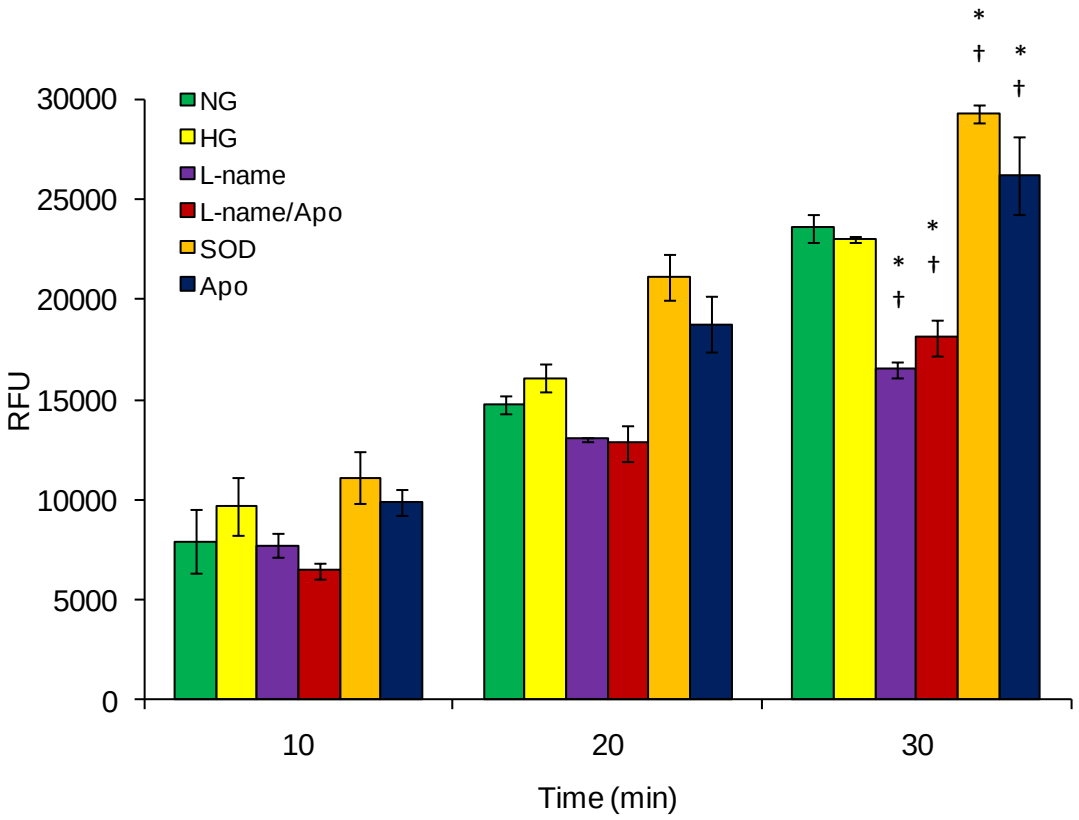
30000
25000
20000
15000
10000
5000
0
RFU
NG
HG
L-name
L-name/Apo
SOD
Apo
10
20
30
Time (min)
*
†
*
†
*
†
*
†

Figure 2a

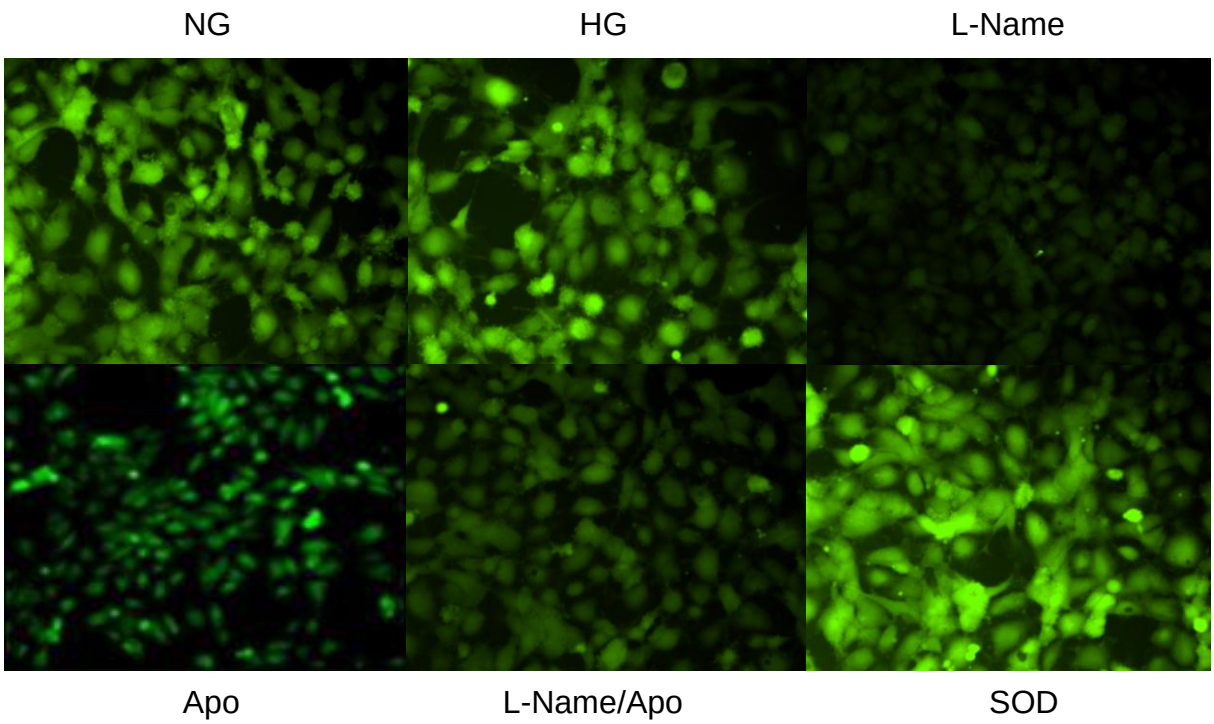

Figure 2b

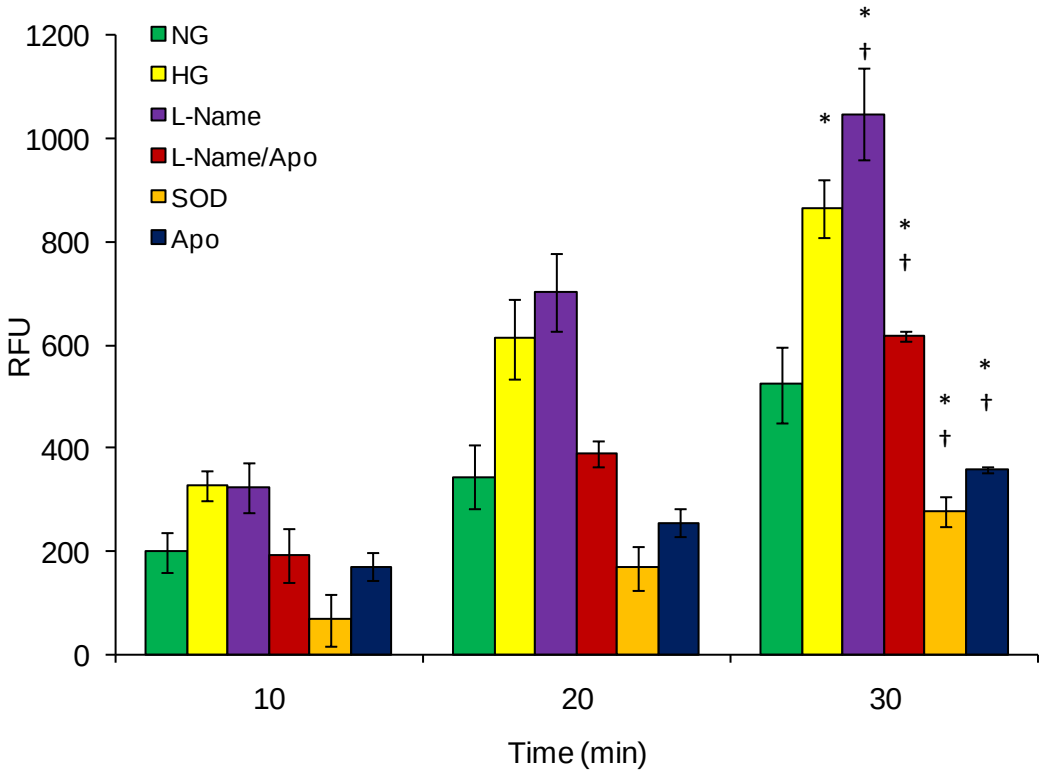
1200
1000
800
600
400
200
0
RFU
NG
HG
L-Name
L-Name/Apo
SOD
Apo
10
20
30
Time (min)
*
†

Figure 3a

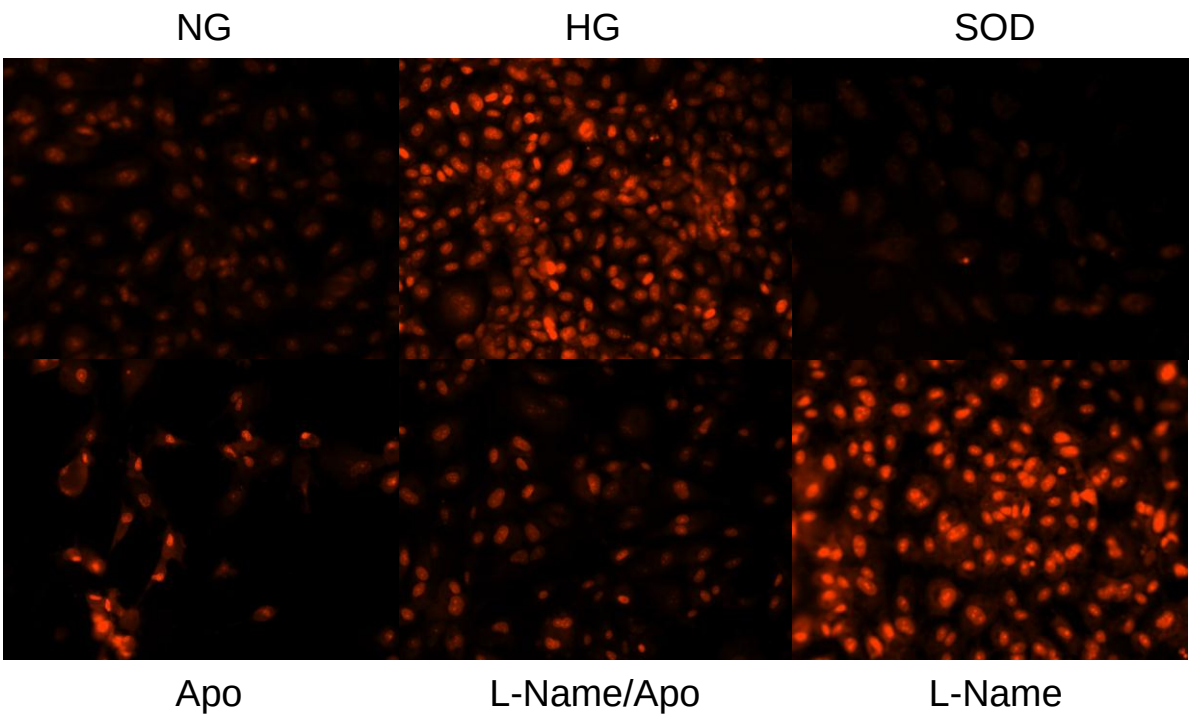

Figure 3b

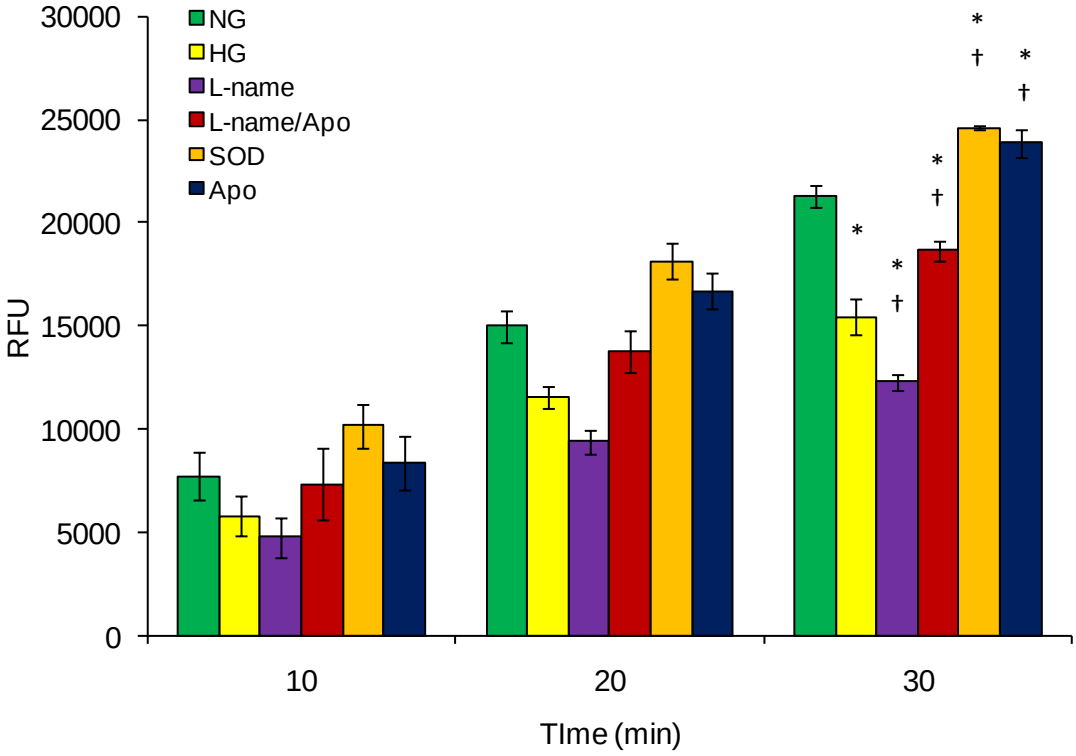
30000
25000
20000
15000
10000
5000
0
RFU
NG
HG
L-name
L-name/Apo
SOD
Apo
10
20
30
TIme (min)
*
†
*
†
*
†
*
†
*
†

Figure 4a

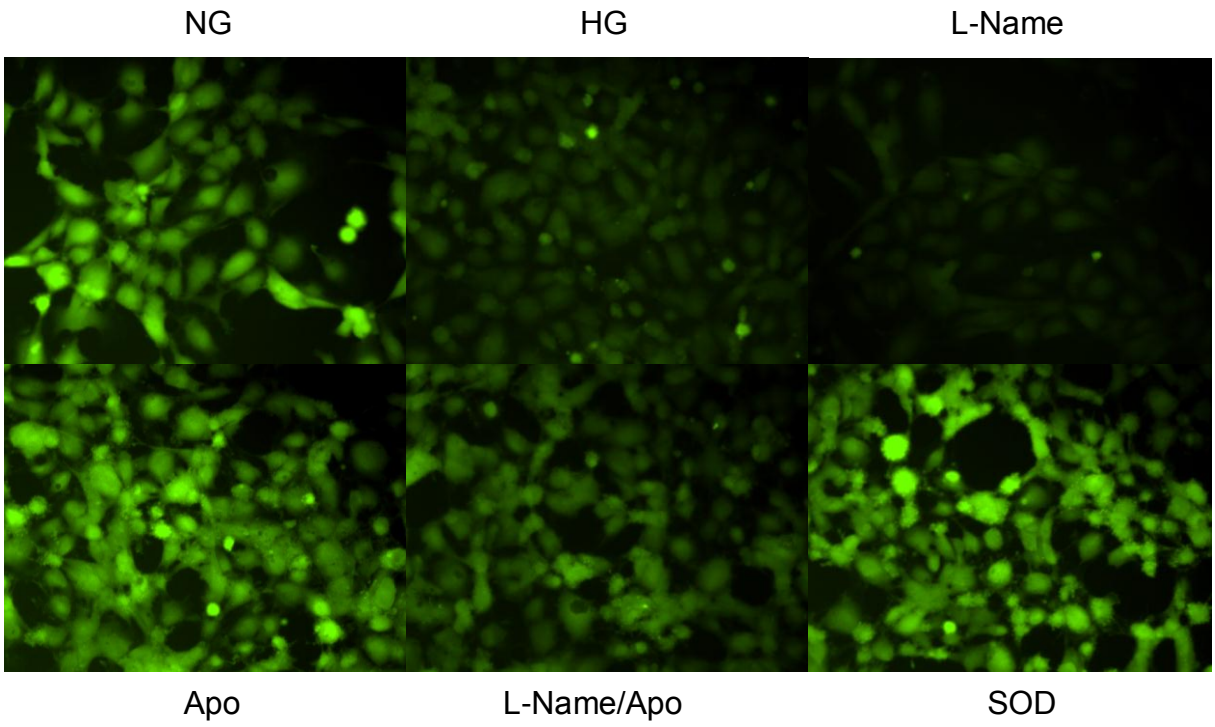

Figure 4b

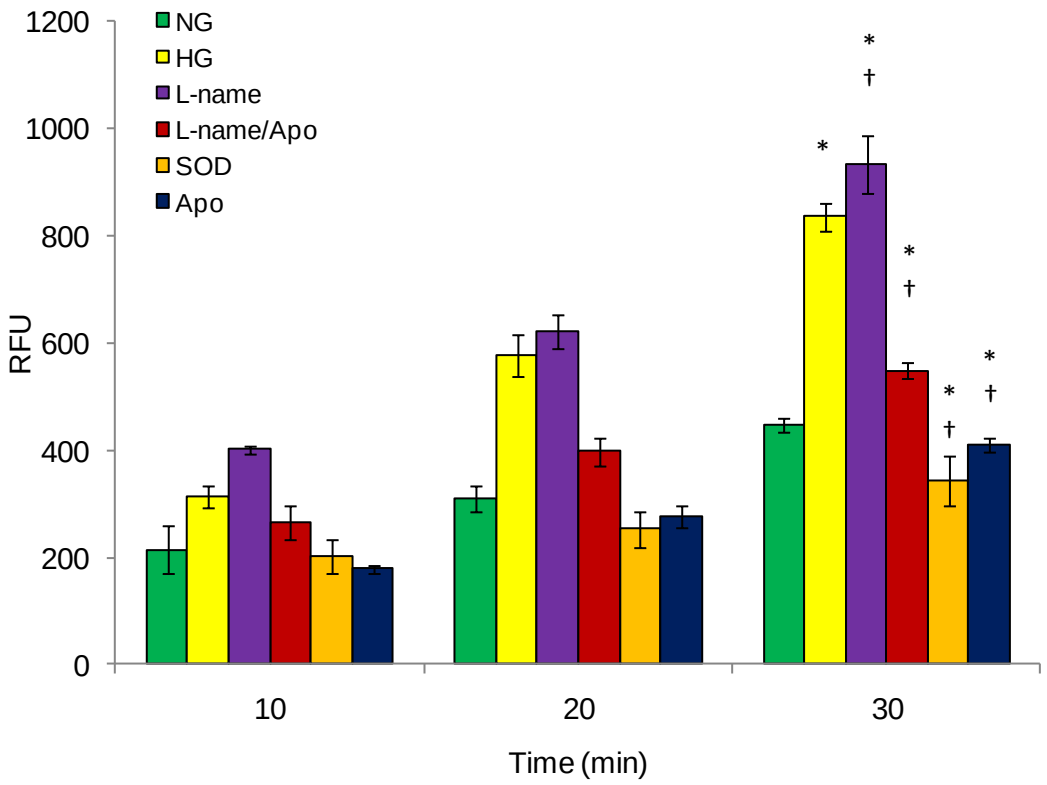
1200
1000
800
600
400
200
0
RFU
NG
HG
L-name
L-name/Apo
SOD
Apo
*
†
10
20
30
Time (min)

Figure 5a

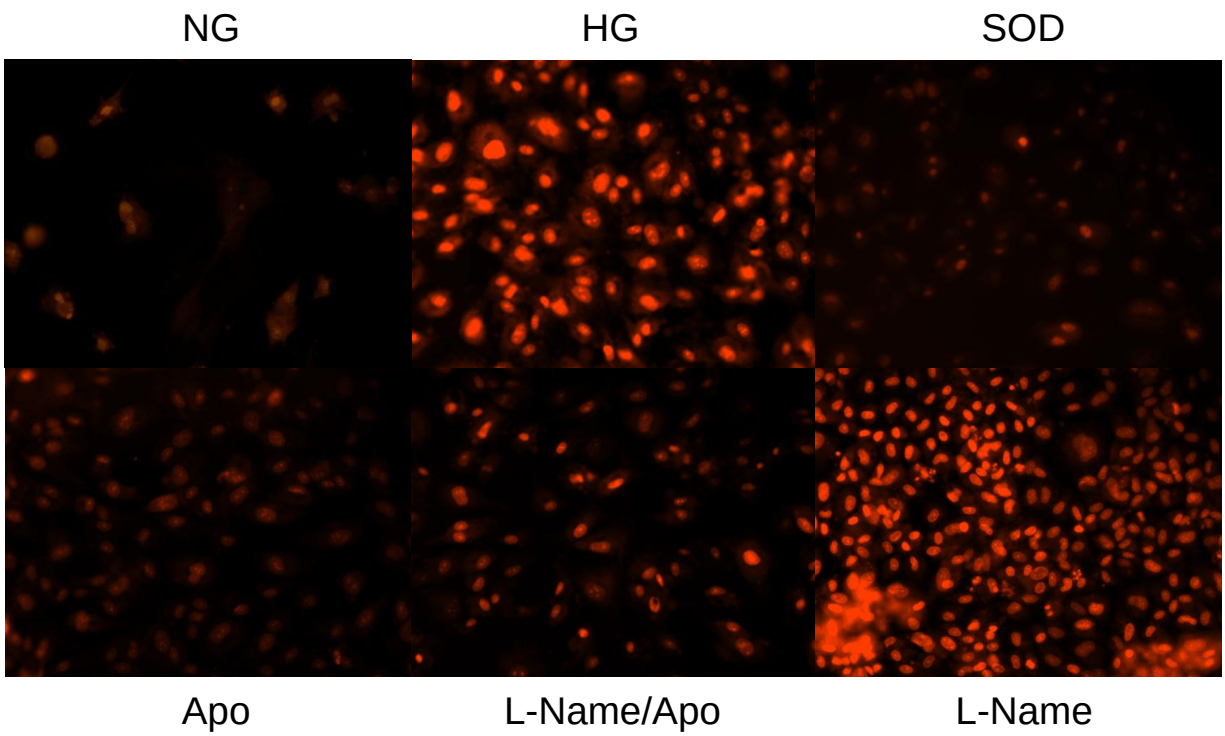

Figure 5b

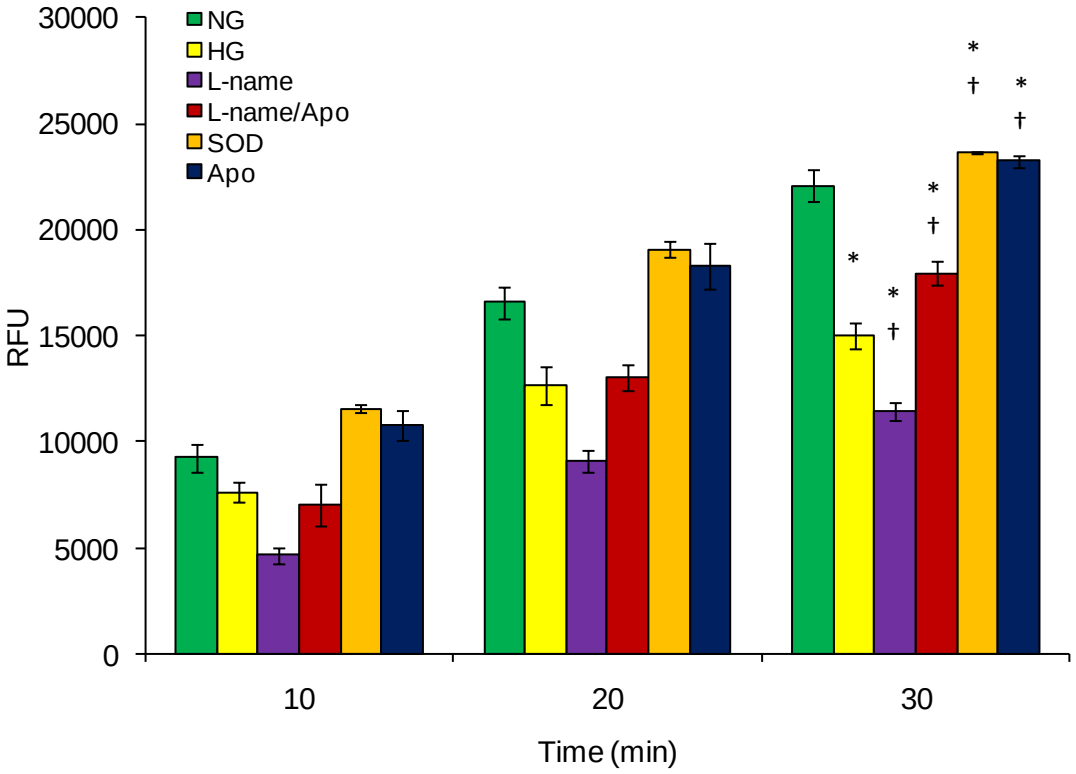
30000
25000
20000
15000
10000
5000
0
RFU
NG
HG
L-name
L-name/Apo
SOD
Apo
10
20
30
Time (min)

Figure 6a

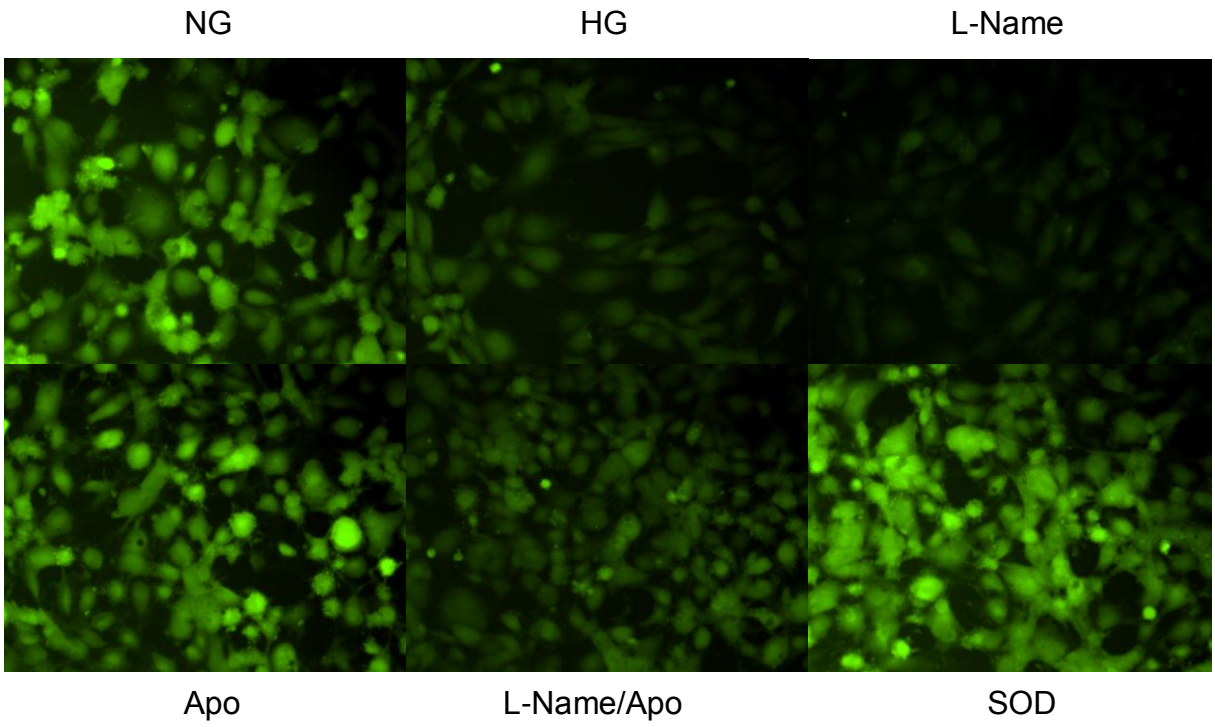

Figure 6b

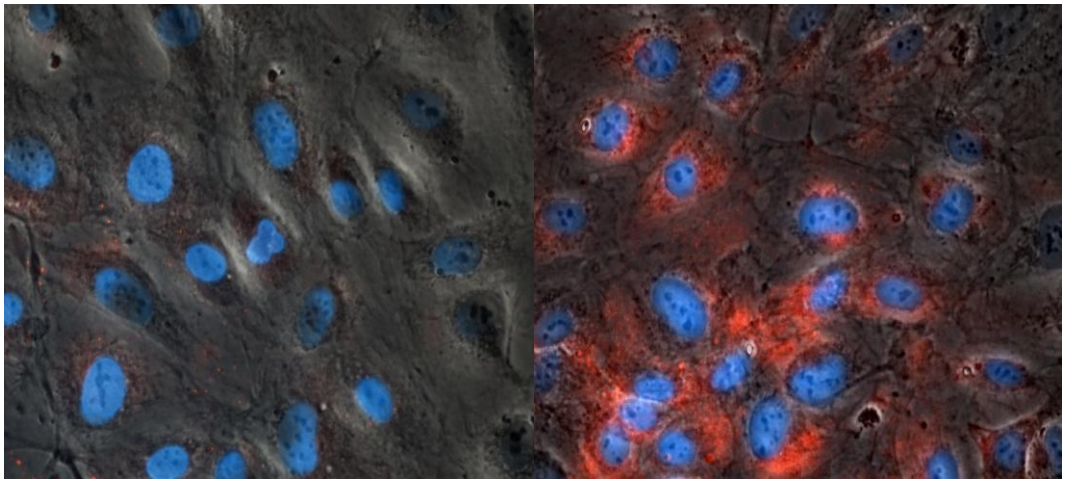

NG **24 hr HG**

Figure 7a

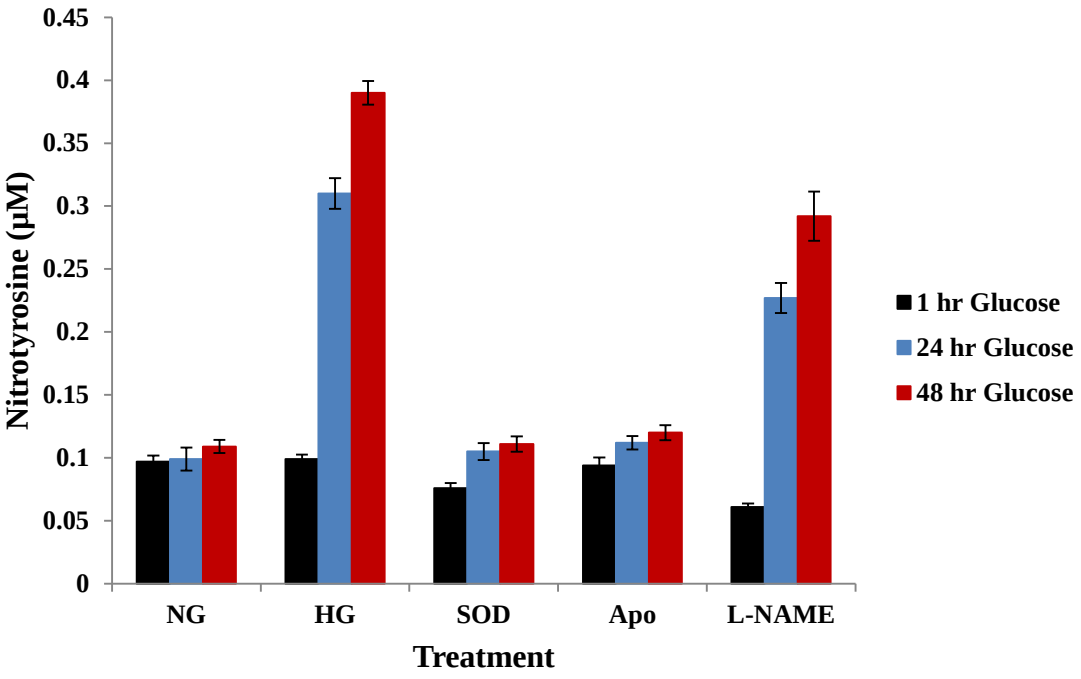
0.45
0.4
0.35
0.3
0.25
0.2
0.15
0.1
0.05
0
Nitrotyrosine (µM)
NG
HG
SOD
Apo
L-NAME
Treatment
1 hr Glucose
24 hr Glucose
48 hr Glucose

Figure 7b

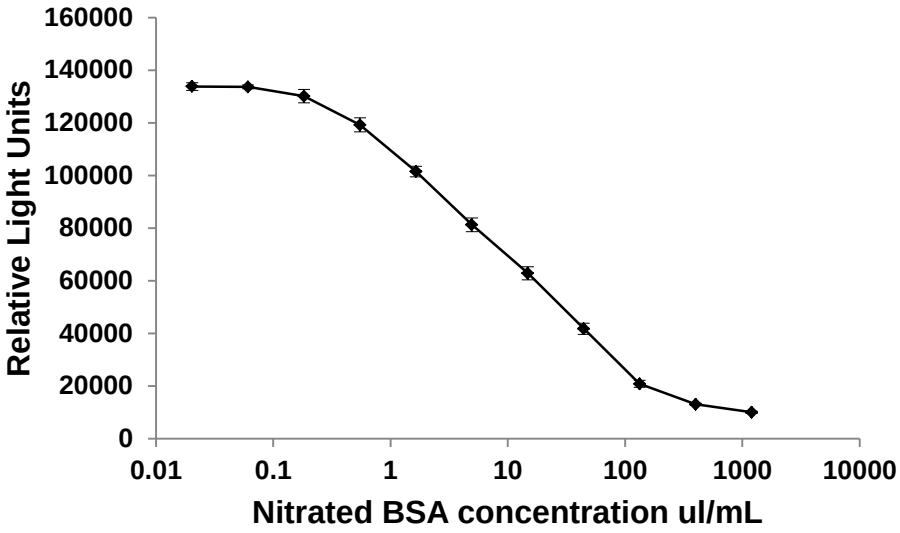
160000
140000
120000
100000
80000
60000
40000
20000
0
Relative Light Units
0.01
0.1
1
10
100
1000
10000
Nitrated BSA concentration ul/mL

Figure 7c

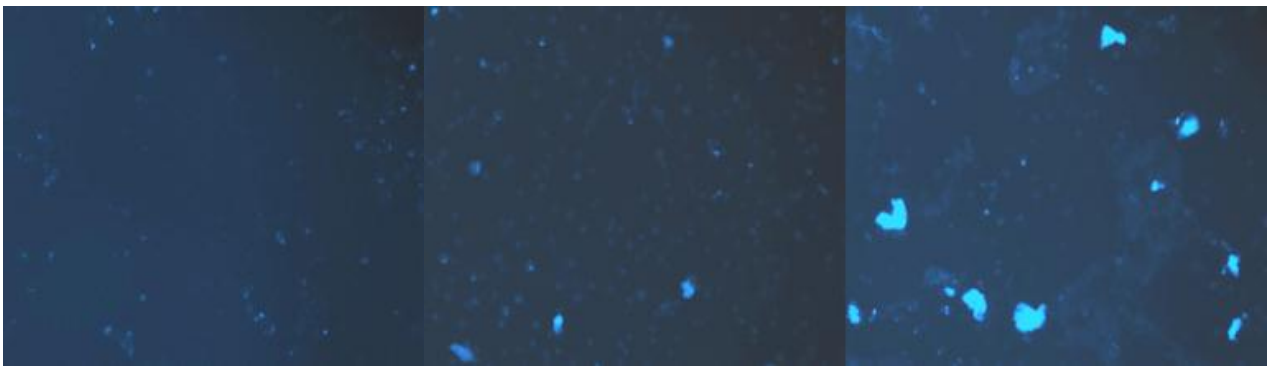

NG HG 24 hr HG 48 hr

Figure 8

Table 1: DHE RFU/min Slopes

Time	NG (RFU/min)	HG (RFU/min)	L-Name (RFU/min)	L-Name/Apo (RFU/min)	SOD (RFU/min)	Apo (RFU/min)
1 hr Slope	**14.3 ± 1.6**	**13.7 ± 1.1**	**25.8 ±2.8 ††**	**14.3 ±0.73**	**5.4 ± 2.3 ††**	**8.7 ± 1.9 ††**
24 hr Slope	**15.1 ± 2.7 ††**	**24.4 ± 2.8 †**	**29.1 ± 3.8 ††**	**19.8 ± 0.82 †, ††**	**6.3 ± 0.48 ††**	**10.0 ± 0.74 ††**
48 hr Slope	**14.7 ± 0.79 ††**	**27.3 ± 1.2 †**	**36.3 ± 1.8 †, ††**	**24.6 ± 0.93 †, ††**	**9.2 ± 1.9 †, ††**	**9.8 ± 0.67 ††**

† - significantly different ($P < 0.05$) Normal Glucose (NG)
†† - significantly different ($P < 0.05$) High Glucose (HG)

Table 2: DAF-FM RFU/min Slopes

Time	NG (RFU/min)	HG (RFU/min)	L-Name (RFU/min)	L-Name/Apo (RFU/min)	SOD (RFU/min)	Apo (RFU/min)
1 hr Slope	**686.3 ± 51.9**	**650.5 ± 47.3**	**536.3 ± 33.4 ††**	**688.3 ± 33.7**	**770.6 ± 6.8 ††**	**774.4 ± 15.5 ††**
24 hr Slope	**680.3 ± 22 ††**	**597 ± 21.2**	**480.7 ± 2.3 †, ††**	**612.1 ± 44.3 †, ††**	**872.4 ± 7.9 †, ††**	**874.1 ± 13 †, ††**
48 hr Slope	**709.8 ± 19.2 ††**	**492.4 ± 22.5 †**	**395.9 ± 11.7 †, ††**	**596.9 ± 36.5 ††**	**985.1 ± 68.7 †, ††**	**880.1 ± 2 ††**

† - significantly different ($P < 0.05$) Normal Glucose (NG)
†† - significantly different ($P < 0.05$) High Glucose (HG)

CHAPTER 4

Angiotensin II Enhances Oxidative and Nitrosative Stress in Hyperglycemic Human Umbilical Vein Endothelial Cells

4.1 Introduction

Renin-angiotensin system (RAS) activation is widely shown to be present in many cardiovascular disorders. Therapeutic regulation of RAS with angiotensin-converting enzyme (ACE) inhibitors is currently a well-established treatment regimen for a number of cardiovascular diseases, such as hypertension and atherosclerosis. More recently, angiotensin type 1 receptor blockers (ARBs) have shown similar promise [143]. Current research is being focused on the role of the RAS in diabetes mellitus, a disorder characterized primarily by chronic inflammation and has emerged as a major risk factor for cardiovascular disease [144-146]. Despite advancements in glucose control, diabetic patients remain at a markedly increased risk of cardiovascular disease. The loss of endothelial function (the development of diabetic endothelial dysfunction) has been implicated both in the development of diabetic macrovascular diseases (e.g. increased incidence and severity of stroke, atherosclerosis, hypertension and myocardial infarction) and in the development of microvascular diseases (neuropathy, nephropathy and retinopathy) [147]. Production of reactive oxygen species (ROS) is increased in both type 1 and type 2 diabetes, contributing not only to the development of diabetes [148], but also significantly to diabetic acceleration of vascular diseases [149, 150]. One important mechanism for ROS-induced vascular damage is oxidative reduction of nitric oxide levels. This leads to endothelial dysfunction that is characterized by a loss in nitric oxide-dependent vasodilatation [151, 152], which has been shown to be impaired in diabetes. The enzyme(s) responsible for production of ROS in diabetes have yet to be fully elucidated. Recent studies by our lab demonstrate that NADPH oxidase (NOX) serves as the predominant source of ROS in high glucose exposed endothelial cells. Uncoupled endothelial nitric oxide synthase (eNOS), however, may be another important source of ROS in the diabetic endothelium [153], likely downstream of NOX [154,

155]. The electron transport chain is also implicated as a potential major contributor of ROS in diabetes. Recent studies suggest that there might be additional cross-talk between the different enzymatic sources of ROS [156]. Nitric oxide synthases produce nitric oxide to scavenge superoxide acting as a potent antioxidant enzyme in the vasculature. Together with other anti-inflammatory and antithrombotic properties of nitric oxide, this antioxidant role of NOS is essential for protection against endothelial dysfunction. Under pathological conditions, however, NOS can convert into a pro-oxidant enzyme, generating superoxide [157]. This "uncoupling" of NOS is thought to have multiple potential mechanisms associated with the oxidative stress pathways involved in the progression of diabetic endothelial dysfunction.

The renin-angiotensin system also represents a major contributor to vascular endothelial dysfunction in macro- and microvascular diseases. Angiotensin II (Ang II) is a circulating vasoconstrictive hormone whose production is often elevated in patients with hypertension and hypercholesterolemia [158]. Production of Ang II is also increased in patients with diabetes, particularly those with hypertension and renal dysfunction [159, 160]. Angiotensin II activates endothelial cell NADPH oxidases via AT1 receptor stimulation [161]. The stimulating effects of angiotensin II on the activity of endothelial cell NADPH oxidases strongly suggests that an activated renin–angiotensin system could cause increased vascular superoxide production and enhance endothelial vascular dysfunction.

A close association exists between signaling pathways and enzymatic nitrosative and oxidative stress activity among endothelial cells and their local environment. Clarification of the mechanisms by which these signaling molecules activate and enhance high-glucose induced endothelial dysfunction would greatly benefit drug design and treatment strategies. The aims of this study are to determine the level of enhancement of angiotensin II on hyperglycemic

endothelial cells and its influence on enzymatic gene expression involved in nitrosative and oxidative stress and endothelial cell damage. Furthermore, we were interested in the potential antagonistic effects of the commonly used angiotensin II receptor blocker (ARB), Losartan, and statin, Simvastatin on high-glucose exposed HUVEC's. We hypothesize that Ang II may mediate common pathological mechanisms involved in the development of different vascular diseases and that high glucose could sensitize endothelial cells to Ang II.

4.2 Materials and Methods

4.2.1 Materials

Pooled HUVEC's, trypsin-EDTA, trypsin neutralizing solution (TNS), HEPES, phenol red-free EBM and EGM-2 bullet kits were obtained from Lonza (Walkersville, PA). Glucose, Angiotensin II, Losartan and Simvastatin were purchased from Sigma-Aldrich (St. Louis, MO). DHE and DAF-FM diacetate were acquired from Invitrogen Molecular Probes (Carlsbad, California). Nitrotyrosine ELISA kit was obtained from Millipore (Billerica, MA). RNA isolation kit was purchased from Qiagen (Germantown, MD). cDNA master mix, PCR mix, PCR 96-well plates and all gene-specific Taqman Probes acquired from Applied Biosystems (Carlsbad, CA). Trizol was obtained from Invitrogen (Carlsbad, CA).

4.2.2 Human Umbilical Vein Endothelial Cell Culture and Treatment Incubation

Pooled primary cell line HUVEC's were cultured in BD falcon 75 cm^2 flasks containing EGM-2 supplemented with 2% heat irradiated fetal bovine serum. The culture flasks were incubated at 37°C in 5% CO_2. Primary cultures were fluid changed 24 hours after seeding and were

subcultured upon reaching 80-90% confluence by the use of 0.25% trypsin-EDTA, inactivated by TNS. Only passages 2-4 were used in the study to avoid passage-dependent cellular modifications. Upon confluency HUVEC's were passaged and seeded at equal density (1×10^4 per well) onto BD Falcon 96 well microplates and allowed to attach overnight in fresh growth media. Once confluent, fresh basal media was then added and treated HUVEC's were incubated with 25mM high glucose for 48 hours. During the final 18 hours of glucose treatment cells were then exposed to Angiotensin II. For the Ang II dose-dependent superoxide and nitric oxide curves we used concentrations ranging from 1×10^{-9} to 1×10^{-3} M. All other experiments in the study used the Ang II dosage of 1×10^{-5} M for treatment with endothelial cells. HUVEC's treated with pharmaceutical agonists, Losartan (750 μM) and Simvastatin (100 μM), were exposed to the drugs during the last 18 hours of glucose and Ang II incubation [162]. Treated basal media was then removed from the well and replaced with phenol-red free basal media to avoid possible fluorescence measurement interference. Cells were then incubated with either 5 μM DHE or 5 μM DAF-FM diacetate for 20 minutes for the measurement of superoxide and NO respectively. Basal media containing either DHE or DAF-FM diacetate was then aspirated from the well and the cells were washed three times with phenol-red free EGM to remove any extracellular fluorescence presence. Fresh phenol-red free media and all respective chemical treatments were added back into each well before fluorescence detection. Osmotic control was assured by incubating HUVEC's with 25mM mannitol for 1, 24 or 48 hours.

4.2.3 Fluorescence Measurement of Superoxide and NO Presence

Fluorescence of DHE and DAF-FM diacetate was monitored with a Synergy 2 Multi-Detection Microplate Reader using Gen5 Microplate Data Collection & Analysis software (BioTek

Instruments Inc., VT, USA). The fluorescence software was programmed to collect readings every two minutes for 30 minutes. For DHE detection of intracellular superoxide the excitation was set to 485/20 nm and emission to 590/35 nm according to Fernandes et al. [93]. DAF-FM diacetate detection of intracellular nitric oxide was measured at excitation 485/20 and emission 545/40 [125]. The plate was read from the bottom and sensitivity of the photomultiplier tube was set to 70. For each assay, final concentrations for each of the treatments were as follows: 5.5 mM and 25 mM glucose, Ang II from 1 x 10^{-9} to 1 x 10^{-3} M.

4.2.4 Nitrotyrosine ELISA

We used a competitive ELISA to measure intracellular nitrotyrosine concentrations. HUVEC's were grown to confluence in 6 well plates and treated with either normal or 48 hour high glucose. Additionally, cells were treated with Ang II (1 x 10^{-5} M) and Losartan (750 μM) or Simvastatin (100 μM. HUVEC's were lysed using a standard RIPA buffer protocol and protein content was standardized via Bradford assay. Equal amounts of protein (50μg) were then aliquoted for use in the ELISA. High binding plates were first coated with antigen, nitrated BSA, and blocked. Next, the competitive ELISA was performed using a nitrotyrosine antibody and a HUVEC lysate sample. HRP-conjugated goat anti-rabbit IgG and LumiGLO® were used for chemiluminescence detection of nitrotyrosine.

First, 100 μL of 5 μg/mL nitrated BSA in 50mM carbonate buffer was added to each well. Next, the plate was incubated for 2 hours at 37°C to ensure adequate binding. The wells were then emptied by inverting the plate over a sink. The plate was then washed two times with 1X TBS-T, then soaked for 2-3 minutes in 1X TBS. Next, we blotted the plate on absorbent paper to remove excess liquid. To eliminate unspecific binding of the antibody, 150 μL per well of 1X blocking

buffer was added to each well and the plate was incubated at 37°C for 1 hour. Lastly, the microplate wells were emptied by inverting the plate over a sink and the plate was blotted on absorbent paper to remove excess liquid.

Next, 50 µL of HUVEC sample was added to the appropriate wells. Then 50 µL of 2X rabbit anti-nitrotyrosine primary antibody was added to each well. The plates were incubated at 37°C for 60 minutes. Next, the wells were emptied by inverting the plate over a sink. We then washed the plate once with TBS-T and three times with 1X TBS to remove all bound antibody-nitrotyrosine complexes. The wells were then emptied by inverting the plate over a sink and the plate was blotted on absorbent paper to remove excess liquid. Now, 100 µL of the secondary 1X goat anti-rabbit IgG, HRP-conjugated antibody was added to each well. The plate was incubated at 37°C for 60 minutes to bind the labeled secondary antibody to any remaining primary antibody on the well surface. The plate was then washed two times with 1X TBS-T and twice with TBS to remove any unbound secondary antibody. The wells were then emptied by inverting the plate over a sink and the plate was blotted on absorbent paper to remove excess liquid. Finally, 75 µL of freshly prepared LumiGLO® chemiluminescent substrate was added to each well and the plate was incubated at room temperature for 10 minutes to complete the reaction. Measurement of nitrotyrosine was performed through the detection of luminescence as relative light units (RLU) using a BioTek Synergy 2 Multi-Detection Microplate Reader. A standard curve using known concentrations of nitrated BSA was generated to provide concentration analysis of each respectively treated HUVEC sample.

4.2.5 Quantitative Real-Time PCR

Total RNA was extracted and purified from 1×10^6 HUVECs grown to confluence in a BD Falcon T-75 flask using a standard Trizol isolation protocol and RNeasy Micro kit (QIAGEN). Briefly, endothelial cells were exposed to normal or high glucose for 48 hours. For the final 18 hours, glucose exposed cells were treated with Ang II (1×10^{-5} M) and Losartan (750 μM) or Simvastatin (100 μM). The concentration of RNA extracted was determined at a wavelength of 260 nm using a Beckman Coulter DU800 (Brea, CA). First-strand complementary DNA (cDNA) was synthesized by using the High Capacity cDNA Reverse Transcription Kit (Applied Biosystems). Total RNA (1 μg) was reverse transcribed to first-strand cDNA in a 20 μL mixture containing reverse transcription 10X reverse transcription buffer (2 μL), 25X deoxyribonucleotide triphosphate (dNTP) Mix (0.8 μL), 10X reverse transcription random primers (2 μL), MultiScribe™ Reverse Transcriptase (1 μL) and nuclease-free H_2O (4.2 μL). The reactions were incubated at 25 °C for 10 min, 37 °C for 120 minutes and then the samples were heated at 85 °C for 5 min. Samples were then either placed on ice for immediate use in PCR experiments or placed in -80 °C for storage. A total of 50 ng cDNA was used for all PCR experiments. All mRNA expression levels were performed by the qRT-PCR technique using a housekeeping gene, beta actin, as an internal standard. The total reaction volume was 25 μL for PCR, which was performed in an Applied Biosystems 7300 Real Time PCR System (Applied Biosystems, Carlsbad, CA). Table 1 shows the list of all TaqMan probes used for each enzyme and endogenous control tested.

4.3 Results

4.3.1 Angiotensin II Sensitivity

We first wanted to determine if there were differences in Ang II sensitivity among normal and high glucose exposed endothelial cells. Figures 1a-b and 2a-b represent superoxide and nitric oxide profiles, respectively, through dose-dependent curves of Ang II treatment on normal and 48 hour high glucose exposed HUVECs. Figure 1a shows the superoxide levels in normal glucose HUVEC's in response to a range of Ang II concentrations (1×10^{-9} to 1×10^{-3} M), while Figure 1b illustrates the change in superoxide levels in high glucose HUVEC's. The results indicate that normal glucose HUVEC's have a lower slope for change in DHE fluorescence levels from that of the high glucose exposed endothelial cells. Additionally, Figure 2a shows the fluorescent values for DAF-FM in normal glucose HUVEC's exposed to Ang II concentrations of 1×10^{-9} to 1×10^{-3} M. Figure 2b gives the nitric oxide levels for HUVEC's exposed to high glucose and Ang II dosages. The figures show that normal glucose endothelial cells have a lower negative slope for change in DAF-FM values compared to that of high glucose HUVEC's.

4.3.2 Gene Expression in Ang II Treated HUVEC's

In order to investigate the gene regulation of enzymatic pathways involved in Ang II stimulation of hyperglycemic endothelial cells, we quantified the mRNA expression levels of eNOS, iNOS, NOX4 and p22phox and calculated the fold increase in expression levels as compared to that of the untreated normal glucose endothelial cells. As seen in Figure 4a and 4b there is no significant increase in eNOS mRNA expression among normal glucose and high glucose exposed HUVEC's in both the Ang II untreated and treated groups. However, iNOS mRNA expression is significantly increased by 9.6 ± 0.3 fold in normal glucose cells treated with Ang II as compared to non-treated normal glucose HUVEC's. Expression of iNOS in Ang II treated high glucose cells shows a significant increase of 19.7 ± 0.5 fold compared to non-treated normal glucose

HUVEC's. Non-treated high glucose cells had a significantly lower increase, 18.4 ± 0.4 fold, in iNOS expression compared to that of Ang II treated high glucose HUVEC's. This illustrates that the synergistic exposure of high glucose and Ang II results in significantly higher increases in iNOS gene expression.

mRNA expression of NOX is also significantly increased by 2.9 ± 0.3 fold in normal glucose cells treated with Ang II as compared to non-treated normal glucose HUVEC's. Expression of NOX4 in Ang II treated high glucose cells shows a significant increase of 13.1 ± 0.7 fold compared to non-treated normal glucose HUVEC's. Non-treated high glucose cells had a significantly lower increase, 5.7 ± 0.2 fold, in NOX4 expression compared to that of Ang II treated high glucose HUVEC's. This illustrates that the synergistic exposure of high glucose and Ang II results in significantly higher increases in NOX4 gene expression.

Gene expression of p22phox was found to have a modest increase of 1.9 ± 0.5 fold in normal glucose cells treated with Ang II as compared to non-treated normal glucose HUVEC's. Expression of p22phox in Ang II treated high glucose cells shows a significant increase of 11.3 ± 0.8 fold compared to non-treated normal glucose HUVEC's. Non-treated high glucose cells had a significantly lower increase, 6.2 ± 0.2 fold, in p22phox expression compared to that of Ang II treated high glucose HUVEC's. This illustrates that the synergistic exposure of high glucose and Ang II results in significantly higher increases in p22phox gene expression.

4.3.3 Pharmacological Effects on Gene Expression in Ang II Treated HUVEC's

Due to recent reports describing the potential for NADPH oxidase activation via angiotensin II interactions with AT1R, we tested the antagonistic effects of the common angiotensin 1 receptor blocker, Losartan, and statin, Simvastatin, on Ang II/high glucose exposed HUVEC's. We were interested in determining if these drugs were able to diminish or reverse the gene upregulation of

oxidant enzymes by Ang II and high glucose. Figure 6a shows that high glucose HUVEC's treated with Losartan had a significant decrease in iNOS gene expression compared to that of high glucose HUVEC's with no treatment, from a 17.9 ± 0.5 fold increase down to only a 3.2 ± 0.3 fold increase compared to that of normal glucose HUVEC's.

4.3.4 Nitrotyrosine Levels

In order to assess the overall oxidative and nitrosative stress induced by increased superoxide-nitric oxide interactions, we measured nitrotyrosine levels in normal and high glucose HUVEC's treated with Ang II. We then tested the antagonistic effects of both Losartan and Simvastatin on the Ang II treated high glucose endothelial cells.

4.4 Discussion

Vascular complications are the leading cause of morbidity and mortality in patients with diabetes. Because the initial injury by hyperglycemia occurs in the blood vessels, endothelial cells are considered to be among the first targets of diabetic vascular disease. Furthermore, endothelial damage and dysfunction plays an important role in the development and progression of diabetic vascular complications [163]. Four main molecular mechanisms have been implicated in glucose-mediated vascular disease: the glucose-induced activation of protein kinase C isoforms, an increased formation of glucose-derived advanced glycation end-products (AGEs), an increased glucose flux through the aldose reductase pathway, and an increased production of reactive oxygen species by pathways such as the renin-angiotensin system [164]; however, the enzymatic mechanisms of endothelial injury by high glucose are not fully understood.

The present data indicate that angiotensin II exposure increases hyperglycemic endothelial cell superoxide levels and increases the gene expression of the ROS generating enzyme NADPH

oxidase subunits $p22^{phox}$ and nox4, while also elevating iNOS mRNA expression. Angiotensin II also reduced nitric oxide bioavailability, which may further enhance oxidative and nitrosative stress in high-glucose exposed endothelial cells, thereby exacerbating endothelial dysfunction. In spite of an increase in iNOS expression, endothelial cell nitric oxide levels are reduced, as upregulation of the NOX subunits facilitates increased peroxynitrite formation. Sensitivity of hyperglycemic endothelial cells to Ang II may be explained by upregulated expression of AT1 receptors on the cell surface and/or enhanced activation of the multiple ROS producing enzymes through amplification of one or more of the molecular signaling pathways. The combination of these events most likely contributes to the elevated nitrotyrosine levels and endothelial dysfunction observed in this high-glucose HUVEC model.

4.4.1 Effects of Angiotensin II Treatment on Superoxide and Nitric Oxide Levels in Normal and High Glucose Exposed Endothelial Cells

The renin-angiotensin system is an enzymatic cascade in which the precursor, angiotensinogen, is converted to the intermediate angiotensin I. Subsequently, angiotensin I is converted to angiotensin II by the coordinated actions of renin and ACE. Additional caspase-dependent pathways for angiotensin II are also present [165]. Angiotensin II is considered the major signaling molecule of the RAS and its functions are known to regulate vasomotor tone, blood pressure, and cardiovascular structure. These functions are primarily via activation of the G-protein–coupled angiotensin II type 1 receptor [166]. The complex cellular interactions of the RAS and hyperglycemia include shared signal transduction pathways, including the PI3 kinase and MAP kinase pathways. Additionally, hyperglycemia activates the RAS by increasing the expression of angiotensinogen and Ang II, which, together, may contribute to the development of

hypertension in patients with diabetes [167]. Ang II acting via AT1 receptors is a powerful stimulus for the generation of ROS in the blood vessels from the NADPH oxidases [168], which become further upregulated in hyperglycemic environments. This increased oxidant stress is instrumental in the progression of endothelial dysfunction, inflammation, smooth muscle hypertrophy, and vascular remodeling.

Vasoactive peptides such as ANG II, which can be synthesized locally in the vasculature, have been implicated in diabetes-associated vascular dysfunctions, including vascular remodeling, hypertrophy, and proliferation of VSMCs [169], leading to impaired relaxation to vasodilators or an enhanced response to vasoconstrictors. The levels of ANG II have been shown to be elevated in plasma from both type 1 and type 2 diabetes and also in experimental models, as well as in endothelial and smooth muscle cells in the presence of high glucose [170], which may contribute to the vascular complications of diabetes. Our data is in agreement with these findings showing that increasing levels of Ang II stimulation of high-glucose exposed HUVEC's results in significantly greater superoxide levels as compared to the same treatment in normal glucose endothelial cells. Furthermore, when compared with normal glucose HUVEC's, nitric oxide levels are greatly reduced in hyperglycemic endothelial cells as concentration of Ang II is increased. This strongly suggests high-glucose endothelial cells are highly sensitive to Ang II interactions, resulting in greater localized oxidative and nitrosative stress via increased AT1R mediated NADPH oxidase activation.

4.4.2 Influence of Angiotensin II on NOS and NOX Gene Expression in Hyperglycemic HUVEC's

The underlying mechanism(s) by which AT_1 receptor activation by high glucose induces vascular dysfunction is not well understood at this time. However, ANG II has been reported to

increase oxidative stress by activating NADPH oxidase, an enzyme responsible for the production of superoxide anion and other reactive oxygen species [171-173]. As shown in Figure 4, our data indicates that Ang II enhances the increase in gene expression of NOX4 and p22phox in high glucose exposed endothelial cells. An ANG II-induced increased expression of $p47^{phox}$ and $p22^{phox}$ has also been shown recently in vascular smooth muscle cells [174]. In addition, a possible explanation for the decreased nitric oxide levels shown in our study may be that increased concentration of Ang II increases expression/activity of the enzymes that are responsible for the formation of nitric oxide and superoxide, leading to increased peroxynitrite formation and an overall net reduction in nitric oxide levels. The excess generation of superoxide, presumably by NADPH oxidase, would scavenge nitric oxide. Studies have suggested that nitric oxide may directly decrease transcription of AT1Rs by binding to DNA [175]. Therefore, a decrease in nitric oxide levels may result in increased AT1R expression. Taken together, it may be possible that ANG II-induced enhanced oxidative stress under hyperglycemic conditions contributes to the enhanced expression of AT1R, leading to a more potent oxidative stress environment. However, the expression of endothelial cell ATR1 still needs to be investigated.

Ang II may increase oxidative stress in the short term by direct activation of NADPH oxidase to form superoxide [161]. Zhang et al demonstrated that Ang II induces immediate release of superoxide in endothelial cells via activation of NADPH oxidase [176]. Another study suggested that Ang II increases NOS enzyme activity, resulting in increased nitric oxide and peroxynitrite production in endothelial cells [177], and the increase in peroxynitrite could be associated with endothelial dysfunction and cardiovascular disease. Our present data suggest that increased interaction of Ang II with hyperglycemic endothelial cells results in enhanced activation of

iNOS, but not eNOS, mRNA expression. This is in agreement with previous in vivo studies of Ang II. However, these studies did not evaluate Ang II-induced effects on gene regulation of enzymes that are major contributors to oxidative stress in hyperglycemia, which was one of the aims of the present study. Our data indicate that Ang II induces iNOS as well as NADPH oxidase expression, which likely contributes to increased endothelial peroxynitrite formation and oxidative/nitrosative stress in high glucose exposed endothelial cells.

4.4.3 Oxidative and Nitrosative Stress Gene Regulation is Reduced by ARBs and Statins

Angiotensin 1 receptor blockers (ARBs) have been show to decrease intracellular production of superoxide in the endothelium and vascular smooth muscle [178]. The reduction in superoxide protects nitric oxide from oxidative degradation to cytotoxic molecules. This will contribute to increased nitric oxide bioactivity by enhancing nitric oxide synthesis and limiting superoxide scavenging. Our data show (Figure 5b) that Losartan treatment reduces the increased expression of NADPH oxidase and iNOS induced by Ang II and high glucose exposure in HUVEC's. This data suggests the blockade of angiotensin 1 receptor, results in decreased oxidant gene upregulation in hyperglycemic endothelial cells.

Statins are thought to inhibit the expression of AT1 receptor upregulation. Furthermore, statins inhibit the production of oxygen derived free radicals by reducing LDL, increasing NO synthesis, and through antioxidant effects [179]. Statins also have an indirect NOX inhibitory action through inhibition of Rac. The ability of statins to block the activation of Rac1 regulates NADPH oxidase, inhibiting the G-protein to translocate to the membrane-bound NOX subunits [180]. The current study shows that simvastatin additionally blunts the expression of membrane subunits p22phox and NOX 4 in hyperglycemic endothelial cells. Consequently, superoxide

levels are significantly reduced in simvastatin-treated HUVEC's. These results indicate that Losartan and Simvastatin protect against endothelial oxidative stress via inhibition of NADPH oxidase-derived superoxide in high glucose exposed HUVEC's. Taken all together, combined therapy with statins and ARBs may have additive beneficial effects on inhibition of oxygen-derived free radical production and improvement in nitric oxide bioactivity. This combined therapy may improve endothelial function in diabetic patients.

4.4.4 Statins and ARBs Reduce Nitrotyrosine Levels in Angiotensin II Treated High Glucose HUVEC's

Interaction of ROS, particularly superoxide with nitric oxide, leads to production of peroxynitrite, which is a highly cytotoxic reactive compound. In turn, peroxynitrite reacts with DNA, lipid and protein molecules. This is important in biomedical research because it can alter protein function, is associated with acute and chronic disease states, and can be a predictor of disease risk. The reactions between nitric oxide and superoxide do not necessarily result in oxidative damage and at low levels can even be cytoprotective [181]. Data has shown that nitrotyrosine abundance is largely a function of ROS interaction with nitric oxide [182]. Our data show that Ang II exposure to hyperglycemic HUVEC's results in increased nitrotyrosine levels. These findings support our data showing Ang II stimulation results in increased NOX and iNOS gene expression in high glucose exposed endothelial cells. This parallel increase in mRNA expression of NOX genes, p22phox and NOX4, and iNOS by HUVEC's suggests a role of increased NADPH oxidase presence and elevated nitric oxide generation via iNOS, in the formation of nitrotyrosine in these endothelial cells. These findings further describe the role of

local Ang II interaction in augmenting oxidative and nitrosative stress of hyperglycemic endothelial cells.

4.5 Conclusions

Results from this study show Ang II exposure leads to an increase in oxidative and nitrosative stress and endothelial iNOS and NADPH oxidase mRNA expression in high glucose HUVEC's. The data strongly suggests that hyperglycemic endothelial cells are sensitized to Ang II and that increased localized concentrations of this signaling molecule in the vasculature enhances oxidative and nitrosative stress pathways. In the presence of the AT1R antagonist losartan and simvastatin, Ang II-induced increases in iNOS, whereas NADPH oxidase gene expression are significantly reduced. This confirms a significant role for ATI1R in the development of diabetic endothelial cell dysfunction. In addition, peroxynitrite formation was enhanced with Ang II exposure. The synergistic effect of Ang II and high glucose suggests that additional, more-complex mechanisms that involve the interaction between free radicals and AT_1 receptors, possibly dependent on certain levels of free radicals locally produced in the vasculature or endothelial cells are responsible for oxidative and nitrosative stress regulation in this HUVEC model. Further studies will be necessary to elucidate the exact mechanisms responsible for this interaction. Nevertheless, our results suggest that combined therapy using the AT_1 receptor blockade and antioxidants may increase the efficacy of treatment for some forms of hypertension in diabetic patients.

Figure Legends

Figure 1. DHE Fluorescence profile for Angiotensin II dose dependent curve in normal and high glucose exposed HUVEC's. (a). The results shown are for SOD concentrations of 1, 10, and 100 U/mL with a total run time of 30 minutes (n = 3). DHE fluorescence of superoxide was measured using a microplate reader and cell-free XO/hypoxanthine system. RFU values were inversely proportional to SOD concentrations. (b)**.** The data represents the average change in DHE fluorescence per minute for the reaction of hypoxanthine with XO in the presence of catalase and SOD. Values were calculated by taking the slope of the linear-fit curve for each fluorescence readings.

Figure 2. Fluorescence profile of DAF-FM DA for Angiotensin II dose dependent curve in normal and high glucose exposed HUVEC's. (a). The data shows DHE fluorescence for superoxide detection in the presence of SNP (n = 3). Fluorescence was measured using a microplate reader and best-fit lines were calculated based on linear-regression. (b). The results shown represent the change in RFU per minute for each measured nitric oxide concentration. Values were calculated by plotting the slopes for each of the nitric oxide concentrations.

Figure 3. mRNA expression of normal and high glucose exposed HUVEC's. (a). The results shown are for measurement of ferricytochrome c absorbance in relation to varying concentrations of SOD. Absorbance values are representative of the level of superoxide reduction of ferricytochrome c in the presence of increasing SOD concentrations. (b). The results are shown for average change per minute in superoxide concentration as a result of SOD concentration. The concentration of

superoxide was determined from absorbance measurements by using the Beer-Lambert law with a molar extinction coefficient of $\Delta\varepsilon = 21{,}000\ M^{-1}cm^{-1}$ and path length calculated to be 0.97473 cm.

Figure 4. Gene expression analysis of normal and high glucose exposed HUVEC's treated with Angiotensin II. (a). The graph illustrates the measurement of ferricytochrome c absorbance in relation to varying concentrations of SNP. Absorbance values are representative of the level of superoxide reduction of ferricytochrome c in the presence of increasing SNP concentrations. (b). The results shown indicate the average change per minute in superoxide concentration as a result of SNP interaction.

Figure 5. Real Time PCR quantification of gene expression in HUVEC's treated with Angiotensin II and Losartan. The reaction rate constant of DHE and superoxide reaction was $2.6 \times 10^5\ M^{-1}s^{-1}$. The superoxide concentration reached a steady-state concentration of 250 nM. The unreacted DHE concentration in the solution reduced to less than 1 nM within first 10 min. This indicates that DHE fluorescence cannot increase linearly over 30 min in experimental measurement as seen in Figure 1.

Figure 6. Gene expression quantification of HUVEC's treated with treated with Angiotensin II and Simvastatin. The increase in RFU plateau around 100 min for the 5 □M initial DHE concentration but remains increasing for 10 □M DHE.

Figure 7. Nitrotyrosine levels in normal and high glucose exposed HUVEC's treated with Angiotensin II. a). The DHE concentration profiles are shown for 5 and 10 □M initial DHE concentrations for 120 min for a reaction rate of (k_{DHE}) $1.01 \times 10^3\ M^{-1}s^{-1}$. We performed kinetic analysis by reducing the reaction rate of DHE with superoxide to better fit the experimental observation of DHE fluorescence in Figure 6. We

obtained the time (=68 min) at which the RFU value was 63.2% of the maximum fluorescence value (1722 RFU) for 5 □M DHE concentration experiments in Figure 6 (which corresponds to one time constant response for a first order system). The reaction rate for which 1.84 □M unreacted DHE (63.2 % of DHE consumed) was at 68 min was 1.01×10^3 $M^{-1}s^{-1}$. The superoxide concentrations reached steady-state concentration of 250 nM not shown. b). The DHE concentration profiles for a higher reaction rate of (k_{DHE}) 2.0×10^3 $M^{-1}s^{-1}$ is shown for 5 and 10 □M initial DHE concentrations for 120 min. Note that, the DHE concentration fall more sharply and reach a plateau at an earlier time points.

Table 1: Taqman Probes

Target	Species	TaqMan Probe Sequence
NOS 3	Human	Hs00167166_m1
NOS 2	Human	Hs01075529_m1
p22phox	Human	Hs00609145_m1
NOX4	Human	Hs00276431_m1
beta-actin	Human	Hs99999903_m1

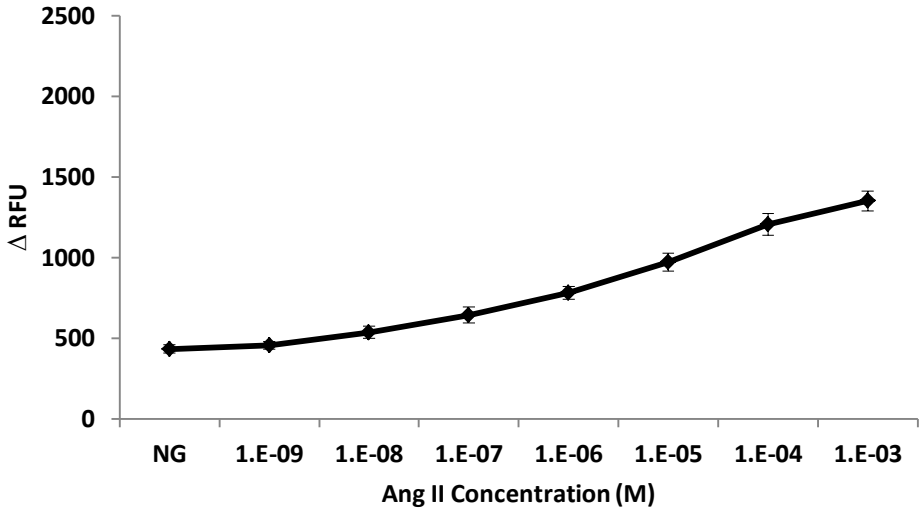
2500
2000
1500
1000
500
0
Δ RFU
NG
1.E-09
1.E-08
1.E-07
1.E-06
1.E-05
1.E-04
1.E-03
Ang II Concentration (M)

Figure 1a

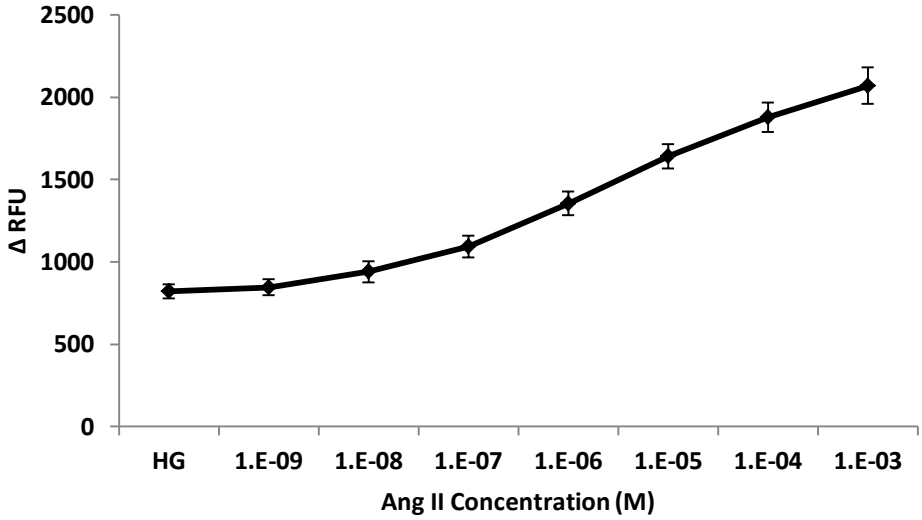
2500
2000
1500
1000
500
0
Δ RFU
HG
1.E-09
1.E-08
1.E-07
1.E-06
1.E-05
1.E-04
1.E-03
Ang II Concentration (M)

Figure 1b

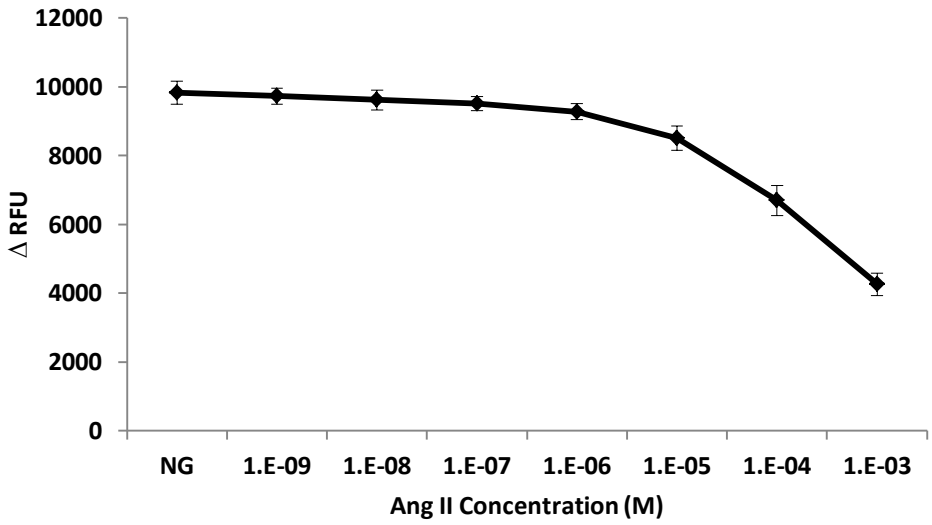
12000
10000
8000
6000
4000
2000
0
Δ RFU
NG
1.E-09
1.E-08
1.E-07
1.E-06
1.E-05
1.E-04
1.E-03
Ang II Concentration (M)

Figure 2a

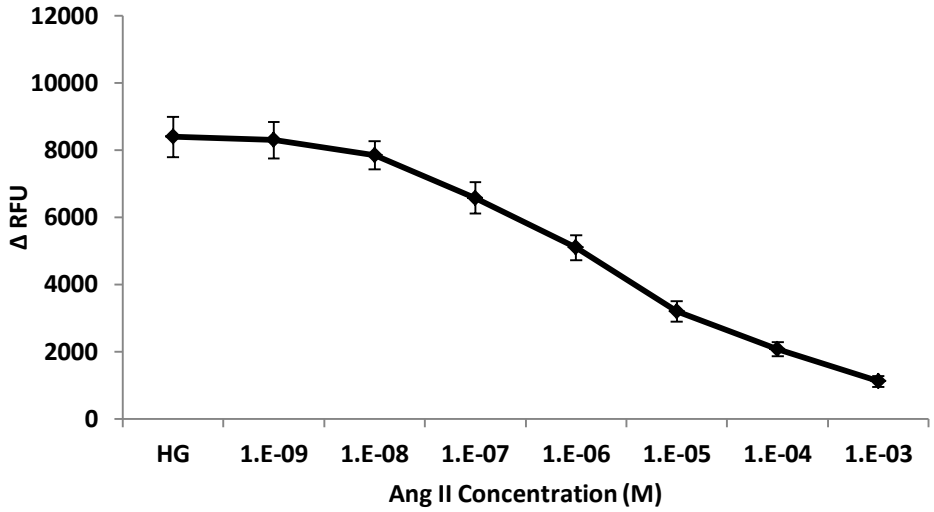
12000
10000
8000
6000
4000
2000
0
Δ RFU
HG
1.E-09
1.E-08
1.E-07
1.E-06
1.E-05
1.E-04
1.E-03
Ang II Concentration (M)

Figure 2b

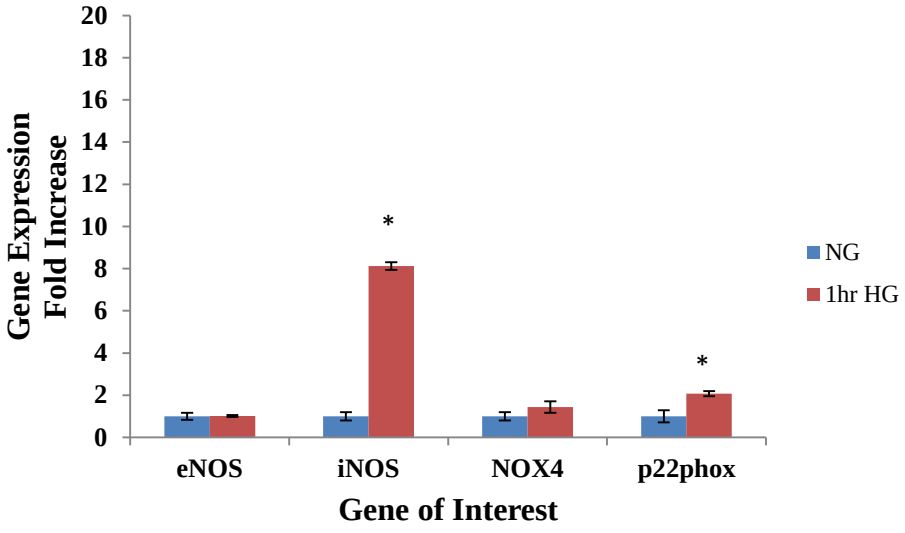
Gene Expression
Fold Increase
20
18
16
14
12
10
8
6
4
2
0
*
*
eNOS
iNOS
NOX4
p22phox
Gene of Interest
NG
1hr HG

Figure 3a

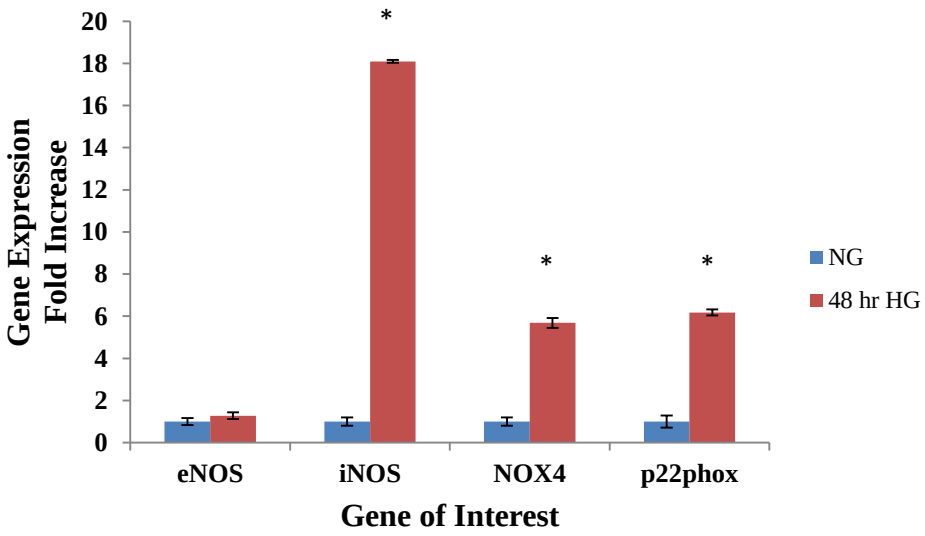
Gene Expression
Fold Increase
20
18
16
14
12
10
8
6
4
2
0
*
*
*
eNOS
iNOS
NOX4
p22phox
Gene of Interest
NG
48 hr HG

Figure 3b

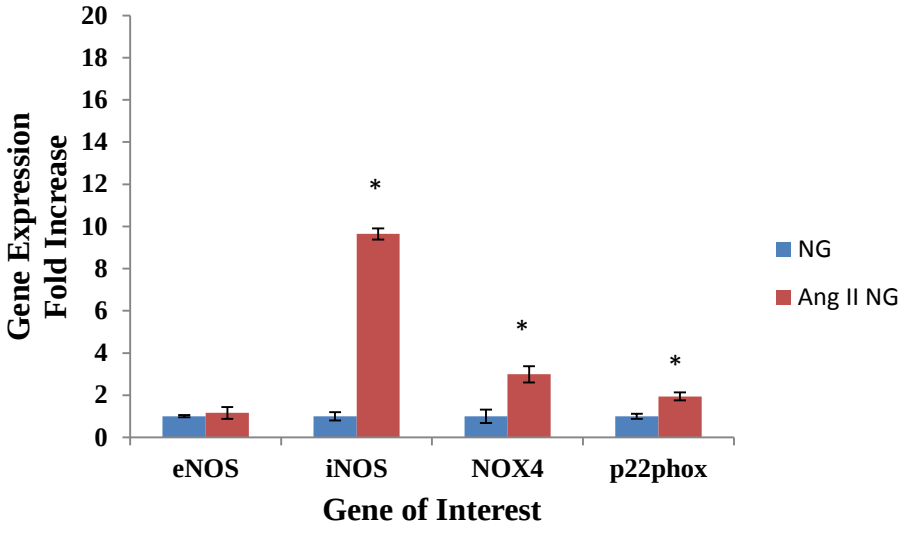
Gene Expression
Fold Increase
20
18
16
14
12
10
8
6
4
2
0
*
*
*
eNOS
iNOS
NOX4
p22phox
Gene of Interest
NG
Ang II NG

Figure 4a

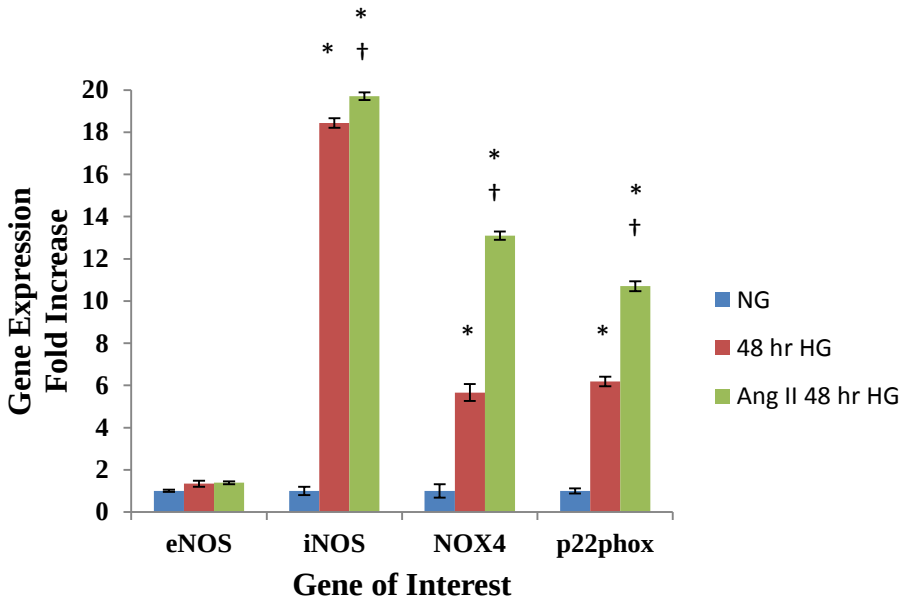
Gene Expression
Fold Increase
20
18
16
14
12
10
8
6
4
2
0
eNOS
iNOS
NOX4
p22phox
Gene of Interest
NG
48 hr HG
Ang II 48 hr HG
*
†

Figure 4b

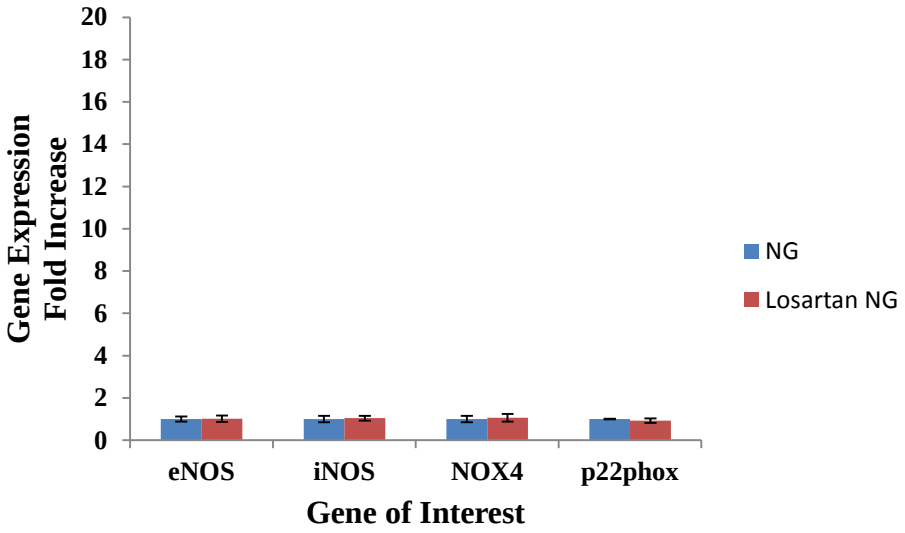
Gene Expression
Fold Increase
20
18
16
14
12
10
8
6
4
2
0
eNOS
iNOS
NOX4
p22phox
Gene of Interest
NG
Losartan NG

Figure 5a

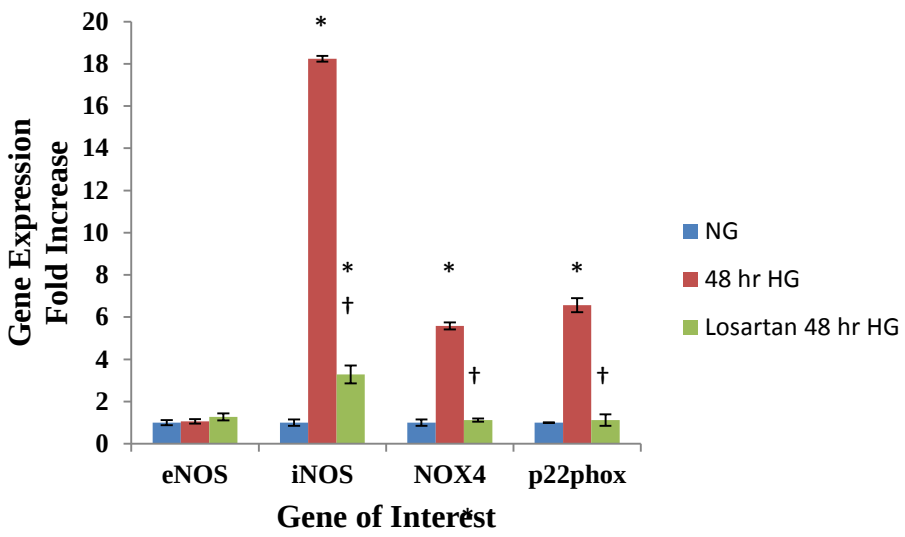
Gene Expression
Fold Increase
20
18
16
14
12
10
8
6
4
2
0
*
*
†
*
†
*
†
eNOS
iNOS
NOX4
p22phox
Gene of Interest
NG
48 hr HG
Losartan 48 hr HG

Figure 5b

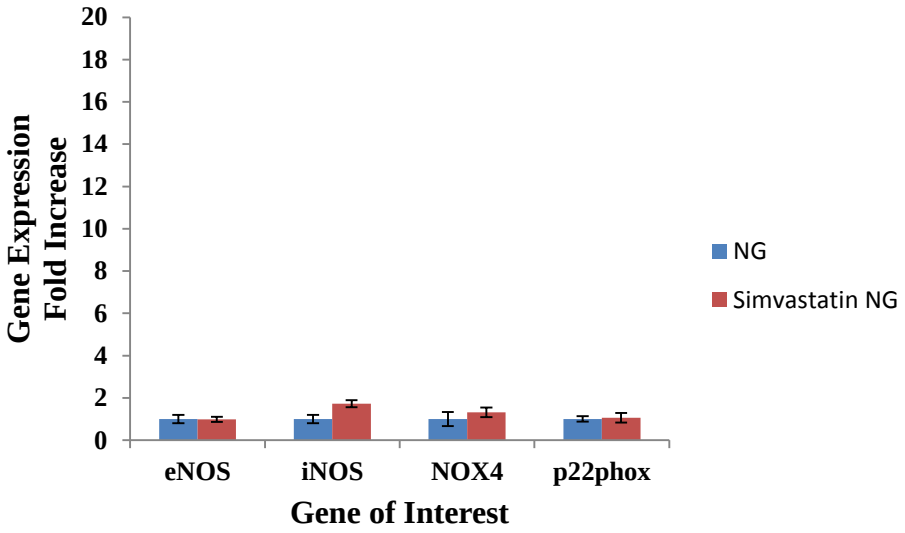
Gene Expression
Fold Increase
20
18
16
14
12
10
8
6
4
2
0
eNOS
iNOS
NOX4
p22phox
Gene of Interest
NG
Simvastatin NG

Figure 6a

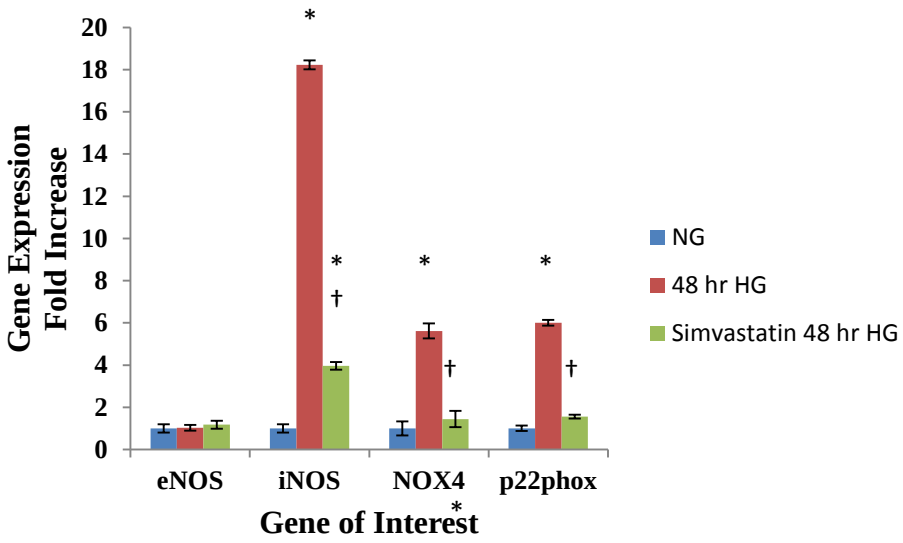
Gene Expression
Fold Increase
20
18
16
14
12
10
8
6
4
2
0
*
*
†
*
†
*
†
*
eNOS
iNOS
NOX4
p22phox
Gene of Interest
NG
48 hr HG
Simvastatin 48 hr HG

Figure 6b

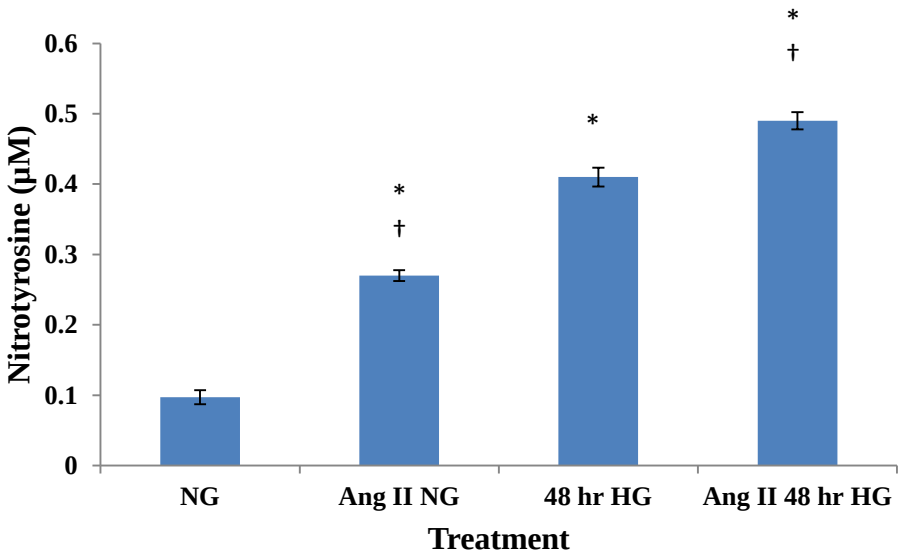
Nitrotyrosine (µM)
0.6
0.5
0.4
0.3
0.2
0.1
0
*
†
*
*
†
NG
Ang II NG
48 hr HG
Ang II 48 hr HG
Treatment

Figure 7a

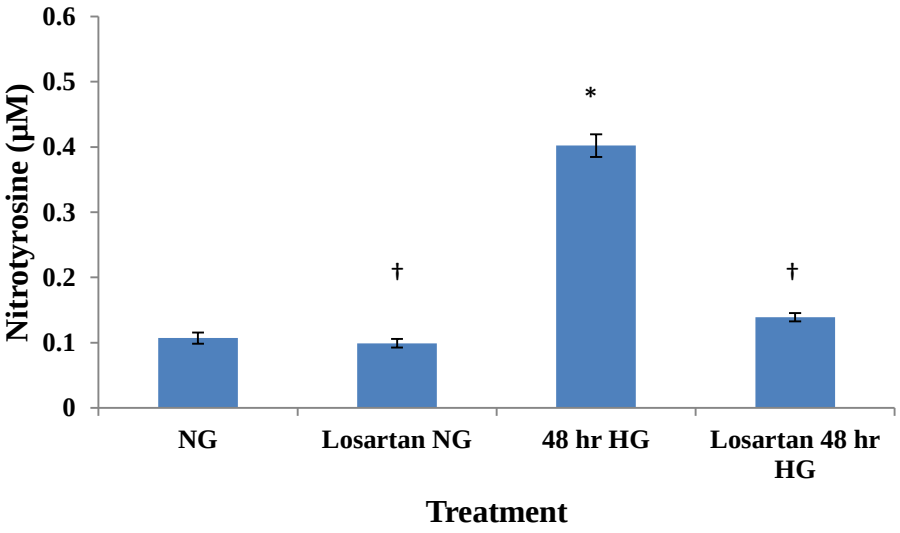
0.6
0.5
0.4
0.3
0.2
0.1
0
Nitrotyrosine (µM)
*
†
†
NG
Losartan NG
48 hr HG
Losartan 48 hr HG
Treatment

Figure 7b

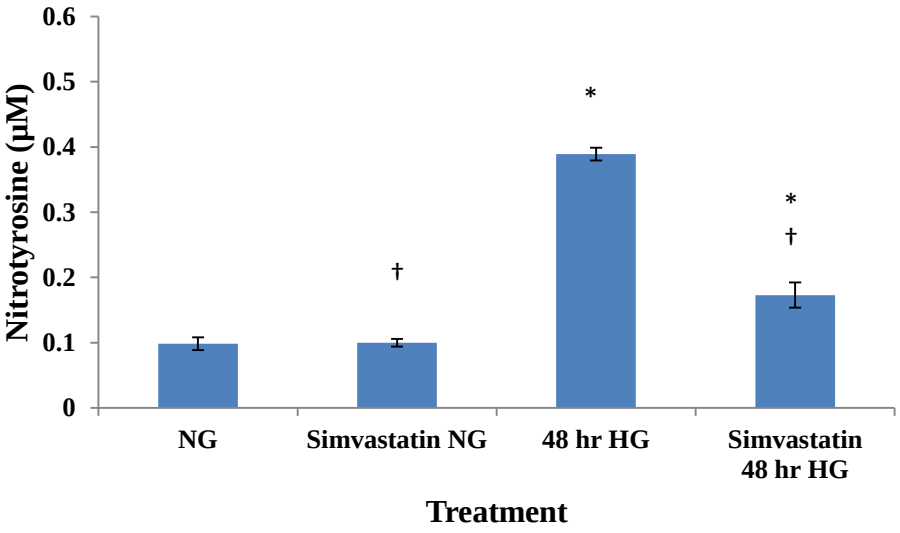
0.6
0.5
0.4
0.3
0.2
0.1
0
Nitrotyrosine (µM)
*
†
*
†
NG
Simvastatin NG
48 hr HG
Simvastatin 48 hr HG
Treatment

Figure 7c

CHAPTER 5

Concluding Remarks and Future Work Recommendations

5.1 Concluding Remarks

Increased extracellular glucose concentration, a principal feature of diabetes mellitus, induces a dysregulation of reactive oxygen and nitrogen generating pathways. These processes lead to a loss of the vascular endothelium to produce biologically active nitric oxide, which impairs vascular function. Reactive oxygen and nitrogen species trigger endothelial cell dysfunction through a multitude of mechanisms and these interrelated pathways have been a focus of numerous researchers. It is well established that hyperglycemia induces excess superoxide production in endothelial cells. Furthermore, past studies have also described the reduced availability of nitric oxide within the endothelial layer. However, the specific pathways, enzymes and gene regulation responsible for the development of high glucose induced oxidative and nitrosative stress is still under intense investigation. The overall aim of the work presented in this dissertation was to provide a more clear understanding of the enzymes and gene regulation responsible for the development of reduced nitric oxide levels and increased superoxide presence, protein damage and apoptosis in high glucose exposed endothelial cells. Through these mechanistic studies we were able to analyze and better describe the interactions between reactive species and the primary enzymes and pathways involved in hyperglycemic endothelial cell dysfunction.

A key factor in the analysis of intracellular superoxide and nitric oxide production is the rate at which the target species is detected compared with the potential rate of reaction of the target with other possible reactants. Previous studies investigating intracellular superoxide and nitric oxide production rates did not consider potential reactant interference in the measurements, while others used detection techniques with reaction rates far lower than those of potential side reactions of the target species. Consequently, these measurements are prone to over- or under-

estimating the actual intracellular levels of superoxide and nitric oxide. We utilized a cell-free system to generate superoxide and nitric oxide in order to more accurately determine the reaction rates of superoxide and nitric oxide with two widely used fluorescent dyes, DHE and DAF-FM diacetate respectively. Absence of in-vivo reactant interference enabled us to better determine the reliability of these fluorophores to detect the highly reactive superoxide and nitric oxide species and also better describe the levels at which superoxide interaction with scavengers such as SOD and nitric oxide begin to interfere with the accuracy of fluorescence measurements. Results obtained from experiments conducted in Chapter 2 show that DHE and DAF-FM diacetate are reliable detectors of superoxide and nitric oxide concentrations in vivo, respectively. However, rates of production are much more difficult to accurately assess due to the varying degree of possible reactant interferences. Therefore, care should be taken in interpreting rate of production reported in oxidative/nitrosative stress studies utilizing fluorescence detection methods.

Next, in Chapter 3 we utilized these fluorescence detection techniques to better describe the oxidative and nitrosative stress levels found in endothelial cells treated with increasing lengths of high-glucose exposure. Furthermore, through the use of specific enzyme inhibitors we were able to more accurately determine the contribution levels of oxidant producing enzymes involved in the excess levels of superoxide and nitric oxide in hyperglycemic HUVEC's. Results from these studies show that NADPH oxidase is the primary contributor to oxidative stress in high glucose exposed HUVEC's. Our work also shows that while hyperglycemia decreases nitric oxide levels, generation of nitric oxide is paradoxically increased. Furthermore, we are able to indirectly confirm this concomitant increase in superoxide and nitric oxide by showing a significant increase in the formation of nitrotyrosine in high glucose exposed endothelial cells. This

illustrates that the parallel increase in superoxide and nitric oxide lead to increased reaction with one another, resulting in higher levels of the cytotoxic peroxynitrite molecule.

To better understand the effects of angiotensin II and high glucose on gene regulation of oxidant generating enzymes involved in oxidative and nitrosative stress pathways, we performed real-time quantitative PCR for NADPH oxidase subunits and nitric oxide synthase isoforms in HUVEC's. The renin-angiotensin system represents a major contributor to vascular endothelial dysfunction in macro- and microvascular diseases. High glucose has been shown to increase both angiotensin converting enzyme activity, as well as local angiotensin II concentrations, in the vasculature. Furthermore, angiotensin II is thought to activate endothelial cell NADPH oxidases via AT1 receptor stimulation. Results from studies found in Chapter 4 show that stimulating effects of angiotensin II on the activity of endothelial cell NADPH oxidases is enhanced in high-glucose exposed HUVEC's. We also show that hyperglycemic endothelial cells are more sensitive to Ang II interaction, resulting in lower levels of nitric oxide bioavailability and increased nitrotyrosine formation. Our results also provide insight into the gene regulation of NADPH oxidase, eNOS and iNOS. Data shows that angiotensin II increases NADPH oxidase and iNOS mRNA levels in high-glucose exposed HUVECs, while eNOS expression is unchanged. This further validates the hypothesis that high glucose initiates a protective response in endothelial cells by upregulating nitric oxide producing enzymes, iNOS, in an attempt to counteract the increased production of superoxide by NADPH oxidase. Unfortunately, this protective measure only exacerbates the oxidative and nitrosative stress environment of the cell, leading to increased cell damage and/or apoptosis.

5.2 Future Work Recommendations

Insights from the experimental analyses of nitric oxide-superoxide interactions conducted in this dissertation further our understanding of the role of oxidative and nitrosative stress in endothelial cells under diabetic pathophysiological conditions. Endothelial cells respond to hyperglycemia by upregulating antioxidant scavenging mechanisms, such as nitric oxide and SOD, and anti-inflammatory actions. However, these potentially protective mechanisms are overwhelmed by the excessive production of oxidants, resulting in further damage and apoptosis. Treatment strategies should be aimed at alleviating the production of reactive oxygen species, rather than increasing antioxidants. An important point produced from our work is the increased sensitivity of hyperglycemic endothelial cells to angiotensin II, the powerful vasoconstrictor. Presumably, this mechanism involves, at least partly, upregulation or activation of angiotensin type 1 receptors on the surface of endothelial cells. Future work should concentrate on determining whether gene and/or protein expression of angiotensin type 1 receptors is increased in response to hyperglycemia and what potential effects may occur from inhibiting the potential over-expression of these receptors. Furthermore, in-depth molecular work on the gene/protein regulation of nitric oxide synthase and NADPH oxidase by hyperglycemic response in endothelial cells will also increase understanding and potential therapeutic targets in diabetes treatment. Focus on the transcriptional regulation of these genes via microRNA, transcriptional factors and histone modifications all represent potential areas of future work in this field. Additionally, a better understanding of the relationship between the signaling pathways and enzyme expression/activation involved in hyperglycemic stress is an area of future interest.